Characterization of the 11β-hydroxysteroid dehydrogenase 1-related short-chain dehydrogenase/reductase DHRS7

Inauguraldissertation

zur

Erlangung der Würde eines Doktors der Philosophie

vorgelegt der Philosophisch-Naturwissenschaftlichen Fakultät der Universität Basel

von Julia Katharina Seibert,

aus Kaiserslautern, Deutschland

Basel, 2015

Genehmigt von der Philosophisch-Naturwissenschaftlichen Fakultät
auf Antrag von Prof. Dr. Alex Odermatt (Fakultätsverantwortlicher) und Prof. Dr. Michael Arand (Korreferent)

_____

Fakultätsverantwortlicher
Prof. Dr. Alex Odermatt

Basel, den 21. April 2015

_____

Dekan
Prof. Dr. Jörg Schibler

Table of Contents

I. Abbreviations

11β-HSD:	11β-hydroxysteroid-dehydrogenase
ACTH:	Adrenocorticotropic hormone
ADHD:	Attention-deficit/hyperactivity disorder
BARD1:	BRCA1 associated RING domain protein 1
BC:	Breast cancer
BCL-2:	B-cell CLL/lymphoma 2
BRCA1/2:	Breast cancer 1/2, Early Onset
BRIP1:	BRCA1 interacting protein C-terminal helicase 1
CAN:	Central nervous system
CDH1:	E-cadherin
CHEK1/2:	Cell cycle checkpoint kinase 1/2
COX-2:	Cyclooxygenase-2
DHEA:	Dehydroepiandrosterone
DHEAS:	Dehydroepiandrosterone sulfate
DHRS7:	Dehydrogenase/Reductase SDR family member 7
DNA:	Deoxyribonucleic acid
DOC:	11-Deoxycorticosterone
EGFR:	Epithelial growth factor receptor
ER:	Estrogen receptor
ERBB2:	V-Erb-B2 avian erythroblastic leukemia viral oncogene homolog
FANCD2:	Fanconi anemia complementation group D2 protein, isoform 1
FGFR:	Fibroblast growth factor receptor
GR:	Glucocorticoid receptor
HCC:	Hepatocellular carcinoma
Her2:	Human epidermal growth factor receptor 2
HPA axis:	Hypothalamic–pituitary–adrenal axis
HPG axis:	Hypothalamic-pituitary-gonadal axis
IC_{50}:	Half maximal inhibitory concentration
IGF-1:	Insulin-like growth factor-1 receptor
LLOQ:	Lower limit of quantification
MAPK:	Mitogen activated protein kinase
MDMA:	3,4-Methylendioxymethamphetamine
MPH:	Methylphenidate
MR:	Mineralocorticoid receptor
mRNA:	Messenger ribonucleic acid

mTOR:	Mammalian target of rapamycin
MYC:	Avian myelocytomatosis viral oncogene homolog
NAD (H):	Nicotinamide adenine dinucleotide (H)
NADP (H):	Nicotinamide adenine dinucleotide phosphate (H)
PCa	Prostate cancer
PPAR:	Peroxisome proliferator-activated receptor
PR:	Progesterone receptor
PSA:	Prostate specific antigen
PSDR1:	Prostate short-chain dehydrogenase/reductase 1
PTEN:	Phosphatase and tensin homolog
PTSD:	Post-traumatic stress disorder
QC:	Quality control
RAD51:	DNA repair protein, *S.cerevisiae* homolog
SCD-1:	Stearoyl-CoA desaturase-1
SDR:	Short-chain dehydrogenase/reductase
SNR:	Signal to noise ration
SPE:	Solid-phase extraction
TMA:	Tissue microarray
TNBC:	Triple negative breast cancer
UPLC-MS/MS:	Ultra-pressure liquid chromatography tandem mass spectrometry
VEGFR:	Vascular endothelial growth factor receptor
Wnt:	Wingless-type MMTV integration site family

1. Summary

Short-chain dehydrogenase/reductase (SDR) enzymes metabolize a broad spectrum of substrates and play a pivotal role in the regulation of different metabolic and signaling pathways. In one part of this thesis the activity and specificity of potential inhibitors of the SDRs were tested. These enzymes, 11β-hydroxysteroid dehydrogenase type 1 and 2 (11βHSD1 and 2), are currently evaluated as potential novel therapeutic targets for several diseases, such as metabolic syndrome, atherosclerosis, osteoporosis and chronic kidney disease. 11βHSD1 is a well characterized SDR and its inhibition was suggested to be beneficial for several metabolic disturbances. In contrast to synthetic compounds, little is known about natural compounds activity on this enzyme. In this thesis, the inhibiting potential of constituents of the extract mastix gum, derived from the plant *Pistacia lentiscus*, on 11βHSD1 activity was examined. All tested mastic gum constituents exhibited an inhibitory potential with low micromolar IC_{50} values and selectivity for 11β-HSD1 over 11β-HSD2 *in vitro*. Compared with compounds currently being developed by several pharmaceutical companies, the mastix gum constituents inhibit 11β-HSD1 with much weaker efficacy. The investigation into the role of mastic gum as a therapeutic agent warrants further research, also to assess possible adverse effects of the plant extract. The constituents of mastic gum may as well target other pathways and it is important to delineate the positive from the negative effects of these molecules.

In another study, the effects of 11β-aminoprogesterone derivatives were evaluated for their potential to inhibit 11βHSD2 *in vitro*. Inhibition of 11βHSD2 is usually avoided in the development of pharmaceuticals, since its systemic inhibition causes sodium and water retention, elevated blood pressure and hypokalemia. Nevertheless, selective 11βHSD2 inhibition has been suggested as a potential therapy for hemodialysis patients suffering from hyperkalemia or for patients with colon cancer. Thus, we tested a series of progesterone derivatives in bioassays and six of them showed selective inhibition of 11β-HSD2 over 11β-HSD1. These compounds offer a good basis for the development of 11β-HSD2 inhibitors with optimized properties for topical applications. However, risk-benefit analysis as well as comparison with other potential selective inhibitors needs to be done. Thus, the assessment of the therapeutic potential of 11β-aminoprogesterone derivatives warrants further research.

The assessment of 11βHSD inhibitors *in vivo* requires analytical methods to detect changes in steroid levels. Therefore, another aim of this thesis was to establish an LC-MS/MS method to quantify corticosteroid hormones. The method was applied in a clinical study on the effects of the recreational drug 3,4-methylenedioxymethamphetamine (MDMA) and the cognitive enhancer Methylphenidate (MPH) on circulating steroid hormones in healthy subjects. The serotonin releaser MDMA showed acute effects on circulating steroids. MDMA significantly increased the plasma concentrations of cortisol by more than 60% compared to control. These effects were not observed with MPH, which stimulates the dopamine and norepinephrine systems. Thus, the findings of this study support the view that serotonin mediates the acute pharmacologically induced stimulation of the Hypothalamic–pituitary–adrenal (HPA) axis in the

absence of other stressors. Since cortisol was elevated but cortisone levels were not altered, an effect on the activities of the glucocorticoid metabolizing 11β-HSD1 and 11β-HSD2 triggered by MDMA and/or MPH could not be fully excluded.

The last and main part of this thesis focused on the “orphan” SDR DHRS7. Given that more than 70 SDRs have been discovered in humans and almost half of them have not been characterized, some “orphan” SDRs may be important therapeutic targets and others may represent “off-targets” if inhibited unintentionally by pharmaceuticals. Hence, “deorphanizing” enzymes is crucial to understand their physiological roles and to evaluate and understand adverse and beneficial drug effects. In this thesis the SDR DHRS7 was identified as a tumor suppressor and possible marker for breast and prostate cancer. DHRS7 protein was found to be decreased with increasing tumor grades in prostate cancer tissue samples. Furthermore, knockdown of DHRS7 increased the aggressiveness of cells *in vitro*. Microarray data suggested the involvement of EMT and/or the BRCA pathway in the DHRS7 mediated effects. In addition, evidence presented in this thesis suggests DHRS7 may also play a role in liver regeneration. To fully understand the mechanism and function of DHRS7 its substrate(s) need to be identified. Applying our steroid analytics the most common steroid hormones could be excluded as substrates of DHRS7 and further research is warranted to “deorphanize” this enzyme. An untargeted omics approach is currently followed for hypothesis generation.

In conclusion, the results presented in this thesis significantly extend our knowledge in the field of SDRs. Firstly, we identified novel, potent, selective inhibitors for two well-characterized 11βHSDs. Secondly, the observed effects of amphetamine-related drugs on steroid hormone levels in the blood suggest that they activate the HPA axis and enhance steroid production rather than altering steroid levels by modifying 11βHSD activities. Finally, this thesis describes a novel role for the “orphan” SDR DHRS7 as a tumor suppressor in breast and prostate cancer. This thesis underlines the importance of “deorphanizing” SDRs, which may play important roles in many metabolic and signaling pathways and may thus be involved in several diseases.

2. Preface

This thesis is divided into three chapters comprising the projects I was involved in. In the first chapter, the characterization of several synthetic and natural compounds inhibiting 11β-hydroxysteroid dehydrogenases (11β-HSDs) is described. Such inhibitors are of potential therapeutic interest; however, their potential for unwanted side-effects has to be carefully investigated and other members of the family of short-chain dehydrogenases (SDRs) including DHRS7 should be considered in the assessment. The first chapter contains two published studies, one where I share first authorship and one where I am co-author. The second chapter describes a project in healthy humans, where the effects of 3, 4-methylendioxymethamphetamine (MDMA) and methylphenidate (MPH) on circulating steroid levels were investigated. In this project I gained deeper insights into the method of liquid chromatography–mass spectrometry (LC-MS/MS) for the quantification of steroids in clinical samples. This method was later used to search for possible substrates of DHRS7. The second chapter contains a study published in the journal of Neuroendocrinology. The final chapter focusses on my main project, the investigation of the "orphan" SDR DHRS7. The results of my experiments provide the first evidence for a role of DHRS7 as a tumor suppressor. This chapter contains a paper submitted to the International Journal of Cancer.

3. Chapter 1: Characterization of novel inhibitors of 11β-Hydroxysteroid dehydrogenases

Introduction

The 11β-hydroxysteroid dehydrogenases (11β-HSDs) belong to the short-chain dehydrogenases/reductases (SDRs), one of the largest enzyme superfamilies, with members identified in all life forms. More than 70 different SDRs are found in humans [2]. Although sequence identity between SDRs is relatively low (15–30%), several motifs are typical for these enzymes, such as the cofactor binding motif TGxxxGxG and the active center motif YxxxK [3]. SDRs share common three-dimensional structures, such as the Rossmann-fold, a structural motif containing a parallel 7 stranded β-sheet surrounded on both sides by α-helices that forms the cofactor binding site and is located at the N-Terminus (Figure 1) [4]. SDRs have a co-factor preference for nicotinamide adenine dinucleotide (H) (NAD(H)) or nicotinamide adenine dinucleotide phosphate (H) (NADP(H)). SDRs catalyze the oxidation and reduction of a wide variety of substrates including sugars, steroids, retinoids, fatty acids and xenobiotics [5]. Several members of this protein family, for example 11β-HSD1 are not restricted to one substrate but exhibit multifunctionality [6].

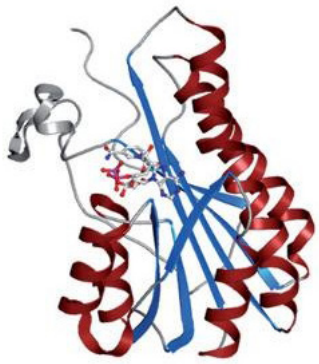

Figure 1: classical SDR structure; Rossmann-fold motif is depicted with beta strands in blue and helices in red; additional domains and secondary structural elements are shown in grey [1].

Due to their broad spectrum of substrates and their pivotal role in the regulation of different metabolic and signaling pathways, dysfunctional SDR enzymes can lead to the progression of several diseases such as Alzheimer's disease, cancer and obesity-related medical conditions [7-9]. Therefore, drugs and xenobiotics targeting SDRs might result in adverse effects. However, some specific SDR members like 11β-HSD1 are considered to be promising pharmacological drug targets [10].

11β-HSD1 is expressed in key metabolic tissues including skeletal muscle, liver and adipose tissue [11, 12]. 11β-HSD1 is strongly associated with the development of obesity, type 2 diabetes, hypertension and the metabolic syndrome [13, 14]. Although the enzyme functions bidirectional, the main reaction catalyzed by 11β-HSD1 is the NADPH-dependent reduction of cortisone to the active steroid hormone cortisol. Cortisol is a glucocorticoid synthesized and released from the adrenal cortex in accordance with a strong circadian rhythm. Secretion of glucocorticoids is under the control of the hypothalamic pituitary adrenal (HPA) axis. After glucocorticoids enter the cell, by free diffusion through the cell membrane, they can be metabolized and the active form, cortisol, can bind to the ligand binding domain of the glucocorticoid

receptor (GR) (Figure 2). Binding of cortisol to GR leads to conformational changes, receptor dimerization and activation of the receptor complex. The “activated” receptor then interacts in the nucleus with critical regulatory sites of genes [15]. The transcription of genes controlling immune response, metabolism and development is triggered either directly by binding of the GR to the promotor region of a gene or indirectly by the interaction of the GR with other transcription factors [16].

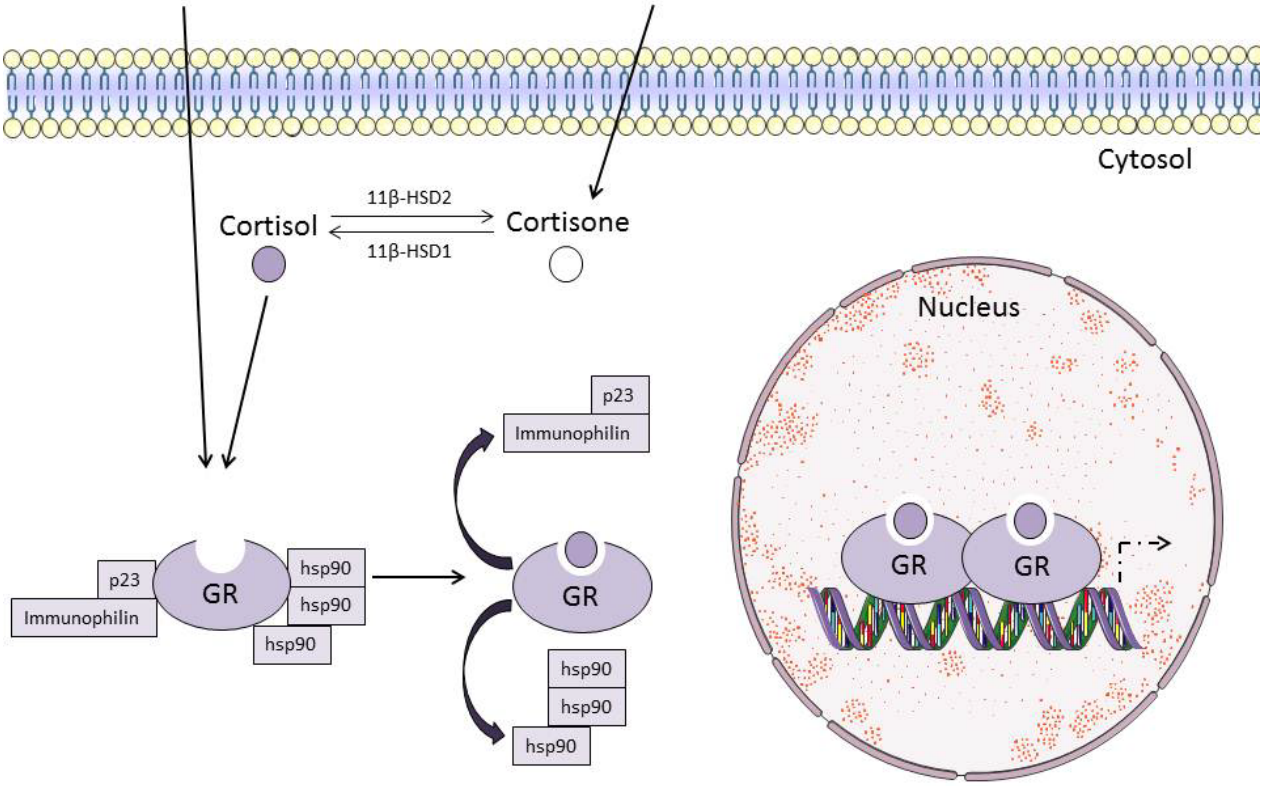

Figure 2: Schematic representation of mechanisms of GR-dependent gene transcription. Glucocorticoids are free to cross the plasma membrane where they can be metabolized by 11β-HSD1/2. Upon binding with cortisol, the GR translocates into the nucleus and modulates gene transcription [modified after [14] using Servier Medical Art software (www.servier.com)]

In the last decade, interconversion of active and inactive glucocorticoids by 11β-HSDs emerged as a key regulatory mechanism of glucocorticoid action [17]. Thus, studies showed that specific 11β-HSD1 inhibitors decrease local cortisol availability and improve insulin sensitivity, glucose tolerance, lipid levels and atherosclerosis via indirect antagonism of the GR [18, 19]. At present, there are several clinical trials ongoing, using 11β-HSD1 inhibitors in patients with metabolic syndrome, type 2 diabetes and cardiovascular disease [20]. The need for selective isozyme inhibitors is important, since the inhibition of 11β-HSD2 results in sodium and water retention, elevated blood pressure and hypokalemia [21]. 11β-HSD2 is a NAD^+-dependent dehydrogenase that acts unidirectional, catalyzing the oxidation of cortisol to its inactive metabolite cortisone. This isozyme is mainly expressed in mineralocorticoid target tissues such as the kidney and colon, where it prevents inappropriate activation of the mineralocorticoid receptor (MR)

by cortisol. Cortisol has been shown to possess binding affinities comparable to that of the physiologic mineralocorticoid aldosterone to the MR [22]. Compounds inhibiting 11β-HSDs non-selectively promote MR activation, which has been linked with the pathogenesis of cardiovascular disease in several clinical studies [23]. On the other hand, MR antagonists showed promising results in the treatment of chronic kidney disease and diabetic nephropathy [24, 25]. Although inhibition of 11β-HSD2 needs to be avoided in most cases, it was recently suggested that 11β-HSD2 inhibitors may be useful to treat chronic hemodialysis patients by increasing potassium loss as a result of cortisol-induced MR activation in the colon [26]. Furthermore, the inhibition of 11βHSD2 showed a suppression in Cyclooxygenase-2 (COX-2) driven prostaglandin E2 production and colorectal tumor growth without any obvious adverse side effects in human [27]. These studies support the hypothesis that 11β-HSD2 inhibition may be a promising therapeutic target, specifically with locally acting enteric inhibitors that are neither systemically absorbed nor influencing renal 11β-HSD2 [28].

The first study of this chapter examined the effect of the oleoresin mastic gum and its constituents, isolated from *Pistacia lentiscus* var. *chia*, on 11β-HSD1 and 2 activities performed in collaboration with Dr. A. Assimopoulou, Dr. D. Schuster and coworkers. *Pistacia lentiscus* is an evergreen tree of the Anacardiaceae family, which is common in the eastern Mediterranean area. The variety chia, commonly known as mastic tree, is uniquely cultivated in southern Chios, a Greek island in the Aegean [29]. The oleoresin of mastic consists of nearly 70 constituents and has been linked to numerous diverse biomedical and pharmacological characteristics, including destruction of bacteria and fungi, reduction of symptoms of autoimmune diseases like Crohn's disease and asthma, protection of the cardiovascular system, induction of apoptosis in human cancer cells and improvement of symptoms in patients with functional dyspepsia [30]. However, many of the potential medical and pharmaceutical properties of mastic gum have only been shown *in vitro* or in animal models. Studies performed in humans, testing mastic gum, are mostly subjective and have contradictory outcomes. Therefore, further research is required to evaluate the potential effects of mastic gum. Recently, mastic gum also showed antidiabetic effects in mice *in vivo* but the exact mechanism remains unknown [31]. However, peroxisome proliferator-activated receptor (PPAR) modulation was discussed as possible mechanism [32]. Glucocorticoid metabolism may also be a possible target of this plant extract. Dr. A. Vuorinen applied a pharmacophore-based virtual screening to filter a natural product database for 11β-HSD1 selectivity. The two main constituents of mastic gum, the triterpenoids masticadienonic acid and isomasticadienonic acid were predicted to bind 11β-HSD1. To support these findings, I performed activity assays for 11β-HSD1 and 2 in cell lysates to test the effect of oleoresin, the acidic fraction and the purified triterpenic acids; masticadienonic acid and isomasticadienoinic acid. The major constituents of the acidic fraction includes; the triterpenic acids oleanonic acid, masticadienonic acid as well as isomasticadienoinic acid.

The second study of this chapter focused on the effect of progesterone and a selection of its metabolites, on the activity of the MR and the 11β-HSDs, since they have been reported to bind to these enzymes [33, 34]. This study was performed in collaboration with Prof. Dr. JC Vederas and coworkers. A previous study showed that the progesterone derivative, 11β-hydroxyprogesterone triggered the activation of MR *in vitro*

and inhibited 11β-HSD1 with an IC_{50} value of 65 nM *in vitro* [34]. However, 11β-hydroxyprogesterone was an equally potent inhibitor of 11β-HSD2 activity in whole cell preparations, with an IC_{50} value of 0.2 μM [35, 36]. In this study, I further evaluated the inhibiting potential of progesterone derivatives on 11β-HSD1 as well as their specificity to inhibit the dehydrogenase reactions and assessed their ability to bind to the MR. Due to high lipophilicity, progesterone possesses low water solubility and hence low bioavailability. Therefore, chemical modifications need to be introduced to improve these parameters [37]. To overcome this problem aminosteroids and amino acid–steroid conjugates are commonly prepared [38]. Following the successful synthesis of several 11β-amino and amino acid progesterone derivatives by Dr. K. Pandya, I tested 17 compounds for their potential to inhibit 11β-HSD1 and 11β-HSD2, as well as for their ability to modulate MR transcriptional activity.

Results and Discussion

The aim of the first study described in this thesis was to investigate the effect of four different constituents of mastic gum on 11β-HSD1 and 2 in cell lysates *in vitro*. To evaluate the selective inhibiting potential of the resin, acidic fraction, masticadienonic acid and isomasticadienonic acid on 11β-HSD1 and 11β-HSD2 a screening was performed at a high concentration, prior to IC_{50} measurements (Figure 3).

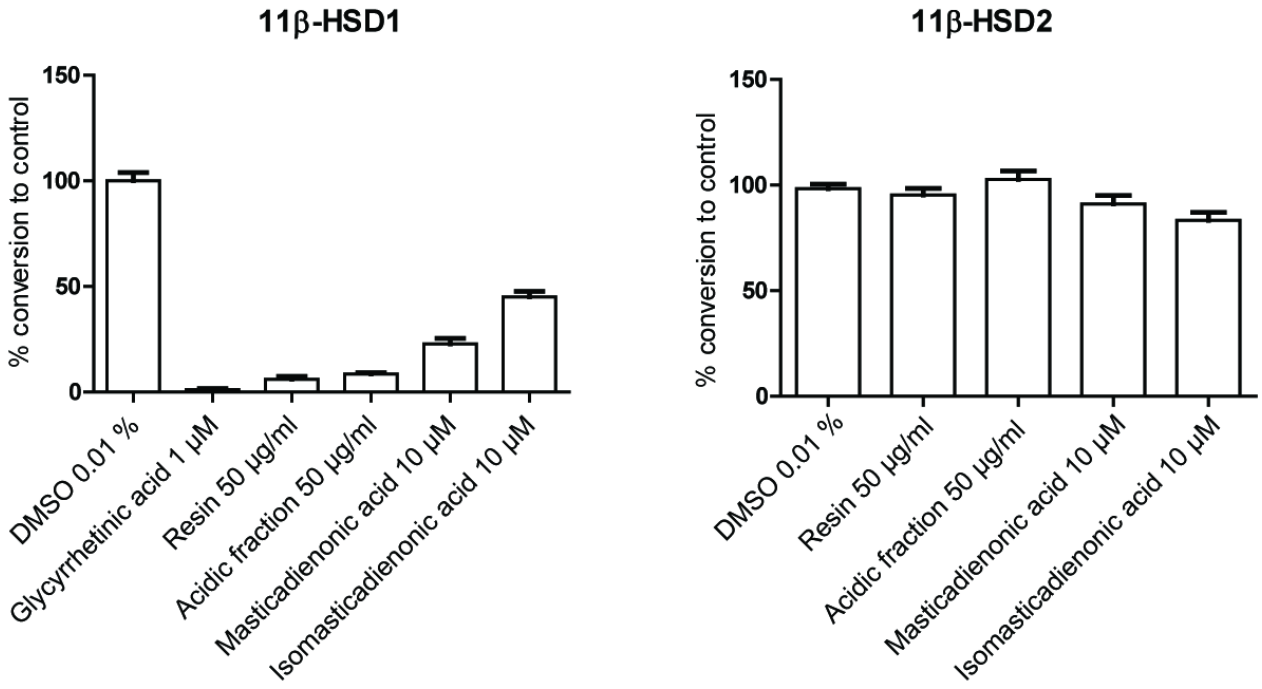

Figure 3: Conversion of radio labeled cortisone by 11β-HSD1 and cortisol by 11β-HSD2. DMSO served as vehicle control and glycyrrhetinic acid (1 μM) as positive control. Data of three independent experiments was normalized to vehicle control and expressed as mean ± SD.

All constituents tested showed inhibiting potential and selectivity for 11β-HSD1 in HEK293 cell lysates, thereby supporting the hypothesis generated by the pharmacophore-based virtual screening model. 11β-HSD2 was not inhibited by any plant constituent, illustrating the selectivity of the compounds.

Following the screening, I determined the IC_{50} values for each of the tested constituents (Figure 4 in the publication). The resin, which contains all the triterpenoids, showed the highest inhibitory potential with an IC_{50} of 1.33 µg/µL. The plant constituents are known to have effects which improve human health [39]. The anti-inflammatory activity of mastic gum for example has been mainly attributed to triterpenoids [40]. Interestingly, purified isomasticadienonic acid gave an IC_{50} of 1.94 µM. This constituent was also reported to be the most active purified compound with respect to the anti-inflammatory action of mastic gum *in vitro* [40]. Compared to oleanonic acid, a main constituent of the acidic fraction of mastic gum, which has been shown to inhibit 11β-HSD1 with high nanomolar IC_{50} values, the inhibiting potential of masticadienonic acid and isomasticadienonic acid is rather low. In summary, I observed for all the tested mastic constituents selectivity for 11β-HSD1 over 11β-HSD2 *in vitro* with low micromolar IC_{50} values.

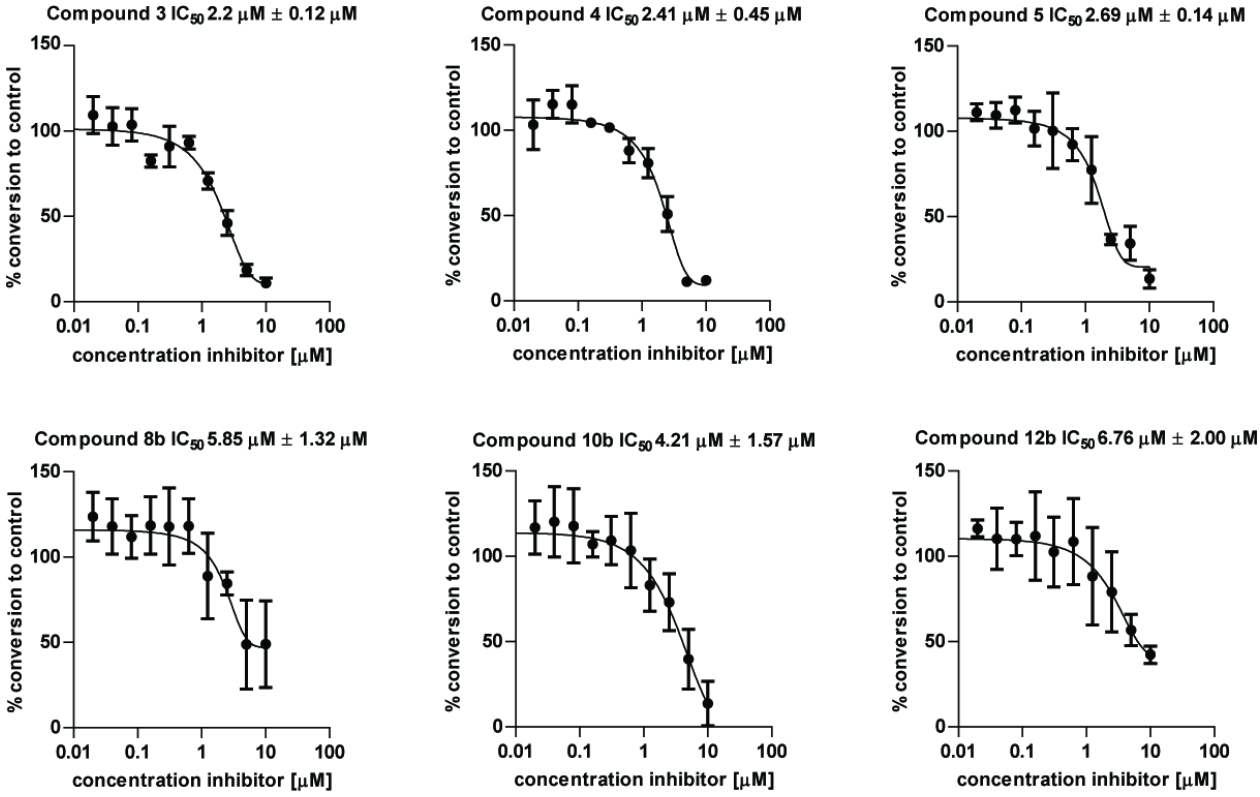

Figure 4: IC_{50} of 11β-HSD2 incubated with progesterone derivatives (Lysates of HEK293 cells expressing recombinant 11β-HSD2 were incubated 10 min at 37 °C in the presence of 50 nM cortisol and 500 µM NAD^+, followed by determination of amount of product formed). Results represent mean ± SD and are derived from three independent experiments.

However, 11β-HSD1 inhibitors have already been developed by several pharmaceutical companies and most of the compounds have high selectivity for 11β-HSD1 over 11β-HSD2 in the low nanomolar range [41]. Clinical studies showed that 11β-HSD1 inhibitors are safe and novel agents for the treatment of type 2 diabetes and metabolic syndrome. Nevertheless, the adverse effects of mastic gum should be evaluated before pharmaceutical use, since the plant extract has been linked to allergic contact dermatitis in humans and increased liver weight in rats [42, 43]. An evaluation of risk-benefit effect of mastic gum compared to other drugs needs to be carried out to validate its potential as a pharmaceutical product. Additionally, possible adverse effects, such as the effect of 11β-HSD1 inhibition on the innate immune response or the negative feedback to the HPA axis, will require careful monitoring during clinical development. In addition, the homology between 11β-HSD1 and other enzymes of the SDR family might lead to non-selective effects [44]. For example, inhibition of the 17β-HSDs may affect sex steroid metabolism and therefore cause abnormalities [45]. Non-Selective inhibition of "orphan" SDR DHRS7, identified as a tumor suppressor in this thesis, is also critical, since it may increase the aggressive potential of cells, which may aid cancer progression. Besides the side effects, the response of the patients is important for the use of 11β-HSD1 inhibitors in therapy. In several phase II studies the response has been observed as heterogeneous and therefore requires the development of pharmacodynamic biomarkers to identify likely 'responders' [45]. Nevertheless, the potential of mastix gum to inhibit 11β-HSD1 may in combination with other mechanisms, contribute to the antidiabetic and anti-inflammatory effects of mastic gum [30]. To evaluate new molecular mechanisms and the pharmacological synergy between several compounds associated with the effects of mastic gum further experiments need to be performed. In the second study, the effects of 11β-aminoprogesterone derivatives were evaluated in cell lysates *in vitro*. In contrast to the mastic gum project this study focused on the inhibition of 11β-HSD2 and MR transactivation. Six of the tested progesterone derivatives showed selective inhibition of 11β-HSD2 over 11β-HSD1 in a preliminary screening (Figure 2 in the publication). While all compounds showed low micromolar IC_{50} values, the highest inhibiting potential was obtained for compound 3, which showed an IC_{50} of 2.2 μM (Figure 4). Compared to glycyrrhetinic acid, which is a nonselective inhibitor for 11β-HSD isozymes but exhibits an IC_{50} of 30 nM for 11β-HSD2 in HEK293 lysates, the newly synthetized compounds have weak inhibiting potential, though possess greater binding to 11β-HSD2 over 11β-HSD1 [46].

This study forms a basis for the development of 11β-aminoprogesterone derivatives, which possess more selective effects on 11β-HSD2 effects compared to their lead compound progesterone and thus may have positive effects in hemodialysis patients suffering from hyperkalemia or in patients with colon cancer. Improvement of the inhibitory potential may be achieved by the modulation of side groups. To ensure the inhibition of 11β-HSD2 in patients and avoid possible side effects occurring with MR targeting in the kidney, it would be an asset if newly designed compounds act locally in the gastrointestinal tract. Further studies *in vitro* and *in vivo* need to be performed to accentuate the potential of 11β-aminoprogesterone derivatives.

Publication: Selective inhibition of 11β-HSD1 by masticadienonic acid and isomasticadienonic acid – constituents of *Pistacia lentiscus* oleoresin as promising antidiabetic drugs

Pistacia lentiscus Oleoresin: Virtual Screening and Identification of Masticadienonic and Isomasticadienonic Acids as Inhibitors of 11β-Hydroxysteroid Dehydrogenase 1

Authors Anna Vuorinen[1], Julia Seibert[2], Vassilios P. Papageorgiou[3], Judith M. Rollinger[4], Alex Odermatt[2], Daniela Schuster[1], Andreana N. Assimopoulou[3]

Affiliations The affiliations are listed at the end of the article

Key words
- *Pistacia lentiscus*
- Anacardiaceae
- 11β-hydroxysteroid dehydrogenase
- virtual screening
- antidiabetic
- diabetes

Abstract

In traditional medicine, the oleoresinous gum of *Pistacia lentiscus* var. *chia*, so-called mastic gum, has been used to treat multiple conditions such as coughs, sore throats, eczema, dyslipidemia, and diabetes. Mastic gum is rich in triterpenes, which have been postulated to exert antidiabetic effects and improve lipid metabolism. In fact, there is evidence of oleanonic acid, a constituent of mastic gum, acting as a peroxisome proliferator-activated receptor γ agonist, and mastic gum being antidiabetic in mice *in vivo*. Despite these findings, the exact antidiabetic mechanism of mastic gum remains unknown. Glucocorticoids play a key role in regulating glucose and fatty acid metabolism, and inhibition of 11β-hydroxysteroid dehydrogenase 1 that converts inactive cortisone to active cortisol has been proposed as a promising approach to combat metabolic disturbances including diabetes. In this study, a pharmacophore-based virtual screening was applied to filter a natural product database for possible 11β-hydroxysteroid dehydrogenase 1 inhibitors. The hit list analysis was especially focused on the triterpenoids present in *Pistacia* species. Multiple triterpenoids, such as masticadienonic acid and isomasticadienonic acid, main constituents of mastic gum, were identified. Indeed, masticadienonic acid and isomasticadienonic acid selectively inhibited 11β-hydroxysteroid dehydrogenase 1 over 11β-hydroxysteroid dehydrogenase 2 at low micromolar concentrations. These findings suggest that inhibition of 11β-hydroxysteroid dehydrogenase 1 contributes to the antidiabetic activity of mastic gum.

Abbreviations

AR:	aromatic ring
11β-HSD:	11β-hydroxysteroid dehydrogenase
GR:	glucocorticoid receptor
H:	hydrophobic area
HBA:	hydrogen bond acceptor
HBD:	hydrogen bond donor
H6PDH:	hexose-6-phosphate dehydrogenase
M:	metal binding area
MR:	mineralocorticoid receptor
NI:	negative ionizable group
PDB:	Protein Data Bank
PI:	positive ionizable group
PPARγ:	peroxisome proliferator-activated receptor γ
XVOL:	exclusion volume

received July 7, 2014
revised January 15, 2015
accepted January 26, 2015

Bibliography
DOI http://dx.doi.org/10.1055/s-0035-1545720
Published online
Planta Med © Georg Thieme Verlag KG Stuttgart · New York · ISSN 0032-0943

Correspondence
Andreana Assimopoulou
Department of Chemical Engineering
Aristotle University of Thessaloniki
Egnatia Street, AUTH Campus
54124 Thessaloniki
Greece
Phone: + 30 23 10 99 42 42
adreana@eng.auth.gr

Introduction

Pistacia lentiscus var. *chia* (Anacardiaceae family) is a tree that grows exclusively on the Greek island Chios. It is mainly exploited for its oleoresinuous gum, the so-called mastic gum [1]. This oleoresin is harvested in a traditional way by longitudinal incisions from the tree as tears or droplets, although an alternative technique called liquid collection has also been applied. In the latter method, the stimulating agent ethrel is used for resin excretion after incision of the tree to increase the mastic gum productivity. The gum harvested by this liquid method is produced in fluid form and has a characteristic odor [2]. In addition to controling cholesterol levels and combating diabetes, the oleoresin has been used for centuries against coughs, sore throats, eczema, stomachaches, kidney stones, pain, and rheumatism [3].

The medicinal effects of *P. lentiscus* are proposed to be caused by the secondary metabolite triterpenes that are found at high concentrations in both the acidic and neutral fractions of *Pistacia*

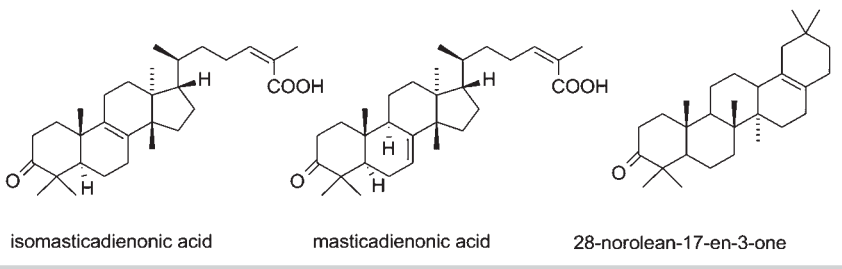

Fig. 1 Main constituents of *P. lentiscus* oleoresin (mastic gum).

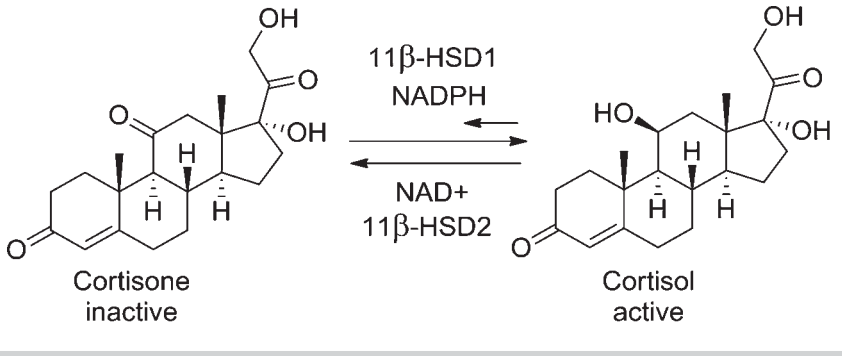

Fig. 2 Interconversion of cortisone to cortisol and vice versa by 11*β*-hydroxysteroid dehydrogenases.

oleoresins. Generally, the triterpenes are derivatives from 11 skeletons: Δ12-oleanene, Δ18-oleanene, 28-nor-Δ17-oleanene, Δ7-tirucallene, 24,25-dehydro-Δ7-tirucallene, Δ8-tirucallene, 24,25-dehydro-Δ8-tirucallene, dammarane, lupane, lupene, and Δ12-lupene [2]. The concentrations of different triterpenes vary with *Pistacia* species and the resin harvest method. The resin from *P. lentiscus* var. *chia* was found to contain 36 triterpenes when harvested in a traditional way and in the case of liquid harvesting, 26 different triterpenes were found [4]. The main constituents in both harvest methods are isomasticadienonic acid, masticadienonic acid, and 28-norolean-17-en-3-one (**Fig. 1**).

In traditional medicine, mastic gum has been used against diabetes, a complex condition where the organism does not respond normally to the absorbed glucose. This is caused either by decreased insulin production (type 1 diabetes) or by insulin resistance, impaired glucose intake, and gluconeogenesis (type 2 diabetes), leading to elevated blood glucose levels [5]. Modern Western medicine combats diabetes by direct insulin injections, insulin sensitizing therapy, or enhancing the insulin secretion. Except for direct insulin injections, the treatment of diabetes involves multiple targets that play a role in glucose intake, gluconeogenesis, insulin sensitivity, and insulin secretion [5]. Among these targets is PPARγ, which enhances insulin sensitivity and fatty acid storage upon activation [6]. In fact, oleanonic acid, a constituent of mastic gum, has been shown to activate PPARγ [7]. An *in vivo* study in rats indicated that daily consumption of mastic gum resulted in a 40% decrease of blood glucose levels in high-fat diet-fed rats that also received streptozotoxin injection according to a protocol that induced diabetes II [8]. In addition, the administration of mastic gum decreased blood glucose levels and improved serum fatty acid levels in diabetic mice [9]. Nevertheless, it is likely that these effects are not only mediated through PPARγ. Thus, to understand the *in vivo* effects of mastic gum, the compounds involved and the underlying mechanisms need to be explored.

One possible explanation for the antidiabetic effects of mastic gum could be an interference with glucocorticoid metabolism. Glucocorticoids regulate carbohydrate and fat metabolism by decreasing glucose uptake and utilization, as well as increasing gluconeogenesis in the liver [10]. By affecting lipolysis and fat distribution, glucocorticoids are associated with the development of dyslipidemia that is often related to type 2 diabetes, metabolic disorders, and Cushing's syndrome. Glucocorticoids act via GRs and MRs, and their intracellular, pre-receptor concentrations are dependent on 11*β*-HSDs (**Fig. 2**) [11]. 11*β*-HSD1 converts cortisone to its active hydroxyl derivative cortisol. This enzyme uses NADPH as a cofactor and the limiting factor of its cortisone-reducing activity is the coexpression with H6PDH that regenerates NADPH from $NADP^+$ [12, 13]. Therefore, *in vivo*, 11*β*-HSD1 acts predominantly as a reductase. In contrast, 11*β*-HSD2 is an NAD^+-dependent dehydrogenase responsible for the oxidative inactivation of cortisol to cortisone [14]. 11*β*-HSD1 is highly expressed in the liver, adrenals, adipose tissue, and skeletal muscles [15], whereas 11*β*-HSD2 is found in the kidneys, colon, and placenta [11, 16].

Since circulating cortisol levels (corticosterone in rodents) affect glucose and lipid metabolism, 11*β*-HSD1 is considered a promising intervention point to treat type 2 diabetes and metabolic disorders [17, 18]. In fact, this hypothesis is supported by biological data; the overexpression of 11*β*-HSD1 in adipose tissue in mice has been shown to cause visceral obesity, hyperglycemia, insulin resistance, and increased serum fatty acid and triglyceride levels [19]. Additionally, high corticosterone concentrations found only in the liver do not cause obesity or central adiposity, but instead cause steatosis, dyslipidemia, hypertension, and mild insulin resistance [20]. 11*β*-HSD1 knockout mice were shown to have an increased adrenal corticosterone production as a result of the impaired hepatic regeneration of active glucocorticoids, and they resisted obesity- or stress-related hyperglycemia [21]. Moreover, 11*β*-HSD1 inhibitors have been shown to improve several meta-

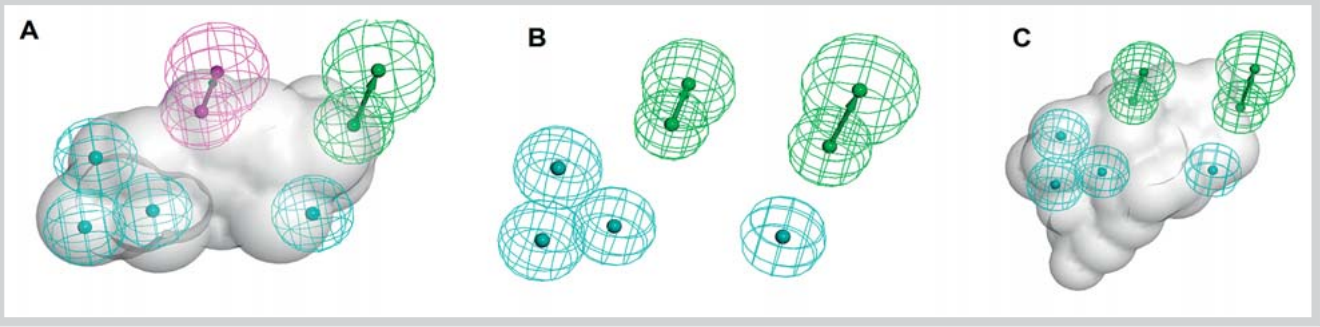

Fig. 3 Pharmacophore models for 11β-hydroxysteroid dehydrogenase 1 inhibition. The original model (**A**), intermediate refined model (**B**), and the final refined model that was used for virtual screening (**C**). The pharmacophore features are color-coded: hydrophobic – cyan, hydrogen bond donor – magenta, hydrogen bond acceptor – green, shape – gray. (Color figure available online only.)

bolic parameters as well as atherosclerosis in mice by decreasing aortic lesions [17,22]. Thus, 11β-HSD1 inhibitors constitute a promising way to treat metabolic syndrome and type 2 diabetes in rodent models. However, when inhibiting 11β-HSD1, selectivity over 11β-HSD2 is important to avoid adverse effects such as severe hypokalemia, hypertension, edema formation, and renal enlargement, which are all consequences of cortisol-dependent MR activation [23].

There is a large number of known 11β-HSD1 inhibitors, mostly small synthetic chemicals [24–26]. In addition, compounds from natural origin have been shown to inhibit 11β-HSD1. Most of these natural compounds are triterpenes, such as corosolic acid, ursolic acid, glycyrrhetinic acid, and its derivatives [27,28]. Because mastic gum is rich in triterpenes, the inhibition of 11β-HSD1 could be one explanation for the observed antidiabetic effects of mastic gum. To test this hypothesis, a virtual screening campaign to search for 11β-HSD1 inhibitors from natural origin was launched. In virtual screening, a database of compounds is filtered to match the query requirements, and it has been considered a suitable tool for setting biological testing priorities also in the natural products field [29,30]. One common way to perform virtual screening is the pharmacophore-based method. In this method, pharmacophore models representing the 3D arrangement of those electrostatic and steric functionalities that make the small molecule active towards its target protein [31] are used as a filter. Pharmacophore models consist of features such as hydrogen bond acceptor (HBA)/hydrogen bond donor (HBD), hydrophobic areas (H), aromatic rings (AR), positively ionizable (PI) and negatively ionizable (NI) groups, as well as metal binding areas (M). Exclusion volumes (XVOLs) – forbidden areas – or a shape can be added to mimic the size and the shape of the binding pocket or active ligands. The result of a virtual screening is a so-called hit list that contains those compounds which chemical functionalities match with the features of the query pharmacophore. These compounds are predicted to be active towards the target.

To support drug development and to discover new 11β-HSD1 inhibitors, a pharmacophore model for 11β-HSD1 inhibition has been developed and reported [32]. This pharmacophore model consisted of six chemical features: four Hs, one HBA, one HBD, and a shape (**Fig. 3A**). The model was theoretically and experimentally successfully validated and used for virtual screening campaigns. However, during the recent years, new 11β-HSD1 inhibitors have been rapidly reported, and the pharmacophore model needed improvement to ensure the best performance. Therefore, it was refined according to the newly published 11β-HSD1 inhibitors to better represent the current state of knowledge. First, the HBD function of the original model was exchanged with an HBA, and the shape restriction was removed (**Fig. 3B**). However, this model was not very restrictive, and therefore, as a further refinement step, a new shape restriction was added (**Fig. 3C**) [33]. This refined model, which was named model 4_{new} in its original publication [33], was employed for the virtual screening of a natural compound database to test the theory of *P. lentiscus* oleoresin constituents as 11β-HSD1 inhibitors prior to *in vitro* testing.

Results

In order to search for natural compounds with antidiabetic activity, especially focusing on the constituents of *P. lentiscus*, a pharmacophore-based virtual screening of the DIOS natural product database was performed. The DIOS database is an in-house database comprising 9676 secondary metabolites from 800 medicinal plants described by Dioscorides in his *De Materia Medica* [34]. The refined 11β-HSD1 model (**Fig. 3C**) returned 305 hits from the virtual screening. The hit list contained 155 terpenes, including 96 triterpenes, among which 27 were from *Pistacia* species and 8 were *P. lentiscus* constituents (**Fig. 4**). Other frequent classes were lipids and flavonoids with 30 and 28 compounds, respectively. Mostly, the triterpenes present in *Pistacia* species were derivatives of masticadienonic and isomasticadienonic acids. The focus of the biological evaluation was set on the whole resin, its acidic fraction containing mainly the above triterpenes, and on purified compounds. Among the eight virtual hits obtained from the species *P. lentiscus,* almost all of them belong to the acidic fraction that was isolated from *P. lentiscus* var. *chia* oleoresin. The two main constituents masticadienonic acid and isomasticadienonic acid were chosen for biological evaluation. The other virtual hits, masticadienolic acid and oleanolic acid, have previously been reported as constituents of *P. lentiscus* var. *chia* [35]; however, they were not detected in the resin batch that was used for biological evaluation [4] and could therefore not be tested. The remaining four hits were excluded because these were not constituents of the *P. lentiscus* var. *chia*, although they were commonly found in *P. lentiscus* L.

After harvesting and isolating the substances of interest, their inhibitory activity against 11β-HSD1 and 11β-HSD2 was tested in lysates of cells expressing the corresponding recombinant human

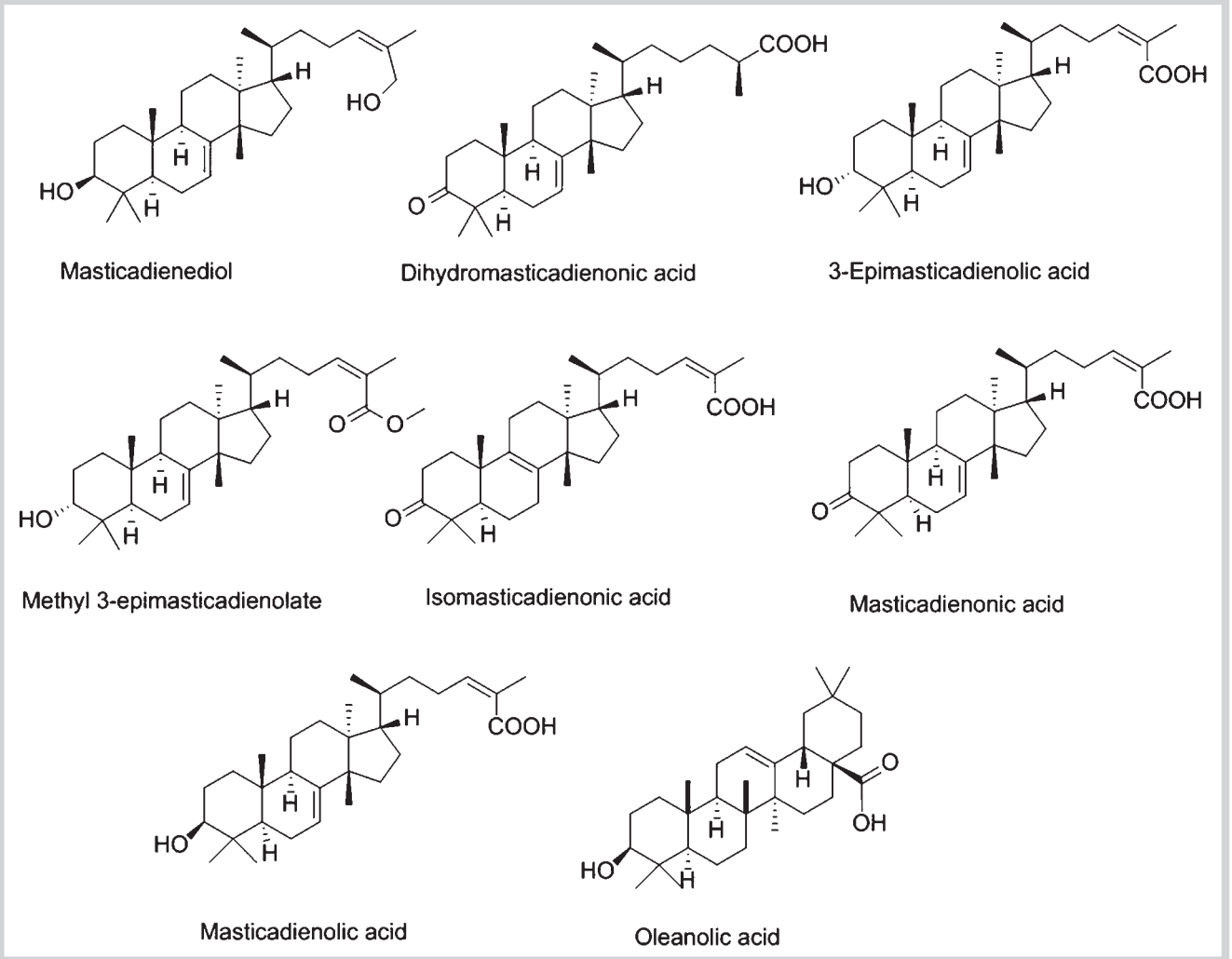

Fig. 4 *P. lentiscus* constituents found by virtual screening.

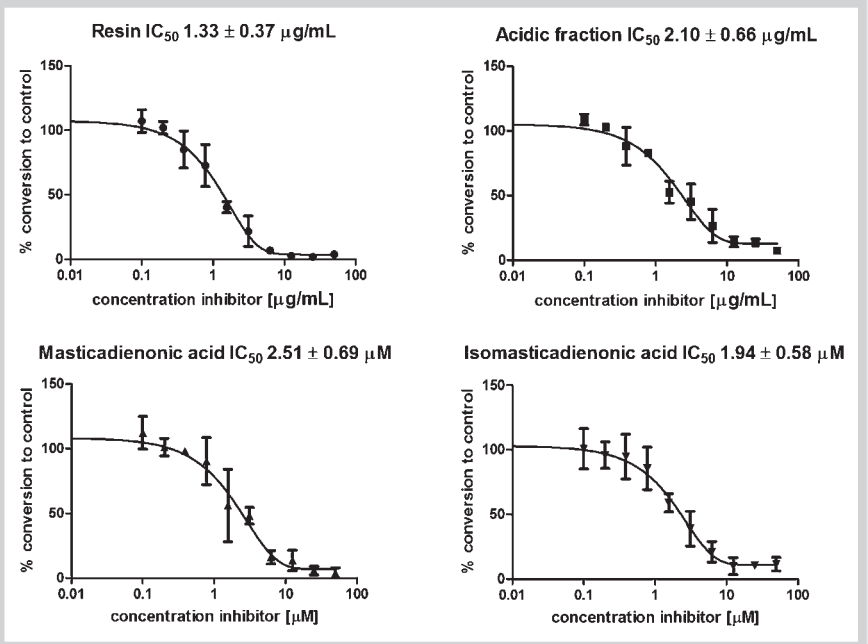

Fig. 5 Activities of *P. lentiscus* var. *chia* oleoresin, acidic fraction, masticadienonic, and isomasticadienonic acids in lysed cells expressing 11β-hydroxysteroid dehydrogenase 1.

enzyme. All four probes, the oleoresin, the acidic fraction of the gum, masticadienonic acid, and isomasticadienonic acid dose-dependently inhibited 11β-HSD1 (**Fig. 5**), but, importantly, not 11β-HSD2 (data not shown). As expected, the oleoresin that contained all the triterpenes turned out to be a potent 11β-HSD1 inhibitor with an IC_{50} value of 1.33 µg/mL, whereas the acidic fraction, containing all the acidic triterpenes, had an IC_{50} of 2.10 µg/mL. Masticadienonic acid and isomasticadienonic acid had IC_{50} values of 2.51 µM and 1.94 µM, respectively. In contrast, the non-selective reference compound glycyrrhetinic acid inhibited 11β-HSD1 and 11β-HSD2 with IC_{50} values of 0.68 ± 0.17 µM and 0.26 ± 0.07 µM, respectively, in line with previously published data [28].

To evaluate how masticadienonic acid and isomasticadienonic acid bind to 11β-HSD1 and to estimate their mechanism of action, they were docked into the respective binding pocket. Both of them aligned well with each other and with the cocrystallized ligand carbenoxolone (**Fig. 6A**). They did not form hydrogen bonds with the catalytic residues, but occupied the binding site, thus preventing the natural ligand from binding. Masticadienonic acid was anchored to the binding site with hydrophobic interactions and with a hydrogen bond with the backbone nitrogen of Leu217 (**Fig. 6B**). Isomasticadienonic acid was proposed to bind similarly to the binding pocket, but it also formed a hydrogen bond with the cofactor NADPH (**Fig. 6C**).

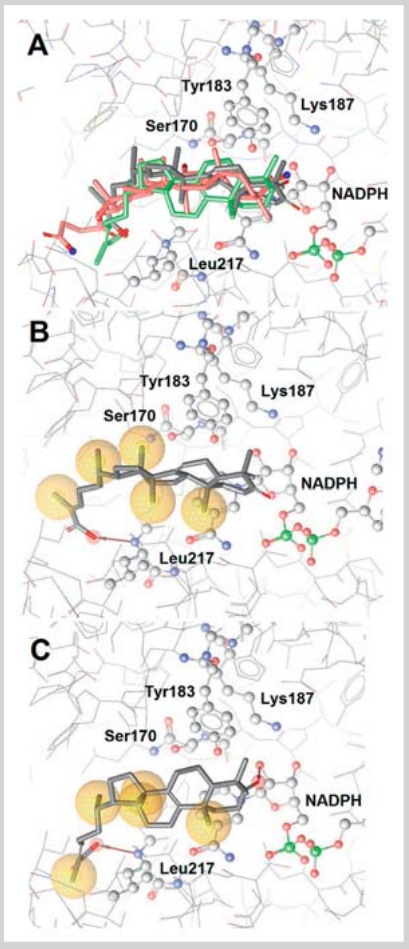

Fig. 6 Predicted binding orientations of masticadienonic and isomasticadienonic acids in the 11β-hydroxysteroid dehydrogenase 1 ligand binding site. Masticadienonic acid (red) and isomasticadienonic acid (green) occupy the same space in the binding pocket compared to the cocrystallized ligand carbenoxolone (gray) (**A**). Masticadienonic acid (**B**) was anchored to the binding pocket with hydrophobic interactions, hydrogen bonds with Leu217, whereas isomasticadienonic acid (**C**) forms an additional hydrogen bond with the cofactor NADPH. Hydrophobic interactions are shown as yellow spheres and hydrogen bonds as red arrows. The catalytic triad Ser-Tyr-Lys, the cofactor, and Leu217 are depicted in ball-and-stick style. (Color figure available online only.)

Discussion

In this study, a pharmacophore-based virtual screening of the natural compound database DIOS was performed. As a virtual screening filter, a previously published and refined pharmacophore model for 11β-HSD1 inhibitors was used. The model successfully recognized triterpenes, from which the majority was from *Pistacia* species. The biological evaluation of the mastic gum oleoresin and its constituents supported the hypothesis of 11β-HSD1 being one of the targets involved in the antidiabetic activity of mastic gum. To support the biological findings, binding orientations for masticadienonic acid and isomasticadienonic acid were predicted. The predicted binding modes were compared with corosolic acid (docking studies reported by Rollinger et al. [27]) and the cocrystallized ligand carbenoxolone. Isomasticadienonic and masticadienonic acids did not have the similar flipped binding orientation predicted for corosolic acid. However, their binding orientations and observed hydrogen bonds with Leu217 and the cofactor as well as the hydrophobic interactions are comparable with those of carbenoxolone. Therefore, masticadienonic and isomasticadienonic acids are suggested to act as competitive 11β-HSD1 inhibitors, like carbenoxolone.

The findings of this study show that the oleoresin of *P. lentiscus* (mastic gum), and especially masticadienonic and isomasticadienonic acids, target 11β-HSD1, which may contribute to a lowered blood glucose and improved serum fatty acids concentrations that have been observed in earlier reports on the treatment of diabetic mice with mastic gum [9]. Moreover, moronic acid, one of the triterpenes present in mastic gum [4], has been shown to exert antihyperglycemic properties in rats and to be a weak 11β-HSD1 inhibitor *in vitro* (22% enzyme inhibition at the concentration of 10 µM) [36]. Other triterpenes with a Δ12-oleanene skeleton, such as oleanolic acid, which was also found as a virtual hit, and its derivatives, have been proven to inhibit 11β-HSD1 with high nanomolar IC_{50} values [37]. However, the activity of oleanonic acid, a mastic gum constituent, is to the best of our knowledge unknown.

There are several studies reporting natural compounds as 11β-HSD1 inhibitors with the potential to be antidiabetic drugs. Nevertheless, most of them, like glycyrrhetinic acid and curcumin, also inhibit 11β-HSD2 and may therefore not be suitable for diabetes treatment [38,39]. Other compounds like flavonone and its derivatives selectively inhibited 11β-HSD1, however, they are rather weak inhibitors [40].

Several constituents of mastic gum acting on the same or different targets could provide an explanation for the antidiabetic actions of mastic gum, such as masticadienonic, isomasticadienonic, and moronic acids inhibiting 11β-HSD1, as well as oleanonic acid activating PPARγ. However, of these compounds, masticadienonic and isomasticadienonic acids are the most potent, experimentally confirmed 11β-HSD1 inhibiting constituents from mastic gum. In addition, at a concentration of 200 µM, oleanonic acid caused a 13-fold activation of PPARγ, whereas masticadienonic and isomasticadienonic acids inhibited 50% of the 11β-HSD1 activity at concentrations of about 2 µM. Based on the previously performed quantification study using an GC-MS technique, these two bioactive compounds (masticadienonic and isomasticadienonic acids) account for 3.4 and 8.9% w/w in mastic gum oleoresin, respectively [4]. Thus, even at low mastic gum concentrations, the pronounced 11β-HSD1 inhibition of these two main constituents as well as probably further contributing congeners may be the main reason for the oleoresin's antidiabetic effects. However, it is currently not clear whether additional

targets are also involved which warrant further studies on the molecular mechanism of the constituents of this traditionally used herbal remedy.

In addition to the explanation for the antidiabetic effects of mastic gum, the findings of this study form an excellent basis for the discovery of new 11β-HSD1 inhibitors from a natural origin. The pharmacophore model has proven it is able to enrich active natural compounds from a large database by identifying masticadienonic and isomasticadienonic acids as new selective 11β-HSD1 inhibitors from natural sources.

Materials and Methods

Virtual screening

For the virtual screening, the DIOS database was composed with the Build 3D database tool of DiscoveryStudio 3.0 (2005–2010 Accelrys Software, Inc.). The database was generated with Best settings and a maximum of 255 conformations per molecule. The pharmacophore model for 11β-HSD1 inhibition was obtained from our pharmacophore model collection. The detailed pharmacophore generation and refinement were described by Schuster et al. [32] and Vuorinen et al. [33]. Briefly, Schuster et al. developed a ligand-based pharmacophore model for 11β-HSD1 inhibitors. The model was trained to enrich the active substances from a set of active and inactive compounds, used for virtual screening, and successfully experimentally validated. During the last years, a vast number of new 11β-HSD1 inhibitors have been developed, and the model needed refinement in order to maintain a good predictive power. The final pharmacophore model used in this present study is a refined version of the model published by Schuster et al. The virtual screening of the DIOS database was performed with the Search 3D database tool of DiscoveryStudio 3.0 (2005–2010 Accelrys Software, Inc.) with Best settings.

Preparation of samples

P. lentiscus var. *chia* oleoresin collected traditionally (crude, large tears) was kindly provided by the Mastic Gum Growers Association (Chios, Greece). The acidic fraction (NaOH) of *P. lentiscus* var. *chia* was isolated as described in [4] after fractionation of the crude *P. lentiscus* var. *chia* oleoresin. Masticadienonic acid and isomasticadienonic acid were isolated by semipreparative HPLC-DAD (Dionex summit – preparative HPLC system) from the acidic fraction of *P. lentiscus* var. *chia* (as prepared above) as described in [41]; their purity was determined by HPLC-DAD also as described in [41]. Their structures were identified by spectroscopic (1D and 2D NMR) and analytical methods (HPLC-MS) (as shown in [41]), and additionally by comparison with published data [4]. All solvents used in this study were LC-MS grade and supplied by Merck.

Biological evaluation

Inhibition of 11β-HSD enzyme activity was performed as described earlier [28]. HEK-293 cells stably expressing human 11β-HSD1 or 11β-HSD2 were harvested by trypsination, followed by centrifugation. The resulting cell pellets were frozen and stored at −80 °C. For the experiments, cell pellets were suspended in TS2 buffer (100 mM NaCl, 1 mM EGTA, 1 mM EDTA, 1 mM $MgCl_2$, 250 mM sucrose, 20 mM Tris-HCl, pH 7.4), sonicated, and immediately used for the activity assay. Cell lysates were incubated for 10 min at 37 °C in a final volume of 22 µL containing either vehicle (0.2% methanol) or the corresponding inhibitor. Glycyrrhetinic acid (Sigma-Aldrich, article G10105, 97% assay purity) was used as a reference compound [28]. Inhibitors were diluted in TS2 buffer from stock solutions (10 mg/mL or 10 mM in methanol). To measure 11β-HSD1 activity, the reaction mixture contained 200 nM [1,2-^{3}H]cortisone and 500 µM NADPH. 11β-HSD2 activity was measured similarly at a final concentration of 50 nM [1,2,6,7-^{3}H] cortisol and 500 µM NAD^+. Reactions were stopped by adding an excess of unlabeled cortisone and cortisol (2 mM each, in methanol). Steroids were separated by TLC, followed by scintillation counting and calculation of the substrate conversion compared to the methanol control. Data were obtained from three independent experiments.

Docking

Masticadienonic acid and isomasticadienonic acid were drawn with ChemBioDraw Ultra 12.0 (1986–2010 CambridgeSoft), and 3D structures were obtained using PipelinePilot (2010 Accelrys Software, Inc.). The X-ray crystal structure of 11β-HSD1 was downloaded from the PDB (www.pdb.org [42]). For 11β-HSD1, the PDB entry 2 BEL [43] was chosen because it is cocrystallized with carbenoxolone, a ligand that is structurally similar to the triterpenoid mastic gum compounds. The docking was performed using GOLD [44,45]. This program uses a genetic algorithm for creating low-energy binding orientations for small molecules into the binding pocket of a protein. The binding site was defined as an 8 Å sphere, centered on the hydroxyl-oxygen of Ser170 (x 3.84; y 22.49; z 13.34). ChemPLP was selected as a scoring function, and the program was allowed to terminate the docking run in case the three best-scored binding orientations were located similarly in the binding site. To ensure acceptable ligand flexibility, the program was set to flip ring corners when exploring the binding orientations. Atom types for the protein and for the ligand were defined by the program. These docking settings were validated by redocking the original ligand, carbenoxolone, for a correct reproduction of the binding mode obtained by crystallography.

Acknowledgements

A.V. is a recipient of a ÖAW DOC grant at the Institute of Pharmacy, University of Innsbruck, Austria. This work was supported by the Swiss National Science Foundation (31 003A_140 961) to A.O., who has a Chair for Molecular and Systems Toxicology by the Novartis Research Foundation. D.S. thanks the Erika Cremer habilitation program of the University of Innsbruck for financial support. A.N.A. and V.P.P. thank Mastic Gum Growers Association (Chios, Greece) for providing samples of *P. lentiscus* var. Chia oleoresin.

Conflict of Interest

The authors declare no conflict of interest.

Affiliations

[1] Institute of Pharmacy/Pharmaceutical Chemistry and Center for Molecular Biosciences Innsbruck (CMBI), Computer Aided Molecular Design Group, University of Innsbruck, Innsbruck, Austria
[2] Department of Pharmaceutical Sciences, Division of Molecular and Systems Toxicology, University of Basel, Basel, Switzerland
[3] Department of Chemical Engineering, Aristotle University of Thessaloniki, Thessaloniki, Greece
[4] Department of Pharmacognosy, Faculty of Life Sciences, University of Vienna, Vienna, Austria

References

1 *Browicz K. Pistacia lentiscus* cv. *chia* (Anacardiaceae) on Chios island. Plant Syst Evol 1987; 155: 189–195
2 *Assimopoulou AN, Papageorgiou VP.* Oleoresins from *Pistacia* species: chemistry and biology. In: Govil JN, Singh VK, Siddiqui NT, editors. Recent progress in medicinal plants natural product II. Houston: Studium Press, LLC; 2007: 145–202
3 *Bozorgi M, Memariani Z, Mobli M, Salehi Surmaghi MH, Shams-Ardekani MR, Rahimi R.* Five *Pistacia* species (*P. vera, P. atlantica, P. terebinthus, P. khinjuk*, and *P. lentiscus*): a review of their traditional uses, phytochemistry, and pharmacology. TheScientificWorldJo 2013; 2013: 1–33
4 *Assimopoulou AN, Papageorgiou VP.* GC-MS analysis of penta- and tetracyclic triterpenes from resins of *Pistacia* species. Part I. *Pistacia lentiscus* var. *chia*. Biomed Chromatogr 2005; 19: 285–311
5 *Rang HP, Dale MM, Ritter JM, Moore PK.* The endocrine pancreas and the control of blood glucose. In: Hunter L, editor. Pharmacology. 5th edition. London: Churchill Livingstone; 2003: 380–393
6 *Berger J, Moller DE.* The mechanisms of action of PPARs. Annu Rev Med 2002; 53: 409–435
7 *Petersen RK, Christensen KB, Assimopoulou AN, Fretté X, Papageorgiou VP, Kristiansen K, Kouskoumvekaki I.* Pharmacophore-driven identification of PPARγ agonists from natural sources. J Comput Aided Mol Des 2011; 25: 107–116
8 *Kokolakis AK.* Analysis and study of the biological activity of the constituents of the resin from the plant *Pistacia lentiscus* var. *chia* (Chios mastic gum) [Master Thesis]. Heraklion: University of Crete; 2008
9 *Georgiadis I, Karatzas T, Korou LM, Agrogiannis G, Vlachos IS, Pantopoulou A, Tzanetakou IP, Katsilambros N, Perrea DN.* Evaluation of Chios mastic gum on lipid and glucose metabolism in diabetic mice. J Med Food 2014; 17: 393–399
10 *Rang HP, Dale MM, Ritter JM, Moore PK.* The pituitary and adrenal cortex. In: Hunter L, editor. Pharmacology. 5th edition. London: Churchill Livingstone; 2003: 409–427
11 *Krozowski Z.* The 11*β*-hydroxysteroid dehydrogenases: functions and physiological effects. Mol Cell Endocrinol 1999; 151: 121–127
12 *Atanasov AG, Nashev LG, Schweizer RAS, Frick C, Odermatt A.* Hexose-6-phosphate dehydrogenase determines the reaction direction of 11*β*-hydroxysteroid dehydrogenase type 1 as an oxoreductase. FEBS Lett 2004; 571: 129–133
13 *Bánhegyi G, Benedetti A, Fulceri R, Senesi S.* Cooperativity between 11*β*-hydroxysteroid dehydrogenase type 1 and hexose-6-phosphate dehydrogenase in the lumen of the endoplasmic reticulum. J Biol Chem 2004; 279: 27017–27021
14 *Arnold P, Tam S, Yan L, Baker ME, Frey FJ, Odermatt A.* Glutamate-115 renders specificity of human 11*β*-hydroxysteroid dehydrogenase type 2 for the cofactor NAD+. Mol Cell Endocrinol 2003; 201: 177–187
15 *Ricketts ML, Verhaeg JM, Bujalska I, Howie AJ, Rainey WE, Stewart PM.* Immunohistochemical localization of type 1 11*β*-hydroxysteroid dehydrogenase in human tissues. J Clin Endocrinol Metab 1998; 83: 1325–1335
16 *Odermatt A, Kratschmar DV.* Tissue-specific modulation of mineralocorticoid receptor function by 11*β*-hydroxysteroid dehydrogenases: An overview. Mol Cell Endocrinol 2012; 350: 168–186
17 *Gathercole LL, Lavery GG, Morgan SA, Cooper MS, Sinclair AJ, Tomlinson JW, Stewart PM.* 11*β*-Hydroxysteroid dehydrogenase 1: translational and therapeutic aspects. Endocr Rev 2013; 34: 525–555
18 *Grundy SM.* Metabolic syndrome pandemic. Arterioscler Thromb Vasc Biol 2008; 28: 629–636
19 *Masuzaki H, Paterson J, Shinyama H, Morton NM, Mullins JJ, Seckl JR, Flier JS.* A transgenic model of visceral obesity and the metabolic syndrome. Science 2001; 294: 2166–2170
20 *Paterson JM, Morton NM, Fievet C, Kenyon CJ, Holmes MC, Staels B, Seckl JR, Mullins JJ.* Metabolic syndrome without obesity: Hepatic overexpression of 11*β*-hydroxysteroid dehydrogenase type 1 in transgenic mice. Proc Natl Acad Sci U S A 2004; 101: 7088–7093
21 *Kotelevtsev Y, Holmes MC, Burchell A, Houston PM, Schmoll D, Jamieson P, Best R, Brown R, Edwards CRW, Seckl JR, Mullins JJ.* 11*β*-Hydroxysteroid dehydrogenase type 1 knockout mice show attenuated glucocorticoid-inducible responses and resist hyperglycemia on obesity or stress. Proc Natl Acad Sci U S A 1997; 94: 14924–14929
22 *Hermanowski-Vosatka A, Balkovec JM, Cheng K, Chen HY, Hernandez M, Koo GC, Le Grand CB, Li Z, Metzger JM, Mundt SS, Noonan H, Nunes CN, Olson SH, Pikounis B, Ren N, Robertson N, Schaeffer JM, Shah K, Springer MS, Strack AM, Strowski M, Wu K, Wu T, Xiao J, Zhang BB, Wright SD, Thieringer R.* 11*β*-HSD1 inhibition ameliorates metabolic syndrome and prevents progression of atherosclerosis in mice. J Exp Med 2005; 202: 517–527
23 *Kotelevtsev Y, Brown RW, Fleming S, Kenyon C, Edwards CRW, Seckl JR, Mullins JJ.* Hypertension in mice lacking 11*β*-hydroxysteroid dehydrogenase type 2. J Clin Invest 1999; 103: 683–689
24 *Barf T, Vallgårda J, Emond R, Häggström C, Kurz G, Nygren A, Larwood V, Mosialou E, Axelsson K, Olsson R, Engblom L, Edling N, Rönquist-Nii Y, Öhman B, Alberts P, Abrahmsén L.* Arylsulfonamidothiazoles as a new class of potential antidiabetic drugs. Discovery of potent and selective inhibitors of the 11*β*-hydroxysteroid dehydrogenase type 1. J Med Chem 2002; 45: 3813–3815
25 *Xu Z, Tice CM, Zhao W, Cacatian S, Ye YJ, Singh SB, Lindblom P, McKeever BM, Krosky PM, Kruk BA, Berbaum J, Harrison RK, Johnson JA, Bukhtiyarov Y, Panemangalore R, Scott BB, Zhao Y, Bruno JG, Togias J, Guo J, Guo R, Carroll PJ, McGeehan GM, Zhuang L, He W, Claremon DA.* Structure-based design and synthesis of 1,3-oxazinan-2-one inhibitors of 11*β*-hydroxysteroid dehydrogenase type 1. J Med Chem 2011; 54: 6050–6062
26 *Böhme T, Engel CK, Farjot G, Güssregen S, Haack T, Tschank G, Ritter K.* 1,1-Dioxo-5,6-dihydro-[4,1,2]oxathiazines, a novel class of 11*β*-HSD1 inhibitors for the treatment of diabetes. Bioorg Med Chem Lett 2013; 23: 4685–4691
27 *Rollinger JM, Kratschmar DV, Schuster D, Pfisterer PH, Gumy C, Aubry EM, Brandstötter S, Stuppner H, Wolber G, Odermatt A.* 11*β*-Hydroxysteroid dehydrogenase 1 inhibiting constituents from *Eriobotrya japonica* revealed by bioactivity-guided isolation and computational approaches. Bioorg Med Chem 2010; 18: 1507–1515
28 *Kratschmar DV, Vuorinen A, Da Cunha T, Wolber G, Classen-Houben D, Doblhoff O, Schuster D, Odermatt A.* Characterization of activity and binding mode of glycyrrhetinic acid derivatives inhibiting 11*β*-hydroxysteroid dehydrogenase type 2. J Steroid Biochem Mol Biol 2011; 125: 129–142
29 *Rollinger JM, Stuppner H, Langer T.* Virtual screening for the discovery of bioactive natural products. Prog Drug Res 2008; 65: 213–249
30 *Wolber G, Rollinger JM.* Virtual screening and target fishing for natural products using 3D pharmacophores. In: Jacoby E, editor. Computational chemogenomics. Boca Raton: Pan Stanford Publishing; 2013: 117–139
31 *Wermuth CG, Ganellin CR, Lindberg P, Mitscher LA.* Glossary of terms used in medicinal chemistry (IUPAC Recommendations). Pure Appl Chem 1998; 70: 1129–1143
32 *Schuster D, Maurer EM, Laggner C, Nashev LG, Wilckens T, Langer T, Odermatt A.* The discovery of new 11*β*-hydroxysteroid dehydrogenase type 1 inhibitors by common feature pharmacophore modeling and virtual screening. J Med Chem 2006; 49: 3454–3466
33 *Vuorinen A, Nashev LG, Odermatt A, Rollinger JM, Schuster D.* Pharmacophore model refinement for 11*β*-hydroxysteroid dehydrogenase inhibitors: search for modulators of intracellular glucocorticoid concentrations. Mol Inf 2014; 33: 15–25
34 *Rollinger JM, Steindl TM, Schuster D, Kirchmair J, Anrain K, Ellmerer EP, Langer T, Stuppner H, Wutzler P, Schmidtke M.* Structure-based virtual screening for the discovery of natural inhibitors for human rhinovirus coat protein. J Med Chem 2008; 51: 842–851
35 *Papageorgiou VP, Bakola-Christianopoulou MN, Apazidou KK, Psarros EE.* Gas chromatographic-mass spectroscopic analysis of the acidic triterpenic fraction of mastic gum. J Chromatogr A 1997; 769: 263–273
36 *Ramírez-Espinosa JJ, García-Jiménez S, Rios MY, Medina-Franco JL, López-Vallejo F, Webster SP, Binnie M, Ibarra-Barajas M, Ortiz-Andrade R, Estrada-Soto S.* Antihyperglycemic and sub-chronic antidiabetic actions of morolic and moronic acids, *in vitro* and *in silico* inhibition of 11*β*-HSD 1. Phytomedicine 2013; 20: 571–576

37 *Blum A, Favia AD, Maser E.* 11β-Hydroxysteroid dehydrogenase type 1 inhibitors with oleanan and ursan scaffolds. Mol Cell Endocrinol 2009; 301: 132–136
38 *Hu GX, Lin H, Lian QQ, Zhou SH, Guo J, Zhou HY, Chu Y, Ge RS.* Curcumin as a potent and selective inhibitor of 11β-hydroxysteroid dehydrogenase 1: improving lipid profiles in high-fat-diet-treated rats. PLoS One 2013; 8: e49976
39 *Gaware R, Khunt R, Czollner L, Stanetty C, Cunha TD, Kratschmar DV, Odermatt A, Kosma P, Jordis U, Claßen-Houben D.* Synthesis of new glycyrrhetinic acid derived ring A azepanone, 29-urea and 29-hydroxamic acid derivatives as selective 11β-hydroxysteroid dehydrogenase 2 inhibitors. Bioorg Med Chem 2011; 19: 1866–1880
40 *Schweizer RAS, Atanasov AG, Frey BM, Odermatt A.* A rapid screening assay for inhibitors of 11β-hydroxysteroid dehydrogenases (11β-HSD): flavanone selectively inhibits 11β-HSD1 reductase activity. Mol Cell Endocrinol 2003; 212: 41–49
41 *Assimopoulou AN, Ganzera M, Stuppner H, Papageorgiou VP.* Determination of penta- and tetra- cyclic triterpenes in *Pistacia lentiscus* resin. Planta Med 2009; 75: PA37
42 *Berman HM, Westbrook J, Feng Z, Gilliland G, Bhat TN, Weissig H, Shindayalov IN, Bourne PE.* The Protein data bank. Nucleic Acids Res 2000; 28: 235–242
43 *Wu X, Kavanagh K, Svensson S, Elleby B, Hult M, Von Delft F, Marsden B, Jornvall H, Abrahamsen L, Oppermann U.* The high resolution structures of human, murine and guinea pig 11-beta-hydroxysteroid dehydrogenase type 1 reveal critical differences in active site architecture. DOI: 10.2210/pdb2bel/pdb; Available online: http://www.rcsb.org/pdb/explore.do?structureId=2bel
44 *Jones G, Willett P, Glen RC, Leach AR, Taylor R.* Development and validation of a genetic algorithm for flexible docking. J Mol Biol 1997; 267: 727–748
45 *Verdonk ML, Cole JC, Hartshorn MJ, Murray CW, Taylor RD.* Improved protein-ligand docking using GOLD. Proteins 2003; 52: 609–623

Publication: Synthesis of sterically encumbered 11β-aminoprogesterone derivatives and evaluation as 11β-hydroxysteroid dehydrogenase inhibitors and mineralocorticoid receptor antagonists.

Bioorganic & Medicinal Chemistry 21 (2013) 6274–6281

Contents lists available at ScienceDirect

Bioorganic & Medicinal Chemistry

journal homepage: www.elsevier.com/locate/bmc

Synthesis of sterically encumbered 11β-aminoprogesterone derivatives and evaluation as 11β-hydroxysteroid dehydrogenase inhibitors and mineralocorticoid receptor antagonists

Keyur Pandya [a,†], David Dietrich [a,†], Julia Seibert [b,†], John C. Vederas [a,*], Alex Odermatt [b,*]

[a] Department of Chemistry, University of Alberta, 11227 Saskatchewan Drive, Edmonton, Alberta T6G 2G2, Canada
[b] Swiss Center for Applied Human Toxicology and Division of Molecular and Systems Toxicology, Department of Pharmaceutical Sciences, University of Basel, Klingelbergstrasse 50, CH-4056 Basel, Switzerland

ARTICLE INFO

Article history:
Received 7 August 2013
Accepted 29 August 2013
Available online 7 September 2013

Keywords:
11Beta-hydroxysteroid dehydrogenase
Mineralocorticoid receptor
Inhibitor
Antagonist
Amino acid–steroid conjugates
Glucocorticoid

ABSTRACT

11β-Hydroxyprogesterone is a well-known nonselective inhibitor of 11β-hydroxysteroid dehydrogenase (11βHSD) types 1 and 2. It also activates the mineralocorticoid receptor (MR). Modulation of corticosteroid action by inhibition of 11βHSDs or blocking MR is currently under consideration for treatment of electrolyte disturbances, metabolic diseases and chronic inflammatory disorders. We established conditions to synthesize sterically demanding 11β-aminoprogesterone, which following subsequent nucleophilic or reductive amination, allowed extension of the amino group to prepare amino acid derivatives. Biological testing revealed that some of the 11β-aminoprogesterone derivatives selectively inhibit 11βHSD2. Moreover, two compounds that did not significantly inhibit 11βHSDs had antagonist properties on MR. The 11β-aminoprogesterone derivatives form a basis for the further development of improved modulators of corticosteroid action.

1. Introduction

Steroids play an important role in maintenance and regulation of various physiological functions. Specifically, the corticosteroids are essentially involved in the regulation of carbohydrate, lipid and protein metabolism, inflammation, and maintenance of water and electrolyte balance. Corticosteroids exert their effects mainly through glucocorticoid receptors (GR) and mineralocorticoid receptors (MR). A chemical hallmark of the endogenous glucocorticoids is the existence of inactive 11-oxosteroids and active 11β-hydroxysteroids that can be interconverted by 11β-hydroxysteroid dehydrogenases (11βHSDs) (Fig. 1).[1] Specifically, there are two isoforms, 11βHSD1 and 11βHSD2, that control tissue- and cell-specific concentrations of active glucocorticoids. 11βHSD1 predominantly catalyzes the reduction of oxosteroids to alcohols, while 11βHSD2 performs the reverse reaction.

Impaired corticosteroid action has been associated with cardiometabolic diseases such as hypertension, atherosclerosis, hyperlipidemia and diabetes as well as psychiatric disorders.[2] Transgenic mice overexpressing 11βHSD1 in adipose tissue develop all typical disturbances observed in metabolic syndrome.[3] Mice overexpressing 11βHSD1 specifically in the liver present with steatosis and rather mild insulin resistance but without obesity.[4] Based on these and additional animal data and clinical observations, inhibition of 11βHSD1-mediated glucocorticoid activation emerged as a promising strategy to treat metabolic diseases, including type 2 diabetes, hyperlipidemia, atherosclerosis and osteoporosis.

Since inhibition of 11βHSD2 in the kidney results in cortisol-induced MR activation with sodium and water retention and hypertension,[5] 11βHSD1 inhibitors used for treatment of metabolic diseases need to be highly selective. Although inhibition of 11βHSD2 needs to be avoided for these applications, it was recently suggested that 11βHSD2 inhibitors may be used to treat patients on hemodialysis in order to achieve potassium loss as a result of cortisol-induced MR activation in the colon,[6] and several glycyrrhetinic acid derived 11βHSD2 inhibitors were

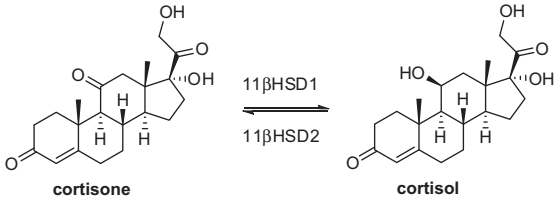

Figure 1. Biological equilibrium between cortisone and cortisol.

* Corresponding authors. Tel.: +1 780 492 5475; fax: +1 780 492 8231 (J.C.V.); tel.: +41 61 267 1530; fax: +41 61 267 1515 (A.O.).
E-mail addresses: john.vederas@ualberta.ca (J.C. Vederas), alex.odermatt@unibas.ch (A. Odermatt).
† These authors contributed equally to this study.

0968-0896/$ - see front matter © 2013 Elsevier Ltd. All rights reserved.
http://dx.doi.org/10.1016/j.bmc.2013.08.068

reported.[7–10] Due to frequent dialysis, sodium retention is limited in these patients.

Some of the adverse cardio-metabolic effects of corticosteroids are likely to be caused by increased activation of MR in cardiomyocytes, adipocytes and macrophage.[2] Excessive activation of MR by aldosterone or cortisol induces detrimental cardiovascular effects, and MR antagonists improved the morbidity and mortality of patients with myocardial infarction or heart failure.[11–13] Furthermore, MR antagonists showed promising results in the treatment of chronic kidney disease and diabetic nephropathy.[14–16] Thus, several pharmaceutical companies are currently developing novel MR antagonists.

Progesterone and some of its metabolites have been reported to bind to MR and inhibit 11βHSDs.[17–19] In the present project, we used 11α-hydroxyprogesterone as a starting point for the synthesis of several 11β-aminoprogesterone derivatives with the goal to identify potential 11βHSD inhibitors and MR antagonists. The lipophilicity of steroids has led chemists to introduce various chemical modifications that can improve their water solubility and bioavailability.[20] Aminosteroids and amino acid–steroid conjugates are commonly prepared to overcome these problems.[21,22] In an effort to obtain selective inhibitors of one of the 11βHSD isoforms, we synthesized a small library of aminosteroid and amino acid–steroid conjugates with the hopes of preparing inhibitors with improved solubility and bioavailability. Based on previous inhibition studies of 11β-hydroxyprogesterone (**1a**),[23] we chose to introduce amino and amino acid functionalities to the 11β-position of progesterone.

This class of molecules presents a synthetic challenge, as only limited examples of 11β substituted progesterone derivatives exist.[24–27] This is based on the steric demands that are introduced by the rigid steroid backbone, as well as the angular methyl groups attached to C10 and C13. Following the successful synthesis of these 11β-amino and amino acid progesterone derivatives, they were assessed for their potential to inhibit 11βHSD1 and 11βHSD2 as well as for their ability to modulate MR transcriptional activity.

2. Results and discussion

2.1. Synthesis

To access the sterically hindered 11β-aminoprogesterone backbone, we started from commercially available 11α-hydroxyprogesterone (**1b**). Attempts to introduce the amino functionality via a number of S_N2-type displacement reactions were unsuccessful. These include displacement via a Mitsunobu reaction with a DNs-protected glycine nucleophile and the Mitsunobu reaction with sodium azide as a nucleophile. In each of these cases the desired 11β-substituted product was not observed, and the major products isolated were a mixture of elimination products (these compounds were not fully purified or characterized). Finally, we followed the modified Mitsunobu protocol of Loibner and Zbiral[28] to synthesize 11β-azidoprogesterone (Scheme 1). Treatment of PPh_3, diethyl azodicarboxylate and phenol with freshly prepared hydrazoic acid[29] and 11α-hydroxyprogesterone (**1b**) gave azido product **2** in 42% yield. After several attempts at the reduction of **2**, it was found that use of a cobalt–boride reduction system[30,31] was optimal. Reduction of the azido species to provide 11β-aminoprogesterone (**3**) was achieved when **2** was refluxed in a $CoCl_2$–$NaBH_4$ mixture. It is important to note these conditions did not reduce the ketones at C3 or C20. Confirmation of the 11β-amino substitution was obtained by X-ray crystallographic analysis (Supplementary information). It should be noted that this represents an improved method to obtain this skeleton relative to that previously reported.[25,26]

To add functionality to the amino steroid, we synthesized a series of conjugates, as shown in Scheme 2. The glycine-functionalized derivative **5** was prepared by reaction of **3** with *t*-butyl bromoacetate, followed by acidic hydrolysis of the *t*-butyl ester. Alternatively, when **3** was treated with *o*-nosyl chloride, sulfonylated derivative **6** was obtained. Finally, we prepared the 3-(ethyl 2-hydroximino-propionate) derivative **7** by direct displacement with the corresponding bromide **13**.[32]

We propose that amino acid conjugates of steroids can provide an important handle that can be further functionalized with a variety of pharmacophores, or to improve water solubility. While derivatives **5** and **7** can provide this functionality, we also hoped to prepare derivatives where the steroid served as a 'side-chain' to an α-amino acid. We attempted to prepare these derivatives using protected α-amino acids bearing a leaving group at the β-position. In cases where the electrophile was not activated (β-bromoalanine), no product was observed. Also, 11β-aminoprogesterone did not alkylate activated aziridines, which have been used in the synthesis of lanthionine derivatives.[33,34]

These results led us to the conclusion that activated, sterically unencumbered electrophiles, such as those used in the synthesis of **4**–**7**, are required to overcome the steric demand that the 11β-aminoprogesterone skeleton provides.

To avoid the challenges of alkylation of **3**, we decided to use a reductive amination approach to increase the diversity of 11β-aminoprogesterone (Scheme 3). When **3** was treated with enantiomerically pure Garner's aldehyde, in the presence of methanol, acetic acid and $NaCNBH_3$, the protected amino–alcohol functionalized derivatives **8a** or **8b** were obtained in 60% yield.[35] It was found that when this reaction was run for longer times (greater than 3–4 h), epimerization at 2′ was observed.

While cooler temperatures and shorter reaction times avoided this problem the diastereomeric products could be separated following deprotection. The acetonide and Boc protecting groups of **8a** or **8b** were hydrolyzed in a warm solution of TFA and water to give amino alcohols **9a** and **9b**.

To convert these amino alcohols to amino acids, we first re-protected the amino group with Boc using standard conditions to yield **10a** or **10b**. Oxidation of these protected amino alcohols was successfully achieved using Jones oxidation conditions. At this point, any diastereomeric products that may have been generated during the reductive amination could be readily separated by silica gel chromatography. The final amino acid products, which are in essence γ-*N*-alkylated 2,3-diaminopropionate (Dap) derivatives, were obtained by TFA cleavage of the Boc protective group to give amino acids **12a** or **12b**.

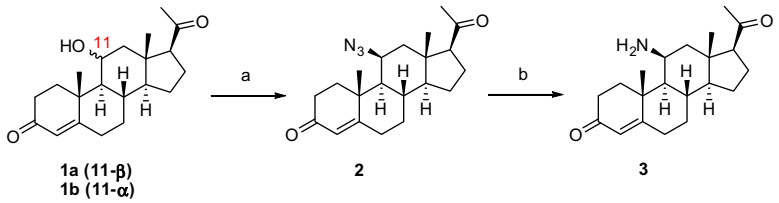

Scheme 1. Synthesis of 11β-aminoprogesterone. (a) PPh_3, diethyl azodicarboxylate, phenol, THF, followed by HN_3 and **1b** (42%); (b) $CoCl_2{\cdot}6H_2O$, $NaBH_4$, H_2O (62%).

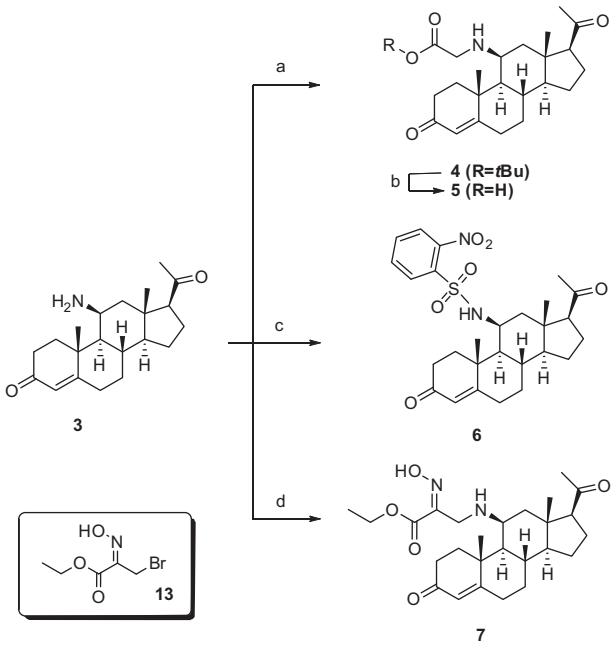

Scheme 2. Synthesis of amine substituted 11β-aminoprogesterone derivatives. (a) *t*-Butyl bromoacetate, Bu_4NI, K_2CO_3, MeCN (75%); (b) TFA, CH_2Cl_2 (89%); (c) *o*-NsCl, pyridine, CH_2Cl_2 (61%); (d) **13**, Bu_4NI, K_2CO_3, MeCN (33%).

2.2. Biological evaluation of compounds

Previous studies showed that **1a** is a potent nonselective inhibitor of both 11βHSD enzymes.[23,36] Morris et al. reported a more pronounced inhibition of 11βHSD2 compared with 11βHSD1 dehydrogenase activity.[23] Interestingly, using rat Leydig cells they observed no inhibition of 11βHSD1 reductase activity. Galignana et al. provided evidence that **1a** is a substrate for both 11βHSD enzymes.[36]

In the present study, we determined the inhibitory activity of **1a** and **1b** and of derivatives of the latter against cortisone reduction by human recombinant 11βHSD1 and cortisol oxidation by human recombinant 11βHSD2 (Fig. 1, Table 1). Both **1a** and **1b** potently inhibited 11βHSD1 reductase activity with IC_{50} of 1.16 ± 0.21 and 0.63 ± 0.13 μM, respectively, and 11βHSD2 dehydrogenase activity with IC_{50} of 0.49 ± 0.06 and 0.40 ± 0.08 μM (Table 1). The novel derivatives of **1b** were then first screened for 11βHSD inhibition at a concentration of 10 μM, and IC_{50} values were determined for compounds showing more than 70% inhibition (Fig. 2).

Table 1
Inhibition of 11βHSD1 and 11βHSD2 by progesterone derivatives

Compound	IC_{50} [μM] (mean ± SD)	
	11βHSD1	11βHSD2
1a	1.16 ± 0.21	0.49 ± 0.06
1b	0.63 ± 0.13	0.40 ± 0.08
3	n.d.	2.20 ± 0.12
4	n.d.	2.41 ± 0.45
5	n.d.	2.69 ± 0.14
7	0.64 ± 0.21	1.05 ± 0.26
8b	n.d.	5.85 ± 1.32
10b	n.d.	4.21 ± 1.57
12b	n.d.	6.76 ± 2.00

Compound **7** with the 3-(ethyl 2-hydroximino propionate) side chain was the only potent 11βHSD1 inhibitor with an IC_{50} of 0.64 ± 0.21 μM. However, **7** was not selective and also potently inhibited 11βHSD2 with an IC_{50} of 1.05 ± 0.26 μM, thus resembling the effect of the parental compound **1b**.

In contrast to 11βHSD1, several of the 11β-amino derivatives preferentially inhibited 11βHSD2, that is **3**–**5**, **8b**, **10b** and **12b**, in the low micromolar range. Interestingly, the *S* stereoisomers of compounds **8**, **10** and **12** retained higher inhibitory activity compared with the *R* forms. In summary, activity against 11βHSD2 can be retained with modifications at position 11 on the steroid backbone. However, compared to **1a** and the parental compound **1b** these 11β-amino derivatives were less active. Nevertheless, they provide a basis for the development of more potent compounds.

In a next step, **1a** and the 11β-aminosteroid derivatives were tested for direct effects on MR transactivation activity using HEK-293 cells expressing human MR and a galactosidase reporter gene under the control of the MR sensitive MMTV promoter. The reference compound **1a**, which has been reported earlier to activate MR in transfected COS-7 cells with an EC_{50} of about 50 nM,[18] showed weak agonist activity in transfected HEK-293 cells with an EC_{50} of 14 ± 5 μM and, as observed previously in the COS-7 cell system, did not act as antagonist.

Among the 11β-aminosteroid derivatives three compounds were active. Compound **12a** activated MR with an EC_{50} of 4.1 ± 1.2 μM but did not act as antagonist, whereas compounds **2** and **6** inhibited aldosterone-induced MR activation with IC_{50} of

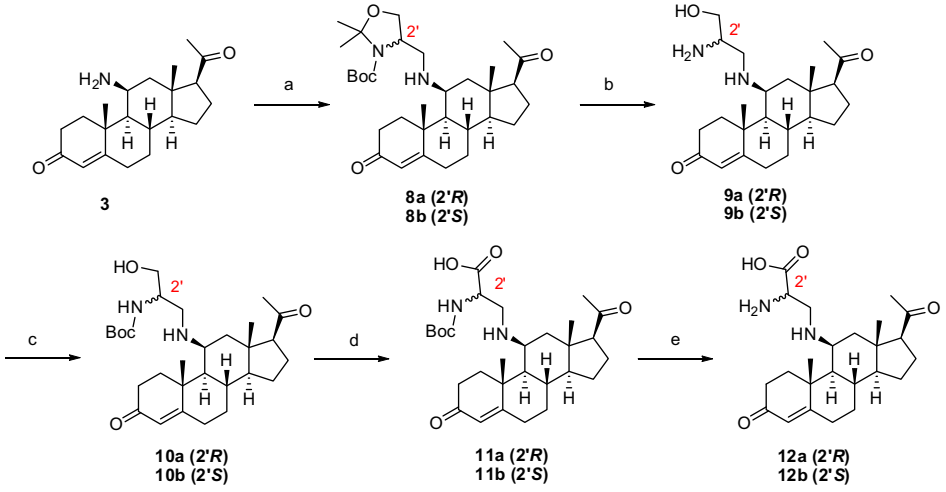

Scheme 3. Synthesis of γ-substituted amino acid derivatives of 11β-aminoprogesterone. (a) (*R*)- or (*S*)-Garner's aldehyde, MeOH, AcOH, then $NaCNBH_3$ (60%); (b) TFA, H_2O 50 °C; (c) Boc_2O, $NaHCO_3$, MeCN, H_2O (78%, two steps); (d) Jones oxidant, acetone (39%); (e) TFA, CH_2Cl_2 (quant).

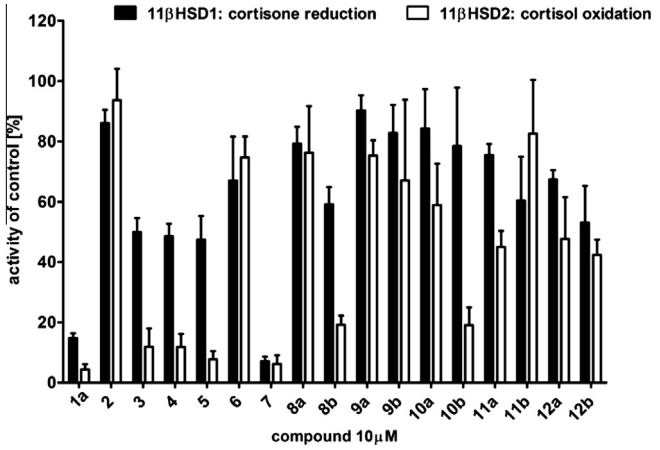

Figure 2. Preliminary inhibition screen of 11βHSD1 and 11βHSD2 by progesterone derivatives at 10 μM. Lysates of HEK-293 cells expressing recombinant human 11βHSD1 or 11βHSD2 were incubated for 10 min at 37 °C in the presence of 200 nM cortisone and 500 μM NADPH to measure 11βHSD1 reductase activity or 50 nM cortisol and 500 μM NAD^+ to measure 11βHSD2 dehydrogenase activity, followed by determination of the amount of product formed. Results (mean ± SD) are from three independent experiments.

3.5 ± 0.2 and 10.9 ± 0.8 μM, respectively, but did not act as an agonist. The reason for the differences in the sensitivity of COS-7 and HEK-293 cells for MR activation remains unknown but may be explained by differences in the experimental procedure and/or the ability of progesterone and its derivatives to enter the cell. Nevertheless, MR modulation by the three aminoprogesterone derivatives **2**, **6** and **12a** was observed at lower concentrations than that by the parental compound **1a**, which has been shown to stimulate sodium absorption in renal cortical collecting duct cells.[18] Thus, future studies are needed to explore the use of these aminoprogesterone derivatives as a basis for the development of suitable MR blockers and to investigate their biological effects.

3. Conclusion

Despite the steric limitations that are imposed on the 11β-position of progesterone, we were able to develop a concise synthesis of 11β-aminoprogesterone (**3**) starting from readily available 11α-hydroxyprogesterone (**1b**). We demonstrated that alkylation of the newly introduced amino functionality is challenging, and only activated unbulky electrophiles were useful. Reductive amination, however did prove to be amenable to extending the functionality of the amine group, and allowed for the synthesis of amino acid derivatives **12a** and **12b**. These amino acid derivatives provide a convenient handle that can be further elaborated in the search for second generation 11βHSD2 inhibitors and MR antagonists. Our results indicate that some of the substituted 11β-aminoprogesterone derivatives prepared display the ability to preferentially inhibit 11βHSD2. Furthermore, we identified two compounds with antagonist properties against the MR (**2** and **6**). The biological effect of these compounds needs to be further investigated in suitable cell and animal models.

4. Experimental details

4.1. Chemistry

All reactions were performed in oven-dried glassware, under a stream of argon. Solvents were purchased from Fisher and used directly, unless otherwise noted. When required, solvents were dried as follows: MeOH was distilled over CaH_2; Et_2O and THF were distilled over sodium in the presence of benzophenone as indicator; CH_2Cl_2 was distilled over CaH_2. Silica gel was purchased from Silicycle (240–400 mesh). Reactions were monitored on silica-coated plates with a fluorescence indicator. All NMR spectra were recorded on Varian Unity or Inova spectrometers, at the indicated frequencies at room temperature. High-resolution mass spectrometry was recorded on an Agilent 6220 oaTOF, with electrospray ionization. Reagents were purchased from Sigma–Aldrich, Alfa–Aesar or 3B Scientific Corporation (11β-hydroxyprogesterone) and used without further purification.

4.1.1. 11β-Azidoprogesterone (2)

The title compound is synthesized by an adapted procedure.[28] Diethyl azodicarboxylate (0.80 mL, 4.6 mmol) is added drop-wise to a stirred solution of (oven-dried) triphenylphosphine (1.2 g, 4.6 mmol) and phenol (0.03 g, 0.3 mmol) in anhydrous THF (2.4 mL) under argon at room temperature. Stirring is continued for 2 min, then hydrazoic acid[37] (3.85 mL of 2.4 M solution in benzene, 9.2 mmol) is added, followed by 11α-hydroxyprogesterone (**1b**, 0.5 g, 1.53 mmol), and the reaction mixture is refluxed for 20 min. A color change from pink to dark brown indicates completion of the reaction. After reduced pressure evaporation of solvent, the crude product is chromatographed twice through silica gel (1st column: CH_2Cl_2–ethyl ether, 9.5:0.5 to 9:1; second column: ethyl ether–hexane 5:5 to 8:2) to yield 11β-azidoprogesterone (**2**, 0.23 g, 42%) as colorless solid. ^{1}H NMR (400 MHz, $CDCl_3$) δ: 5.67 (d, J = 1.7 Hz, 1H), 4.17–4.15 (m, 1H), 2.51–2.35 (m, 5H), 2.24–2.18 (m, 2H), 2.18–2.09 (m, 4H), 2.05–1.93 (m, 1H), 1.91–1.75 (m, 2H), 1.74–1.65 (m, 2H), 1.41 (s, 3H), 1.39–1.23 (m, 2H), 1.17–0.96 (m, 3H), 0.90 (s, 3H). ^{13}C NMR (100 MHz, $CDCl_3$) δ: 208.7, 199.3, 171.4, 122.4, 63.5, 57.6, 57.4, 55.1, 42.5, 42.4, 39.0, 35.0, 33.6, 32.3, 31.7, 31.5, 31.2, 24.1, 22.6, 20.4, 14.4. HRMS (ESI) $C_{21}H_{29}N_3O_2Na^+$ m/z: 378.2152 (expected), 378.2142 (found). FTIR (MeOH thin film) cm^{-1}: 3244, 3015, 2987, 2091, 1710, 1676, 1479. $[\alpha]_D$: +274 (c 0.87, CH_2Cl_2).

4.1.2. 11β-Aminoprogesterone (3)

To a suspension of azide **2** (1.9 g, 5.4 mmol) and $CoCl_2{\cdot}6H_2O$ (3.8 g, 16.1 mmol) in water (10 mL) at room temperature, a solution of $NaBH_4$ (0.92 g, 24.1 mmol) in H_2O (25 mL) is added drop-wise (to subside an excessive foaming) with stirring. The appearance of a black precipitate indicates the formation of a cobalt boride species. The mixture is then stirred at reflux for 3.5 h. Upon completion of the reaction, the solution is allowed to cool back to room temperature, which is then diluted with ethyl acetate (30 mL). The resulting biphasic mixture is filtered through Celite and the aqueous layer is separated. The aqueous phase is extracted several times, first with ethyl acetate (3 × 30 mL) and then with CH_2Cl_2 (3 × 30 mL). The combined organic phases are dried (Na_2SO_4) and concentrated under reduced pressure, and further purified on silica gel by flash column chromatography (100% ethyl acetate followed by CH_2Cl_2–MeOH, 9.5:0.5) to give the pure amine **3** (1.1 g, 62%) as a colorless solid. ^{1}H NMR (500 MHz, $CDCl_3$) δ: 5.67 (d, J = 1.7 Hz, 1H), 3.62 (br s, 1H), 2.51–2.34 (m, 5H), 2.26–2.21 (m, 1H), 2.20–2.09 (m, 5H), 2.07–2.00 (m, 1H), 1.97–1.88 (m, 2H), 1.79–1.68 (m, 2H), 1.44 (s, 3H), 1.35–1.28 (m, 2H), 1.15–1.03 (m, 3H), 0.92 (s, 3H). ^{13}C NMR (125 MHz, $CDCl_3$) δ: 209.0, 199.3, 172.2, 122.2, 64.4, 58.4, 56.2, 48.7, 43.1, 39.2, 35.0, 33.9, 32.9, 32.0, 31.4, 31.1, 29.8, 24.4, 22.6, 21.6, 16.6. HRMS (ESI) $C_{21}H_{31}NO_2$-H^+ m/z: 330.2428 (expected), 330.2426 (found). FTIR (MeOH thin film) cm^{-1}: 3381, 3323, 2928, 2874, 1701, 1667, 1446, 1388 $[\alpha]_D$: +208 (c 0.93, CH_2Cl_2). MP: 142–145 °C.

4.1.3. *t*-Butyl 11β-aminoprogesteronyl acetate (4)

To a mixture of amine **3** (0.100 g, 0.3 mmol), *t*-butyl bromoacetate (88 μL, 0.6 mmol), tetrabutyl ammonium iodide and 4 Å MS

(0.222 g, 0.6 mmol) in acetonitrile (5 mL) is added K_2CO_3 (0.166 g, 1.2 mmol) under argon at room temperature. This mixture is then stirred at reflux for 9 h. The resulting mixture is filtered through Celite and the solvent is removed under reduced pressure. The residue is dissolved in CH_2Cl_2 (10 mL) and extracted several times with water (2 × 5 mL) followed by brine (1 × 5 mL). The organic phase is dried (Na_2SO_4), concentrated under reduced pressure, and further purified by silica gel flash column chromatography (ethyl acetate–hexane, 1:1) to give the pure title compound **4** (0.101 g, 75%) as an off-white solid. ^{1}H NMR (600 MHz, $CDCl_3$) δ: 5.67 (s, 1H), 3.42 (d, J = 16.8 Hz, 1H), 3.29–3.10 (m, 2H), 2.52–2.35 (m, 5H), 2.25–2.20 (m, 1H), 2.19–2.15 (m, 1H), 2.15–2.13 (m, 4H), 2.08–2.03 (m, 1H), 1.99–1.90 (m, 1H), 1.90–1.85 (m, 1H), 1.79–1.73 (m, 1H), 1.72–1.66 (m, 1H), 1.56 (s, 3H), 1.48 (s, 9H), 1.35–1.28 (m, 1H), 1.18 (dd, J = 11.4, 4.5 Hz, 1H), 1.14–1.02 (m, 3H), 0.92 (s, 3H). ^{13}C NMR (125 MHz, $CDCl_3$) δ: 209.1, 199.6, 172.5, 171.8, 121.8, 81.4, 64.2, 58.5, 56.1, 55.0, 50.6, 43.3, 40.7, 39.2, 34.6, 34.0, 33.2, 32.0, 31.7, 31.5, 28.1, 24.4, 22.7, 21.8, 15.2. HRMS (ESI) $C_{27}H_{41}NO_4H^+$ m/z: 444.3108 (expected), 444.3115 (found). FTIR (MeOH thin film) cm^{-1}: 3032, 2934, 1731, 1703, 1671, 1367, 1234, 1158. $[\alpha]_D$: +137 (c 2.00, CH_2Cl_2).

4.1.4. 11β-Aminoprogesteronyl acetic acid TFA salt (5)

A solution of ester **4** (0.100 g, 0.23 mmol) in CH_2Cl_2 (2 mL) is treated with excess trifluoroacetic acid (4 mL), and stirred at room temperature for 6 h. After completion of the reaction, the solvent is evaporated under reduced pressure and the resulting residue is dried on high vacuum to yield the title amino acid **5** (0.101 g, 89%) as a fluffy white solid. ^{1}H NMR (500 MHz, CD_3OD) δ: 5.73 (d, J = 1.5 Hz, 1H), 4.08–4.01 (m, 3H), 2.64–2.50 (m, 4H), 2.42 (dt, J = 16.7, 4.8 Hz, 1H), 2.39–2.32 (m, 1H), 2.28 (dt, J = 13.5, 5.0 Hz, 1H), 2.16 (s, 3H), 2.16–1.94 (m, 3H), 1.95–1.82 (m, 2H), 1.81 (dd, J = 15.5, 5.0 Hz, 1H), 1.72 (dd, J = 11.8, 4.2 Hz, 1H), 1.58 (s, 3H), 1.43–1. 26 (m, 3H), 1.23–1.14 (m, 1H), 0.89 (s, 3H). ^{13}C NMR (125 MHz, $CDCl_3$) δ: 211.3, 200.9, 172.8, 170.0, 123.0, 64.2, 58.4, 57.5, 55.5, 42.3, 39.4, 39.1, 35.2, 34.2, 33.6, 32.4, 32.3, 31.0, 27.7, 24.8, 23.9, 22.0, 14.6. HRMS (ESI) $C_{23}H_{33}NO_4H^+$ m/z: 388.2482 (expected), 388.2483 (found). FTIR (MeOH thin film) cm^{-1}: 3197, 2962, 1699, 1678, 1422, 1199. $[\alpha]_D$: +112 (c 1.44, H_2O).

4.1.5. 11β-*N*-*ortho*-Nitrobenzenesulfonyl-aminoprogesterone (6)

Amine **3** (0.2 g, 0.6 mmol) is mixed with *o*-nitrobenzenesulfonyl chloride (1.33 g, 6 mmol) and pyridine (0.48 mL, 6.0 mmol) in CH_2Cl_2 (5 mL) and then stirred at reflux for 12 h. The resulting mixture is diluted further with additional CH_2Cl_2 (5 mL) and then extracted with water (2 × 5 mL) and brine (1 × 5 mL). The organic phase is dried (Na_2SO_4), concentrated under reduced pressure, and further purified on silica gel by flash column chromatography (CH_2Cl_2 followed by ethyl acetate–CH_2Cl_2, 2:8) to give pure title compound **6** (0.19 g, 61%) as a light yellow solid. ^{1}H NMR (500 MHz, $CDCl_3$) δ: 8.19–8.13 (m, 1H), 7.93–7.87 (m, 1H), 7.83–7.73 (m, 2H), 5.68 (d, J = 1.6 Hz, 1H), 5.48 (d, J = 10.4 Hz, 1H), 4.46 (dtd, J = 10.0, 4.7, 2.3 Hz, 1H), 2.51–2.35 (m, 4H), 2.30–2.20 (m, 2H), 2.09–1.96 (m, 3H), 1.96–1.80 (m, 2H), 1.77 (s, 3H), 1.76–1.63 (m, 2H), 1.49 (s, 3H), 1.48–1.43 (m, 1H), 1.31–1.19 (m, 2H), 1.15–0.99 (m, 2H), 0.53 (s, 3H). ^{13}C NMR (125 MHz, $CDCl_3$) δ: 207.8, 199.2, 170.4, 147.8, 136.2, 133.7, 133.4, 129.6, 125.7, 122.7, 63.8, 57.3, 55.2, 51.4, 44.4, 41.9, 39.1, 34.8, 33.9, 32.7, 31.8, 31.7, 30.7, 24.3, 22.6, 21.0, 16.1. HRMS (ESI) $C_{27}H_{34}N_2O_6SNa^+$ m/z: 537.2030 (expected), 537.2028 (found). FTIR (MeOH thin film) cm^{-1}: 3388, 3092, 2942, 2881, 1700, 1667, 1542, 1450, 1355, 1166. $[\alpha]_D$: +275.6 (c 1.13, CH_2Cl_2).

4.1.6. Ethyl 2-(hydroxyimino)-3-bromopropanoate (13)

The title compound was synthesized as per the literature procedure.[32] Briefly, a stirred solution of ethyl bromopyruvate (3.6 mL, 28.5 mmol) in $CHCl_3$ (85 mL) and CH_3OH (57 mL), is treated with hydroxylamine hydrochloride (2.00 g, 28.5 mmol) at room temperature. The mixture is stirred overnight at room temperature and then concentrated to dryness. The residue is dissolved in CH_2Cl_2 (40 mL), washed with 0.1 N HC1 (20 mL) and brine (20 mL), and dried over Na_2SO_4. Evaporation of the solvent gives crystalline material, which is recrystallized (CH_2Cl_2–hexane) to yield the desired product (3.96 g, 68%) as white needles. ^{1}H NMR (500 MHz, $CDCl_3$) δ: 9.33 (s, 1H), 4.38 (q, J = 7.2 Hz, 2H), 4.27 (s, 2H), 1.38 (t, J = 7.2 Hz, 3H). ^{13}C NMR (125 MHz, $CDCl_3$) δ: 161.7, 147.9, 62.5, 30.1, 14.3. HRMS (ESI) $C_5H_8BrNO_3Na^+$ m/z: 231.9580 (expected), 231.9579 (found). FTIR (MeOH thin film) cm^{-1}: 3445 (br), 3275, 3057, 2987, 1724, 1472, 1326, 1225, 1184, 1035. Mp: 77–78 °C.

4.1.7. 11β-*N*-3-(*O*-Ethyl-2-hydroxyimino-propanoyl)-aminoprogesterone (7)

To a mixture of amine **3** (0.05 g, 0.15 mmol), and oxime **13** (0.065 g, 0.3 mmol), in acetonitrile (1 mL) is added tetrabutyl ammonium iodide (0.110 g, 0.3 mmol), K_2CO_3 (0.085 g, 0.6 mmol) and 4 Å MS under argon at room temperature. The mixture is stirred at reflux for 12 h, and then filtered through Celite. The filtrate is evaporated under reduced pressure, and the residue is dissolved in CH_2Cl_2 (2 mL) and extracted with water (2 × 2 mL) followed by brine (1 × 2 mL). The organic phase is dried (Na_2SO_4), concentrated under reduced pressure, and further purified by silica gel column chromatography (ethyl acetate–CH_2Cl_2, 1:1) to give pure title compound **7** (0.025 g, 33%) as a light yellow solid. ^{1}H NMR (500 MHz, $CDCl_3$) δ: 8.97 (s, 1H), 5.66 (d, J = 1.6 Hz, 1H), 4.31 (q, J = 7.1 Hz, 2H), 3.81 (d, J = 12.9 Hz, 1H), 3.63 (d, J = 13.0 Hz, 1H), 3.19 (s, 1H), 2.54 (dd, J = 13.8, 2.2 Hz, 1H), 2.50–2.29 (m, 5H), 2.24–2.18 (m, 1H), 2.19 (td, J = 4.6, 3.7, 2.1 Hz, 1H), 2.15 (s, 3H), 2.15–2.05 (m, 1H), 2.06–1.97 (m, 1H), 1.91–1.79 (m, 2H), 1.79–1.61 (m, 2H), 1.42 (s, 3H), 1.35 (t, J = 7.1 Hz, 3H), 1.33–1.22 (m, 2H), 1.15 (dd, J = 11.5, 4.7 Hz, 1H), 1.14–1.00 (m, 2H), 0.89 (s, 3H). ^{13}C NMR (125 MHz, $CDCl_3$) δ: 209.2, 199.8, 172.6, 163.6, 152.5, 121.9, 64.3, 62.2, 58.4, 56.1, 55.4, 43.2, 40.9, 39.4, 34.5, 34.1, 33.2, 32.0, 31.8, 31.5, 29.9, 24.5, 22.6, 21.6, 15.4, 14.4. HRMS (ESI) $C_{26}H_{38}N_2O_5H^+$ m/z: 459.2853 (expected), 459.2853 (found). FTIR (MeOH thin film) cm^{-1}: 3300, 3058, 2934, 1703, 1668, 1449, 1357, 1189, 1015. $[\alpha]_D$: +152 (c 0.75, CH_2Cl_2).

4.1.8. 11β-*N*-(3-(*N*-Tertbutyloxycarbonyl-*N*,*O*-acetonide-1-hydroxy-2(*R*)-amino-propyl))-aminoprogesterone (8a)

This is prepared by adaptation of a known protocol.[35] The following is a representative example; both diastereoisomers **8a** and **8b** are generated following the same protocol. To a solution of **3** (330 mg, 1 mmol) in dry MeOH (11 mL), containing acetic acid (1% v/v), is added (*S*)-Garner's aldehyde (230 mg, 1 mmol), and the mixture is stirred at room temperature under an atmosphere of argon for 45 min. The resultant imine is reduced by the addition of $NaCNBH_3$ (80 mg, 1.25 mmol) in two portions over 30 min. This is stirred at room temperature for another 2 h, at which point the reaction is quenched with water (5 mL). The organic solvent is evaporated, more water is added (5 mL), and the aqueous layer is extracted with CH_2Cl_2 (3 × 15 mL). The combined organic extracts are dried over Na_2SO_4, evaporated and the residue is purified by silica gel chromatography (CH_2Cl_2–MeOH, 96:4). The title product is obtained as a white foam (325 mg, 60%). ^{1}H NMR (500 MHz, $CDCl_3$) δ: 5.66 (s, 1H), 4.08–3.92 (m, 2H), 3.91–3.82 (m, 1H), 3.22–3.11 (m, 1H), 3.09–2.91 (m, 2H), 2.66–2.41 (m, 5H), 2.27–2.09 (m, 5H), 2.08–2.02 (m, 2H), 1.93–1.80 (m, 2H), 1.79–1.64 (m, 2H), 1.60 (s, 3H), 1.51 (br s, 15H), 1.35–1.24 (m, 2H), 1.19 (dd, J = 11.5, 4.5 Hz, 1H), 1.71–1.01 (m, 2H), 0.84 (s, 3H). ^{13}C NMR (125 MHz, CD_3OD) δ: 208.9, 199.5, 172.4, 152.6, 121.8, 93.9, 80.8, 66.4, 64.2, 58.1, 57.2, 55.1, 55.0, 49.5, 48.9, 43.2, 39.9, 39.3, 34.5, 33.9, 33.1, 31.8, 31.7, 31.5, 28.3, 24.3, 22.6, 21.6, 15.5. HRMS (ESI)

$C_{32}H_{50}N_2O_5Na^+$ *m/z*: 565.3612 (expected), 565.3605 (found). FTIR (MeOH thin film) cm^{-1}: 3053, 2974, 2934, 2878, 1699, 1671, 1617, 1389, 1174, 1086. $[\alpha]_D$: +138 (*c* 0.74, CH_2Cl_2).

4.1.9. 11β-*N*-(3-(*N*-Tertbutyloxycarbonyl-*N*,*O*-acetonide-1-hydroxy-2(*S*)-amino-propyl))-aminoprogesterone (8b)

^1H NMR (500 MHz, $CDCl_3$) δ: 5.67 (s, 1H), 4.01–3.86 (m, 3H), 3.91–3.82 (m, 1H), 3.15 (br s, 1H), 3.11–3.02 (m, 2H), 2.58–2.30 (m, 5H), 2.30–2.19 (m, 2H), 2.15 (s, 3H), 2.10–1.98 (m, 2H), 1.96–1.80 (m, 4H), 1.75 (s, 3H), 1.60 (s, 6H), 1.50 (br s, 9H), 1.40–1.21 (m, 2H), 1.20–1.17 (m, 1H), 1.17–1.00 (m, 2H), 0.87 (s, 3H). ^{13}C NMR (125 MHz, CD_3OH) δ: 208.8, 199.7, 169.4, 155.9, 122.7, 95.4, 83.0, 66.8, 64.1, 63.0, 58.2, 56.7, 55.9, 50.9, 43.1, 41.4, 40.6, 39.4, 34.5, 33.6, 33.2, 31.8, 31.4, 30.9, 28.2, 24.3, 22.6, 21.6, 15.5. HRMS (ESI) $C_{32}H_{50}N_2O_5Na^+$ *m/z*: 565.3612 (expected), 565.3605 (found). FTIR (MeOH thin film) cm^{-1}: 3056, 2972, 2935, 2879, 1699, 1671, 1389, 1365, 1207, 1172. $[\alpha]_D$: +90 (*c* 0.6, CH_2Cl_2).

4.1.10. 11β-*N*-(3-(1-Hydroxy-2(*R*)-amino-propyl))-aminoprogesterone TFA salt (9a)

The following is a representative example; both diastereoisomers **9a** and **9b** are generated following the same protocol. The fully protected amino alcohol appended aminoprogesterone **8a** (250 mg, 0.46 mmol) is stirred in a mixture of trifluoroacetic acid and water (6 mL, 5:1 mixture) at 50 °C for 16 h. The solvents are evaporated on a high-vacuum rotary evaporator, and then co-evaporated with water (3 × 10 mL), and dried on high vacuum, to afford the desired product as a white trifluoroacetate salt. This product was used without further purification. Analytical samples and those used for assay were further purified by HPLC. ^1H NMR (600 MHz, D_2O) δ: 5.83 (s, 1H), 4.22–4.16 (m, 1H), 4.16–4.11 (m, 1H), 3.99–3.93 (m, 2H), 3.93–3.88 (m, 1H), 3.64–3.56 (m, 1H), 2.73 (t, *J* = 9.2 Hz, 1H), 2.70–2.64 (m, 1H), 2.61–2.51 (m, 2H), 2.46 (dt, *J* = 17.0, 5.0 Hz, 1H), 2.37 (ddd, *J* = 14.8, 4.8, 2.6 Hz, 1H), 2.24 (s, 3H), 2.19–2.09 (m, 2H), 2.09–1.98 (m, 3H), 1.95–1.81 (m, 4H), 1.43 (s, 3H), 1.42–1.32 (m, 2H), 1.27–1.16 (m, 1H), 0.89 (s, 3H). ^{13}C NMR (125 MHz, D_2O) δ: 216.0, 203.4, 175.2, 129.1, 121.2, 62.8, 61.5, 57.6, 56.8, 53.7, 48.3, 46.8, 41.3, 38.0, 36.9, 33.1, 32.5, 31.8, 31.1, 30.7, 23.2, 22.6, 20.2, 13.3. HRMS (ESI) $C_{24}H_{38}N_2O_3H^+$ *m/z*: 403.2955 (expected), 403.2948 (found). FTIR (MeOH thin film) cm^{-1}: 3101, 2949, 2564, 1715, 1426, 1212, 1161. $[\alpha]_D$: +91.5 (*c* 1.8, H_2O).

4.1.11. 11β-*N*-(3-(1-Hydroxy-2(*S*)-amino-propyl))-aminoprogesterone TFA salt (9b)

^1H NMR (600 MHz, D_2O) δ: 5.83 (d, *J* = 1.6 Hz, 1H), 4.18–4.15 (m, 2H), 4.07–4.00 (m, 1H), 3.98 (m, 1H), 3.89 (dd, *J* = 13.9, 6.2 Hz, 1H), 3.81–3.75 (m, 1H), 2.77–2.64 (m, 2H), 2.62–2.51 (m, 2H), 2.46 (dt, *J* = 17.2, 5.1 Hz, 1H), 2.39–2.34 (m, 1H), 2.24 (s, 3H), 2.22–2.12 (m, 2H), 2.10–1.98 (m, 3H), 1.97–1.82 (m, 4H), 1.45 (s, 3H), 1.44–1.31 (m, 2H), 1.28–1.16 (m, 1H), 0.88 (s, 3H). ^{13}C NMR (125 MHz, D_2O) δ: 216.1, 203.7, 175.4, 129.2, 121.2, 62.9, 62.1, 57.5, 56.7, 53.7, 48.5, 46.3, 41.4, 37.9, 36.5, 33.1, 32.5, 31.8, 31.1, 30.7, 23.3, 22.5, 20.3, 13.1. HRMS (ESI) $C_{24}H_{38}N_2O_3H^+$ *m/z*: 403.2955 (expected), 403.2948 (found). FTIR (MeOH thin film) cm^{-1}: 3087, 2960, 2570, 1703, 1435, 1210, 1168. $[\alpha]_D$: +89 (*c* 0.62, CH_2Cl_2).

4.1.12. 11β-*N*-(3-(1-Hydroxy-2(*R*)-tertbutyloxycarbonyl-aminopropyl))-aminoprogesterone (10a)

The following is a representative example; both diastereoisomers **10a** and **10b** are generated following the same protocol. The deprotected amino alcohol **9a** (0.46 mmol) is dissolved in a water–acetonitrile mixture (6 mL, 1:2 mixture), to which is added $NaHCO_3$ (116 mg, 1.4 mmol) and di-*t*-butyl-dicarbonate (105 mg, 0.48 mmol). The mixture is stirred at room temperature for 2 h, at which point the starting material is completely consumed as evidenced by TLC analysis (CH_2Cl_2–MeOH, 95:5). The solution is basified with NaOH (three drops of a 3 M solution), and extracted with ethyl acetate (3 × 30 mL). The combined organic extracts were dried over Na_2SO_4, concentrated and purified by silica gel chromatography (CH_2Cl_2–MeOH, 95:5), to yield the desired product (181 mg, 78% over two steps). ^1H NMR (600 MHz, $CDCl_3$) δ: 5.69 (s, 3H), 5.14–5.02 (br s, 1H), 3.78–3.64 (m, 3H), 3.18–3.11 (br s, 1H), 3.00–2.91 (m, 1H), 2.96 (dd, 1H, *J* = 11.0, 3.7 Hz), 2.75–2.65 (m, 1H), 2.52–2.43 (m, 3H), 2.40–2.30 (m, 1H), 2.26–2.21 (m, 1H), 2.19–2.12 (m, 4H), 2.12–2.02 (m, 3H), 1.94–1.82 (m, 3H), 1.81–1.69 (m, 2H), 1.61–1.56 (m, 1H), 1.52 (s, 3H), 1.48–1.43 (m, 9H), 1.36–1.25 (m, 3H), 1.26–1.20 (m, 2H), 0.88 (s, 3H). ^{13}C NMR (125 MHz, $CDCl_3$) δ: 209.1, 199.4, 172.1, 156.2, 122.1, 79.9, 65.7, 64.2, 58.3, 55.7, 52.1, 49.9, 43.2, 40.3, 39.3, 34.7, 34.0, 33.2, 31.9, 31.8, 31.6, 29.9, 28.5, 24.5, 22.8, 22.0, 15.5. HRMS (ESI) $C_{29}H_{46}N_2O_5H^+$ *m/z*: 503.3479 (expected), 503.3470 (found). IR (MeOH cast film) cm^{-1}: 3385.4, 2933.3, 1702.2, 1667.7, 1616.1, 1523.0, 1452.8, 1365.1, 1171.4, 1031.8, 700.4. $[\alpha]_D$: +135.6 (*c* 0.90, MeOH).

4.1.13. 11β-*N*-(3-(1-Hydroxy-2(*S*)-tertbutyloxycarbonyl-aminopropyl))-aminoprogesterone (10b)

^1H NMR (600 MHz, $CDCl_3$) δ: 5.66 (s, 1H), 4.99 (br s, 1H), 3.72 (dd, 2H, *J* = 4.1, 1.9 Hz), 3.65–3.49 (m, 1H), 3.17–3.13 (m, 1H), 3.10–3.04 (m, 1H), 2.52–2.39 (m, 4H), 2.38–2.32 (m, 1H), 2.24–2.19 (m, 1H), 2.16–2.11 (m, 4H), 2.11–2.06 (m, 1H), 2.05–1.99 (m, 1H), 1.91–1.88 (m, 1H), 1.87–1.80 (m, 1H), 1.79–1.65 (m, 2H), 1.59–1.53 (m, 3H), 1.46 (s, 3H), 1.44–1.40 (m, 9H), 1.30–1.23 (m, 2H), 1.22–1.18 (m, 1H), 1.11–1.03 (m, 2H), 0.84 (s, 3H). ^{13}C NMR (125 MHz, $CDCl_3$) δ: 209.0, 199.4, 172.1, 156.5, 122.1, 80.0, 64.2, 58.4, 56.0, 55.8, 52.9, 49.7, 43.2, 40.4, 39.3, 34.8, 34.0, 33.2, 31.9, 31.8, 31.6, 29.9, 28.5, 24.4, 22.8, 21.8, 15.5. HRMS (ESI) $C_{29}H_{46}N_2O_5H^+$ *m/z*: 503.3479 (expected), 503.3471 (found) IR (MeOH cast film) cm^{-1}: 3375.4, 2931.5, 1701.8, 1668.4, 1616.0, 1522.7, 1452.3, 1390.5, 1364.9, 1171.3, 1030.3, 703.2. $[\alpha]_D$: +120.9 (*c* 0.86, MeOH).

4.1.14. 11β-*N*-(3-(1-Carboxy-2(*R*)-tertbutyloxycarbonyl-aminopropyl))-aminoprogesterone (11a)

The following is a representative example; both diastereoisomers **11a** and **11b** are generated following the same protocol. The Jones reagent (2 M final concentration) is prepared freshly by dissolution of CrO_3 (100 mg, 1 mmol) in water (0.5 mL) followed by the addition of concentrated H_2SO_4 (0.085 mL, 1.5 mmol). The Boc-protected amino alcohol **10a** (127 mg, 0.25 mmol) is stirred at room temperature in HPLC-grade acetone (2.5 mL). Oxidation is achieved by the slow addition of freshly prepared Jones reagent (0.26 mL of a 2 M solution, 0.53 mmol), over 5 min, followed by stirring at room temperature for a further 1.5 h. The progress of the reaction is followed by TLC analysis (CH_2Cl_2–MeOH, 8:2). Once the reaction is deemed complete excess Jones reagent is quenched with *i*PrOH (1 mL), and the entire mixture is evaporated. The residue is suspended in water (20 mL) and extracted with CH_2Cl_2 (2 × 15 mL) followed by ethyl acetate (2 × 15 mL). The combined organic extracts are dried over Na_2SO_4, evaporated and purified by silica gel chromatography (CH_2Cl_2–MeOH, 4:1), to yield the product as a pure white solid (50 mg, 39%). ^1H NMR (600 MHz, CD_3OD) δ: 5.64 (s, 1H), 4.19–4.09 (m, 1H), 3.75–3.64 (m, 1H), 3.49–3.41 (m, 1H), 3.03–2.94 (m, 1H), 2.64 (dd, 1H, *J* = 15.0, 1.9 Hz), 2.60–2.45 (m, 3H), 2.40–2.24 (m, 3H), 2.17–2.06 (m, 3H), 2.00–1.89 (m, 2H), 1.89–1.76 (m, 2H), 1.63–1.58 (m, 1H), 1.60–1.49 (m, 4H), 1.49–1.40 (m, 9H), 1.40–1.31 (m, 1H), 1.31–1.22 (m, 2H), 1.19–1.09 (m, 1H), 0.90 (s, 3H). ^{13}C NMR (125 MHz, CD_3OD) δ: 210.0, 200.2, 174.2, 172.7, 156.4, 121.2, 79.5, 63.0, 57.3, 55.3, 54.6, 48.5, 41.5, 38.4, 37.6, 33.4, 33.0, 32.5, 31.1, 31.0, 29.7, 27.3, 23.5, 22.3, 19.8, 13.0. HRMS $C_{29}H_{44}N_2O_6H^+$ (ESI) *m/z*:

517.3272 (expected), 517.3264 (found) IR (MeOH cast film) cm^{-1}: 3390.1, 2936.2, 1705.0, 1671.5, 1484.2, 1454.5, 1365.7, 1167.2, 1058.5, 1029.2, 871.6. $[\alpha]_D$: +80.0 (*c* 1.10, MeOH).

4.1.15. 11β-*N*-(3-(1-Carboxy-2(*S*)-tertbutyloxycarbonyl-amino-propyl))-aminoprogesterone (11b)

^{1}H NMR (600 MHz, CD_3OD) δ: 5.66 (s, 1H), 4.18–4.10 (m, 1H), 3.76–3.68 (m, 1H), 3.26 (d, 1H, *J* = 6.2 Hz), 2.81 (app d, 1H, *J* = 13.9 Hz), 2.62 (app t, 1H, *J* = 9.1 Hz), 2.60–2.41 (m, 2H), 2.39–2.23 (m, 1H), 2.19 (s, 3H), 2.15–2.04 (m, 3H), 1.98–1.86 (m, 3H), 1.86–1.76 (m, 1H), 1.76–1.64 (m, 1H), 1.65–1.59 (m, 1H), 1.51 (s, 3H), 1.45–1.40 (m, 9H), 1.38–1.22 (m, 3H), 1.20–1.08 (m, 1H), 0.80 (s, 3H). ^{13}C NMR (125 MHz, CD_3OD) δ: 210.0, 200.5, 178.1, 173.3, 156.6, 121.0, 79.5, 63.3, 57.8, 54.9, 53.8, 48.2, 42.1, 38.6, 37.9, 33.7, 33.1, 33.0, 31.2, 30.1, 29.0, 27.3, 23.6, 21.9, 20.4, 13.4. HRMS (ESI) $C_{29}H_{44}N_2O_6H^+$ *m*/*z*: 517.3272 (expected), 517.3268 (found). IR (MeOH cast film) cm^{-1}: 3413.3, 2935.2, 1702.6, 1671.2, 1482.2, 1392.7, 1366.4, 1244.6, 1165.5, 1029.1, 867.8. $[\alpha]_D$: +131.0 (*c* 1.10, MeOH).

4.1.16. 11β-*N*-(3-(1-Carboxy-2(*R*)-amino-propyl))-aminoprogesterone TFA salt (12a)

The following is a representative example; both diastereoisomers **12a** and **12b** are generated following the same protocol. The Boc-protected amino acid derivative **11a** (11 mg, 0.02 mmol) is stirred at room temperature in a CH_2Cl_2–TFA mixture (0.5 mL, 3:1 mixture) for 30 min. The solvent is evaporated, followed by co-evaporation with water (3 × 1 mL), to yield the amino acid **12a** as a TFA salt (quant). ^{1}H NMR (500 MHz, D_2O) δ: 5.79 (br s, 1H), 4.08 (dd, 1H, *J* = 12.5, 4.0 Hz), 4.05–4.01 (m, 1H), 3.79 (dd, 1H, *J* = 11.7, 4.0 Hz), 3.41 (app t, 1H, *J* = 12.2 Hz), 2.73–2.66 (m, 1H), 2.62–2.49 (m, 3H), 2.43 (dt, 1H, *J* = 17.3, 5.0 Hz), 2.36–2.30 (m, 1H), 2.21–2.16 (m, 4H), 2.14–2.09 (m, 1H), 2.05–1.96 (m, 3H), 1.91–1.77 (m, 4H), 1.48 (app s, 3H), 1.40–1.30 (m, 2H), 1.24–1.13 (m, 1H), 0.85 (app s, 3H). ^{13}C NMR (125 MHz, D_2O) δ: 216.2, 203.9, 175.7. 171.7, 120.9, 62.9, 56.7, 56.6, 53.3, 47.5, 45.5, 41.4, 38.1, 36.5, 32.8, 32.7, 32.0, 31.1, 30.7, 30.7, 23.3, 22.5, 20.1, 13.1. HRMS (ESI) $C_{24}H_{36}N_2O_4H^+$ *m*/*z*: 417.2748 (expected), 417.2741 (found) IR (MeOH cast film) cm^{-1}: 2945.7, 1676.9, 1422.8, 1362.3, 1294.5, 1202.9, 1134.6, 1027.8, 836.7, 721.4. $[\alpha]_D$: +56.6 (*c* 0.8, MeOH).

4.1.17. 11β-*N*-(3-(1-Carboxy-2(*S*)-amino-propyl))-aminoprogesterone TFA salt (12b)

^{1}H NMR (500 MHz, D_2O) δ: 5.80 (app s, 1H), 4.18 (dd, 1H, *J* = 12.1, 4.0 Hz), 4.17 (m, 1H), 3.78 (dd, 1H, *J* = 12.8. 4.0 Hz), 3.62 (app t, 1H, *J* = 12.5 Hz), 2.69 (app t, 1H, *J* = 9.0 Hz), 2.67–2.60 (m, 1H), 2.58–2.47 (m, 2H), 2.40 (dt, 1H, *J* = 17.3, 5.0 Hz), 2.35–2.29 (m, 1H), 2.30–2.16 (m, 4H), 2.15–2.08 (m, 1H), 2.03–1.91 (m, 3H), 1.91–1.77 (m, 4H), 1.45 (app s, 3H), 1.40–1.30 (m, 2H), 1.25–1.11 (m, 1H) 0.81 (app s, 3H). ^{13}C NMR (125 MHz, D_2O) δ: 216.1, 203.9, 175.4, 171.5, 121.2, 62.9, 57.0, 53.9, 53.7, 46.0, 43.7, 41.4, 38.2, 37.0, 33.1, 32.6, 31.8, 31.2, 30.8, 30.6, 23.2, 22.5, 20.4,13.3. HRMS (ESI) $C_{24}H_{36}N_2O_4H^+$ *m*/*z*:: 417.2748 (expected), 417.2741 (found) IR (MeOH cast film) cm^{-1}: 2957.8, 2881.1, 1676.5, 1431.0, 1360.6, 1203.7, 1137.5, 835.8, 799.2, 721.8. $[\alpha]_D$: +114.1 (*c* 0.80, MeOH).

4.2. Biology

All experiments were performed with intact HEK-293 cells or homogenates of cells expressing recombinant human proteins. Construction of expression plasmids of 11β-HSD1 and 11β-HSD2 and of MR and reporter gene have been described earlier.[38,39] [1,2-^{3}H]-cortisone was purchased from American Radiolabeled Chemicals (St. Louis, MO), [1,2,6,7-^{3}H]-cortisol from Perkin Elmer (Waltham, MA, USA), cell culture media from Invitrogen (Carlsbad, CA), aldosterone from Steraloids (Wilton, NH, USA) and all other chemicals from Sigma–Aldrich Chemie GmbH (Buchs, Switzerland) of the highest grade available.

4.2.1. 11βHSD enzyme activity

Inhibition of 11βHSD enzyme activity was measured as described earlier.[10] Briefly, HEK-293 cells stably expressing human 11βHSD1 or 11βHSD2 were harvested by centrifugation and cell pellets were frozen and stored at −80 °C. Cell pellets were suspended in TS2 buffer (100 mM NaCl, 1 mM EGTA, 1 mM EDTA, 1 mM $MgCl_2$, 250 mM sucrose, 20 mM Tris–HCl, pH 7.4), sonicated and immediately used for activity assay. Cell lysates were incubated for 10 min at 37 °C in a final volume of 22 μL, containing either vehicle (0.2% DMSO) or the corresponding inhibitor. Inhibitors were diluted in TS2 buffer from stock solutions (10 mM in DMSO). To measure 11βHSD1 activity, the reaction mixture contained 200 nM [1,2-^{3}H]cortisone and 500 μM NADPH. 11βHSD2 activity was measured similarly at a final concentration of 50 nM [1,2,6,7-^{3}H] cortisol and 500 μM NAD^+. Reactions were stopped after 10 min by adding an excess of unlabeled cortisone and cortisol (2 mM each, in methanol). Steroids were separated by TLC, followed by scintillation counting and calculation of substrate conversion. Data were obtained from three independent experiments.

4.2.2. MR transactivation activity

The effect of compounds on the transcriptional activity of MR was measured as described earlier.[40] Briefly, 150,000 HEK-293 cells/well of a poly-L-lysine coated 24-well plate were incubated for 24 h, followed by transfection using calcium phosphate precipitation with pMMTV-lacZ β-galactosidase reporter (0.20 μg/well), pCMV-LUC luciferase transfection control (0.04 μg/well) and plasmid for human recombinant MR (0.35 μg/well). The medium was changed 6 h post-transfection and cells were incubated for another 18 h. Cells were washed twice with charcoal-treated DMEM containing 10% FBS and incubated with various concentrations of compounds in the absence of presence of 10 nM aldosterone and for 24 h. Cells were washed once with PBS and lysed with 50 μL lysis buffer of the Tropix kit (Applied Biosystems, Foster City, CA) supplemented with 0.5 mM dithiothreitol. Lysed samples were frozen at −80 °C prior to analysis of β-galactosidase activity using the Tropix kit and luciferase activity using a luciferine-solution. Data were normalized to the ratio of β-galactosidase to luciferase activity of the vehicle control and were obtained from three independent experiments.

4.2.3. Calculations and statistical analysis

Enzyme kinetics was analyzed by nonlinear regression using the four parameter logistic curve fitting. All data (mean ± SD) were obtained from at least three independent experiments and significance was assigned using the ratio *t*-test in the GraphPad Prism 5 software.

Acknowledgments

We thank Mark Miskolzie for assistance with NMR analysis, Dr. Angie Morales-Izquierdo and Dr. Randy Whittal for help with mass spectrometry, and Dr. Robert McDonald (University of Alberta) for crystallographic analysis of compound **3**. Funding for K.P., D.D., and J.C.V. was provided by the Natural Sciences Engineering and Research Council of Canada (NSERC) and by the Canada Research Chair in Bioorganic and Medicinal Chemistry. A.O. and J.S. were supported by the Swiss National Science Foundation Grant 31003A_140961. A.O. has a Chair for Molecular and Systems Toxicology by the Novartis Research Foundation.

Supplementary data

Supplementary data (Tables of crystallographic experimental details of **3**, along with structural diagrams) associated with this article can be found, in the online version, at http://dx.doi.org/10.1016/j.bmc.2013.08.068.

References and notes

1. Stewart, P. M.; Krozowski, Z. S. *Vitam. Horm.* **1999**, *57*, 249.
2. Odermatt, A.; Kratschmar, D. V. *Mol. Cell. Endocrinol.* **2012**, *350*, 168.
3. Masuzaki, H.; Paterson, J.; Shinyama, H.; Morton, N. M.; Mullins, J. J.; Seckl, J. R.; Flier, J. S. *Science* **2001**, *294*, 2166.
4. Paterson, J. M.; Morton, N. M.; Fievet, C.; Kenyon, C. J.; Holmes, M. C.; Staels, B.; Seckl, J. R.; Mullins, J. J. *Proc. Natl. Acad. Sci. U.S.A.* **2004**, *101*, 7088.
5. Stewart, P. M.; Wallace, A. M.; Valentino, R.; Burt, D.; Shackleton, C. H.; Edwards, C. R. *Lancet* **1987**, *2*, 821.
6. Farese, S.; Kruse, A.; Pasch, A.; Dick, B.; Frey, B. M.; Uehlinger, D. E.; Frey, F. J. *Kidney Int.* **2009**, *76*, 877.
7. Gaware, R.; Khunt, R.; Czollner, L.; Stanetty, C.; Da Cunha, T.; Kratschmar, D. V.; Odermatt, A.; Kosma, P.; Jordis, U.; Classen-Houben, D. *Bioorg. Med. Chem.* **2011**, *19*, 1866.
8. Beseda, I.; Czollner, L.; Shah, P. S.; Khunt, R.; Gaware, R.; Kosma, P.; Stanetty, C.; Del Ruiz-Ruiz, M. C.; Amer, H.; Mereiter, K.; Da Cunha, T.; Odermatt, A.; Classen-Houben, D.; Jordis, U. *Bioorg. Med. Chem.* **2010**, *18*, 433.
9. Stanetty, C.; Czollner, L.; Koller, I.; Shah, P.; Gaware, R.; Cunha, T. D.; Odermatt, A.; Jordis, U.; Kosma, P.; Classen-Houben, D. *Bioorg. Med. Chem.* **2010**, *18*, 7522.
10. Kratschmar, D. V.; Vuorinen, A.; Da Cunha, T.; Wolber, G.; Classen-Houben, D.; Doblhoff, O.; Schuster, D.; Odermatt, A. *J. Steroid Biochem. Mol. Biol.* **2011**, *125*, 129.
11. Pitt, B.; Remme, W.; Zannad, F.; Neaton, J.; Martinez, F.; Roniker, B.; Bittman, R.; Hurley, S.; Kleiman, J.; Gatlin, M. *N. Eng. J. Med.* **2003**, *348*, 1309.
12. Pitt, B.; Zannad, F.; Remme, W. J.; Cody, R.; Castaigne, A.; Perez, A.; Palensky, J.; Wittes, J. *N. Eng. J. Med.* **1999**, *341*, 709.
13. Zannad, F.; McMurray, J. J.; Krum, H.; van Veldhuisen, D. J.; Swedberg, K.; Shi, H.; Vincent, J.; Pocock, S. J.; Pitt, B. *N. Eng. J. Med.* **2011**, *364*, 11.
14. Bertocchio, J. P.; Warnock, D. G.; Jaisser, F. *Kidney Int.* **2011**, *79*, 1051.
15. van den Meiracker, A. H.; Baggen, R. G.; Pauli, S.; Lindemans, A.; Vulto, A. G.; Poldermans, D.; Boomsma, F. *J. Hypertens.* **2006**, *24*, 2285.
16. Sato, A.; Hayashi, K.; Naruse, M.; Saruta, T. *Hypertension* **2003**, *41*, 64.
17. Souness, G. W.; Latif, S. A.; Laurenzo, J. L.; Morris, D. J. *Endocrinology* **1995**, *136*, 1809.
18. Rafestin-Oblin, M. E.; Fagart, J.; Souque, A.; Seguin, C.; Bens, M.; Vandewalle, A. *Mol. Pharmacol.* **2002**, *62*, 1306.
19. Funder, J. W. *Curr. Hypertens. Rep.* **2007**, *9*, 112.
20. Salunke, D. B.; Hazra, B. G.; Pore, V. S. *Curr. Med. Chem.* **2006**, *13*, 813.
21. Szendi, Z.; Dombi, G.; Vincze, I. *Monatsh. Chem.* **1996**, *127*, 1189.
22. Lange, W. E.; Stein, M. E. *J. Pharm. Sci.* **1964**, *53*, 435.
23. Morris, D. J.; Latif, S. A.; Hardy, M. P.; Brem, A. S. *J. Steroid Biochem. Mol. Biol.* **2007**, *104*, 161.
24. Lecomte, V.; Stephan, E.; Vaissermann, J.; Jaouen, G. *Steroids* **2004**, *69*, 17.
25. Rausser, R.; Finckenor, C. G.; Weber, L.; Hershberg, E. B.; Oliveto, E. P. *J. Org. Chem.* **1966**, *31*, 1346.
26. Rausser, R.; Weber, L.; Hershberg, E. B.; Oliveto, E. P. *J. Org. Chem.* **1966**, *31*, 1342.
27. Dao, K. L.; Hanson, R. N. *Bioconjugate Chem.* **2012**, *23*, 2139.
28. Loibner, H.; Zbiral, E. *Helv. Chim. Acta* **1977**, *60*, 417.
29. Afonso, C. M.; Barros, M. T.; Godinho, L. S.; Maycock, C. D. *Tetrahedron* **1994**, *50*, 9671.
30. Salunke, D. B.; Ravi, D. S.; Pore, V. S.; Mitra, D.; Hazra, B. G. *J. Med. Chem.* **2006**, *49*, 2652.
31. Fringuelli, F.; Pizzo, F.; Vaccaro, L. *Synthesis* **2000**, 646.
32. Ottenheijm, H. C. J.; Plate, R.; Noordik, J. H.; Herscheid, J. D. M. *J. Org. Chem.* **1982**, *47*, 2147.
33. Diaper, C. M.; Sutherland, A.; Pillai, B.; James, M. N. G.; Semchuk, P.; Blanchard, J. S.; Vederas, J. C. *Org. Biomol. Chem.* **2005**, *3*, 4402.
34. Liu, H. Q.; Pattabiraman, V. R.; Vederas, J. C. *Org. Lett.* **2007**, *9*, 4211.
35. Chhabra, S. R.; Mahajan, A.; Chan, W. C. *J. Org. Chem.* **2002**, *67*, 4017.
36. Galigniana, M. D.; Vicent, G. P.; Burton, G.; Lantos, C. P. *Steroids* **1997**, *62*, 358.
37. Wolff, H. *Organic Reactions*; John Wiley and Sons: New York, 1959.
38. Odermatt, A.; Arnold, P.; Stauffer, A.; Frey, B. M.; Frey, F. J. *J. Biol. Chem.* **1999**, *274*, 28762.
39. Odermatt, A.; Arnold, P.; Frey, F. J. *J. Biol. Chem.* **2001**, *276*, 28484.
40. Chantong, B.; Kratschmar, D. V.; Nashev, L. G.; Balazs, Z.; Odermatt, A. *J. Neuroinflamm.* **2012**, *9*, 260.

4. Chapter 2: Effects of 3,4-methylenedioxymethamphetamine and methylphenidate on circulating steroids in healthy humans

Introduction

The illicit, recreational drug 3,4-methylenedioxymethamphetamine (MDMA) or “ecstasy” is a powerful central nervous system stimulant, mostly used by dance clubbers, which can generate feelings of euphoria, energy surge, elevated mood, enhanced bonding with others and psychedelic effects [47]. However, MDMA abuse also has many, though rare, adverse effects, such as liver damage, extended depressed mood, rhabdomyolysis, serotonin syndrome, multiorgan failure, cardiovascular events, arrhythmias and death caused by dehydration [48]. Nevertheless, the recreational drug was suggested as treatment for post-traumatic stress disorder (PTSD) [49]. However, because of the possible side effects, pharmaceutical use of MDMA is questionable [50]. MDMA is a methamphetamine derivative with many similarities to the parent compound. It has a particular affinity for the serotonin transporter and can release up to 80% of available serotonin, but like methamphetamine, it also stimulates the release of dopamine, norepinephrine and other neurotransmitters [51]. Many studies show that MDMA triggers changes in hypothalamic–pituitary–adrenal (HPA) axis, resulting in the increased release of adrenocorticotropic hormone (ACTH) and glucocorticoids, such as the hormone cortisol. Several studies in humans supported this hypothesis by showing increased levels of plasma cortisol following MDMA administration [52-54]. In a controlled study under laboratory conditions in healthy volunteers, an acute MDMA use increased cortisol levels by 50-100 % [53]. Several investigators tested the changes in cortisol levels in dance clubbers before and after MDMA use and found up to an 800% increase in cortisol levels [54]. Since glucocorticoids are involved in a wide range of psychobiological functions including memory, sleep, appetite, impulsivity, neuronal damage, and hippocampal activity, the suggested changes in HPA axis activity may be involved in many of the diverse effects of recreational ecstasy [53, 55]. The effects of MDMA on other steroid hormones has also been studied, but mostly in small cohorts of human subjects or animal studies and some of the results are contradictive. MDMA intake was reported to suppress the hypothalamic-pituitary-gonadal (HPG) reproductive axis of male rats, resulting in, amongst others a decrease in testosterone levels [56]. However, a study performed in dance clubbers showed increased levels of the androgen testosterone [52]. Furthermore plasma dehydroepiandrosterone (DHEA), a precursor for androgens as well as estrogens, was found to be increased in experienced volunteers (regular MDMA users) after ecstasy intake [57]. The mineralocorticoid aldosterone was also shown to be increased in rats after acute administration [58]. However, the effects of MDMA on a wider range of corticosteroids have not yet been studied in humans. To better understand the effects of MDMA on the brain there is a need to measure the steroid hormones in human plasma following MDMA administration.

In contrast to MDMA, methylphenidate (MPH), a piperidine derivative structurally related to amphetamines, exerts its psychomotor stimulant effects via dopamine and norepinephrine but not through serotonin. MPH is used in the clinic for the treatment of attention-deficit/hyperactivity disorder (ADHD), the most common behavioral disorder during childhood and adolescence. However, MPH is also misused as a cognitive enhancer primarily among university students [59]. The beneficial effects of MPH on ADHD patients include the reduction of impulsivity and the improvement of disruptive behavior, sustained attention, short-term memory and social responsiveness [60]. Several human studies reveal that MPH treatment influence the neuroendocrine systems, thus affect the levels of DHEA, testosterone and cortisol [59, 61, 62]. This suggests that the therapeutic effects of MPH in ADHD treatment may be through changes in steroid levels. DHEA and DHEA-S are precursors for sex hormones; however, they also exert multiple effects on the central nervous system (CNS), affecting emotion and mood, neural plasticity, neuroprotection, sleep, inhibiting aggressive-impulsive behavior, improving attention and memory. Previously, significant inverse correlations between clinical symptomatology and levels of DHEA in humans with ADHD were indicated. The beneficial effects of MPH were suggested to be linked with increasing DHEA levels [60, 63]. However, the global effects of MPHs on the steroidal system remain unknown. Additionally, several studies show the influence of MPH in human development is critical. Chronic exposure to MPH during development showed changes in behavior as well as in steroid hormone plasma levels in developing rats [64, 65]. MPH treatment was also linked with puberty delay in male non-human primates [66]. These results highlight the need for further research, to improve understanding of the effects of stimulants on the developing nervous system and the potential lasting effects resulting from drug exposure in early life phases. Steroid hormones may play a key role in the therapeutic and adverse effects of MPH.

Since MDMA and MPH are widely misused drugs and pharmacodynamic interactions of both are likely, the comparison between the combined intake versus a single drug administration could give insights into mechanism of the beneficial as well as the unwanted side effects. Additionally, the combination of both drugs in a single study may be of clinical importance for assessing the risks of combined psychostimulant misuse. Given that serotonin release plays a role in MDMA, but not in the MPH mechanism of action, the comparison of both drugs might provide further information as to their underlying mechanisms. Since both, MDMA and MPH share an enhancing effect on norepinephrine neurotransmission, resulting in sympathomimetic and psychostimulant effects, and they are otherwise indirect serotonergic or dopaminergic agonists, it makes them promising pharmacological molecules to evaluate the role of serotonin and dopamine as activators of the HPA axis. In a study performed in healthy volunteers MPH and MDMA shared some subjective amphetamine-type effects; however, MDMA increased positive mood more than MPH and MPH enhanced activity and concentration more than MDMA. Besides, the combined use of MPH and MDMA did not show an increase in psychoactive effects compared with either drug alone, but potentially enhanced cardiovascular and adverse effects [67].

The second project of this thesis focused on the measurement of eleven steroid hormones in plasma samples of healthy volunteers after a single dose intake of MDMA, MPH or a combination of both (Figure

5) in collaboration with Dr. M. Liechti and coworkers. The steroid panel consisted of hormones from the mineralocorticoid, glucocorticoid as well as androgen family. During the study performed by Dr. C Hysek, 16 subjects (8 men, 8 women) were treated with MDMA (125 mg), MPH (60 mg), MDMA + MPH and placebo on 4 separate days using a double-blind, cross-over study design. Plasma samples were taken 1 hour prior and 0, 0.33, 0.67, 1, 1.5, 2, 2.5, 3, 3.5, 4, 6, 8, and 24 h following the administration of the drugs or placebo. I supported the study by extracting, measuring and quantitating the following steroids: cortisol, cortisone, corticosterone, 11-dehydrocorticosterone, aldosterone, 11-deoxycorticosterone (DOC), dehydroepiandrosterone (DHEA), dehydroepiandrosterone sulfate (DHEAS), androstenedione and testosterone.

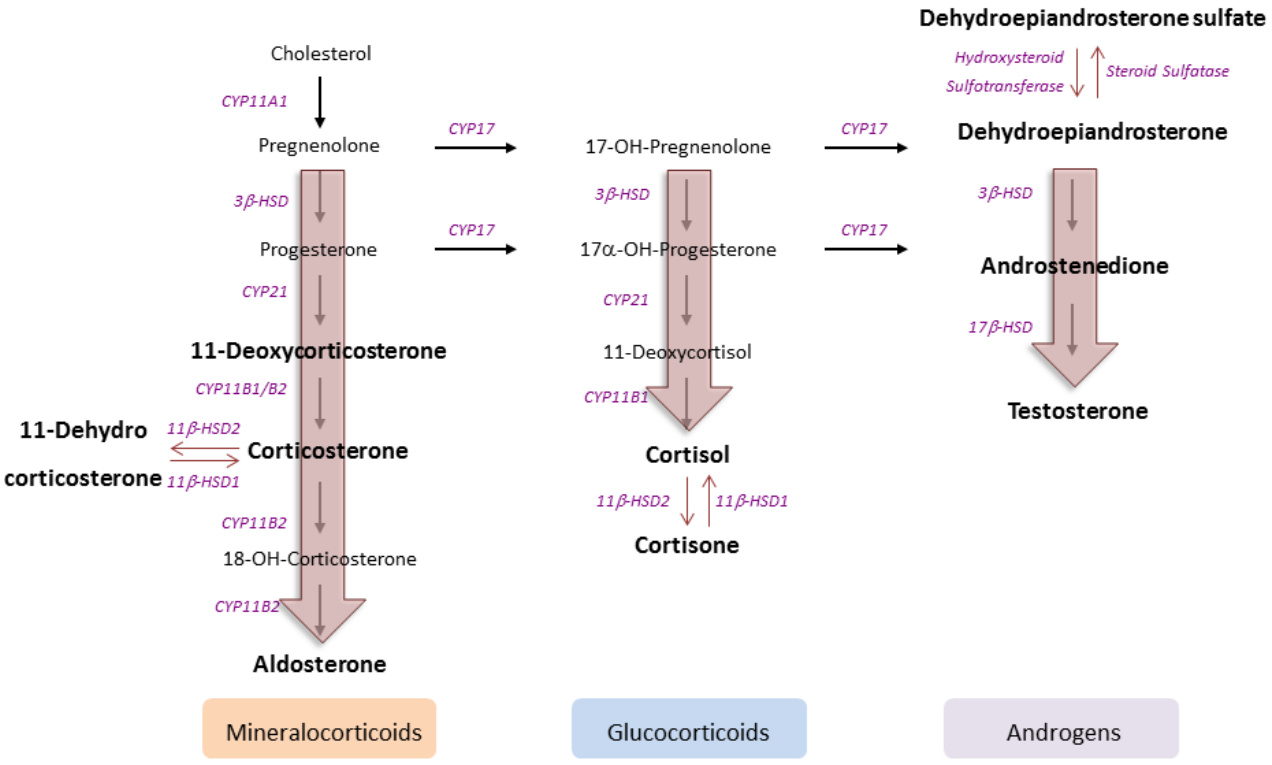

Figure 5: Steroidogenesis of mineralocorticoids, glucocorticoids and androgens. Highlighted steroids were measured with LC-MS/MS (modified after KEGG [68]).

Low-dose steroids may provide insights into the function and effects of psychoactive drugs. However, the extremely low levels of some steroids in plasma and the insufficient sensitivity/selectivity of current analytical methods depict a significant challenge for the evaluation of steroid plasma levels. Therefore, a method for an ultrasensitive quantification of steroids in plasma samples was developed. The basis of the analyses performed in this study was an ultra-pressure liquid chromatography tandem mass spectrometry (UPLC-MS/MS) method developed and validated with the help of Dr. C. Penno. This was achieved by the combination of a selective solid-phase extraction (SPE) with a highly sensitive UPLC-MS/MS analysis. To validate the quality of the newly developed method we determined the extraction efficiency with five

replicates of untreated pooled human plasma, which were extracted twice consecutively. Extraction efficiency was determined by comparing the amount of steroid extracted in both procedures. Values of lower limit quantification (LLOQ) were obtained by assessing the signal to noise (SNR) ratio at lower calibration range. A signal equal or higher than five times that of the baseline was considered the LLOQ, with accuracy between 80 and 120% of the true value and coefficient of variation of 20%. Identical criteria were used to determine the SNR of a given sample. To determine intra-day precision and accuracy, quality assessment of the method was performed with untreated human plasma samples (quality control 1 (QC1)) spiked with known concentrations of steroids (QC2 and QC3) using 5 replicates, respectively (Table 1). To summarize our sample extraction and UPLC-MS/MS method generated reliable and reproducible results. The only exception was DHEAS, which showed a recovery rate of only approximately 50% following extraction. Due to the low extraction recovery and the fact that the measured DHEAS values were low, these values should only be used for qualitative comparison.

				Precision (coefficient of variation %)		
Steroid hormone	Extraction Efficiency (%)	LLOQ (nM)	SNR	QC1 (Endogenous)	QC2 (spiked with +50% of endogenous)	QC3 (spiked with +100% of endogenous)
Cortisol	88 ± 1	0.2	11 ± 2	4	4.4	3
Cortisone	92 ± 2	0.2	10 ± 3	4	4.4	3
Corticosterone	90 ± 2	0.2	10 ± 1	7.4	6	4.8
11-Dehydrocorticosterone	85 ± 2	0.06	12 ± 2	15.5	8.5	7.6
Aldosterone	86 ± 4	0.2	6 ± 2	11.2	5.6	18
DOC	88 ± 2	0.2	6 ± 2	8.7	6.4	10.7
Androstenedione	96 ± 7	0.2	21 ± 3	7	10.5	7.3
Testosterone	97 ± 4	0.3	25 ± 4	6.7	4	6.9
DHEA	98 ± 4	1	7 ± 2	14	4.6	8.9
DHEAS	49 ± 2	3	8 ± 3	1.8	7.8	7.9

Table 1: Method qualification LC-MS/MS 12 steroids measurement including assessed extraction efficiency, LLOQ, SNR as well as precision

Results and Discussion

Following rigorous quality control and development of the UPLC-MS/MS method, the measurement of the steroid hormones cortisol, cortisone, corticosterone, 11-dehydrocorticosterone, aldosterone, DOC, DHEA, DHEAS, androstenedione and testosterone were performed. MDMA significantly increased the plasma concentrations of cortisol by over 60% compared to control, which is comparable to what was reported earlier [54]. The dramatic differences between plasma cortisol levels following MDMA intake reported in dance clubbers versus the clinically assessed volunteers could be a consequence of environmental as well as physical factors such as temperature, crowding and prolonged dancing, which may also influence the psychobiological effects of MDMA [55]. Another important co-factor is the regular use of MDMA compared with healthy volunteers screened and identified as drug naive. Additionally, the possible use of other psychoactive drugs by dance clubbers, including alcohol, amphetamine, cannabis, cocaine and nicotine could play a role in the more pronounced change of cortisol levels. Circadian rhythm, sleeping habits and stress of the volunteers may also play a role in the differences observed [69]. Furthermore, corticosterone, 11 dehydrocorticosterone, and DOC plasma levels increased, supporting the hypothesis that MDMA can influence changes in the HPA axis, thus resulting in increased release of glucocorticoids. On the other hand, the glucocorticoid cortisone showed no change. Notably, MDMA increased both the sum of cortisol + cortisone levels and cortisol/cortisone ratio, suggesting an increase in HPA axis stimulation and possibly reduced or saturated 11β-HSD2 enzyme function. The 11β-HSD2 enzyme catalyzes the reduction of the active glucocorticoid cortisol to the inactive form cortisone [70]. MDMA also moderately increased aldosterone levels compared with placebo. Interestingly, significant positive correlations were found between the MDMA-induced peak elevation of DOC, a mineralocorticoid precursor, and aldosterone and the peak increase in systolic blood pressure ($R_s = 0.38$ and 0.40, respectively, both $p < 0.05$, $n = 30$), which supports a role for of MDMA in mineralocorticoid action [67]. On the other hand, MDMA did not alter the levels of DHEA, DHEAS, androstenedione or testosterone. Compared to placebo, MPH did not affect any of the steroid concentrations and it neither synergized nor inhibited the effects of MDMA on circulating steroids. In the context of recreational drug use, steroid hormones such as cortisol or DHEA may contribute to or modulate substance-induced acute psychotropic and reinforcing effects [71]. For example, MDMA-induced increases in plasma cortisol levels have previously been shown to correlate with subjective “drug liking” in response to MDMA in a laboratory study [57]. Stress-induced increases in cortisol were also correlated with positive mood responses to other recreational drugs [72]. In summary, the serotonin releaser MDMA has acute effects on circulating steroids. These effects are not observed after stimulation of the dopamine and norepinephrine systems as with MPH. The present findings support the view that serotonin rather than dopamine and norepinephrine mediates the acute pharmacologically induced stimulation of the HPA axis in absence of other stressors.

Publication: Acute effects of 3,4-methylenedioxymethamphetamine and methylphenidate on circulating steroid levels in healthy subjects.

Original Paper

Neuro
-endocrinology

Neuroendocrinology 2014;100:17–25
DOI: 10.1159/000364879

Received: March 19, 2014
Accepted after Revision: May 26, 2014
Published online: June 5, 2014

Acute Effects of 3,4-Methylenedioxymethamphetamine and Methylphenidate on Circulating Steroid Levels in Healthy Subjects

Julia Seibert[a] Cédric M. Hysek[b] Carlos A. Penno[a] Yasmin Schmid[b]
Denise V. Kratschmar[a] Matthias E. Liechti[b] Alex Odermatt[a]

[a]Swiss Center for Applied Human Toxicology and Division of Molecular and Systems Toxicology, Department of Pharmaceutical Sciences, University of Basel, and [b]Psychopharmacology Research Group, Division of Clinical Pharmacology and Toxicology, Department of Biomedicine and Department of Clinical Research, University Hospital and University of Basel, Basel, Switzerland

Key Words
MDMA · Methylphenidate · Steroid · Cortisol · Aldosterone · Testosterone

Abstract
3,4-Methylenedioxymethamphetamine (MDMA, 'ecstasy') and methylphenidate are widely used psychoactive substances. MDMA primarily enhances serotonergic neurotransmission, and methylphenidate increases dopamine but has no serotonergic effects. Both drugs also increase norepinephrine, resulting in sympathomimetic properties. Here we studied the effects of MDMA and methylphenidate on 24-hour plasma steroid profiles. 16 healthy subjects (8 men, 8 women) were treated with single doses of MDMA (125 mg), methylphenidate (60 mg), MDMA + methylphenidate, and placebo on 4 separate days using a cross-over study design. Cortisol, cortisone, corticosterone, 11-dehydrocorticosterone, aldosterone, 11-deoxycorticosterone, dehydroepiandrosterone (DHEA), dehydroepiandrosterone sulfate (DHEAS), androstenedione, and testosterone were repeatedly measured up to 24 h using liquid chromatography-tandem mass spectroscopy. MDMA significantly increased the plasma concentrations of cortisol, corticosterone, 11-dehydrocorticosterone, and 11-deoxycorticosterone and also tended to moderately increase aldosterone levels compared with placebo. MDMA also increased the sum of cortisol + cortisone and the cortisol/cortisone ratio, consistent with an increase in glucocorticoid production. MDMA did not alter the levels of cortisone, DHEA, DHEAS, androstenedione, or testosterone. Methylphenidate did not affect any of the steroid concentrations, and it did not change the effects of MDMA on circulating steroids. In summary, the serotonin releaser MDMA has acute effects on circulating steroids. These effects are not observed after stimulation of the dopamine and norepinephrine systems with methylphenidate. The present findings support the view that serotonin rather than dopamine and norepinephrine mediates the acute pharmacologically induced stimulation of the hypothalamic-pituitary-adrenal axis in the absence of other stressors.

J. Seibert, C.M. Hysek, M.E. Liechti and A. Odermatt contributed equally to this work.

Matthias E. Liechti
Division of Clinical Pharmacology and Toxicology
University Hospital Basel, Hebelstrasse 2
CH–4031 Basel (Switzerland)
E-Mail matthias.liechti@usb.ch

Alex Odermatt
Division of Molecular and Systems Toxicology
Department of Pharmaceutical Sciences, University of Basel, Klingelbergstrasse 50
CH–4056 Basel (Switzerland)
E-Mail alex.odermatt@unibas.ch

KARGER

E-Mail karger@karger.com
www.karger.com/nen

0028–3835/14/1001–0017$39.50/0

Introduction

Many recreational drugs activate the hypothalamic-pituitary-adrenal (HPA) axis to release adrenocorticotropic hormone (ACTH) and corticosteroids [1]. The neurochemical mechanisms involved in HPA axis activation depend on the particular drug and mostly involve corticotropin-releasing factor stimulation in the hypothalamus [1–3]. HPA axis activation by cocaine and amphetamine and its derivatives is thought to be mediated by increases in brain monoamines, including dopamine (DA), norepinephrine (NE), and serotonin (5-hydroxytryptamine, 5-HT) [1]. Few studies have examined which of these monoamines contribute the most to HPA axis activation in animals [1], and even less data are available for humans. For example, cocaine inhibits the uptake of all three monoamines (DA, NE, and 5-HT), and all three may be involved in cocaine-induced HPA axis activation. Dopaminergic and adrenergic receptor antagonists reduced the corticosterone response to cocaine in rodents [4–6]. Additionally, the blockade of 5-HT receptors also decreased the ACTH response to cocaine in rats [5].

3,4-Methylenedioxymethamphetamine (MDMA; 'ecstasy') primarily releases 5-HT in the brain via the serotonin transporter (SERT) and NE via the NE transporter (NET) [7]. Methylphenidate is an amphetamine derivative used for the treatment of attention-deficit/hyperactivity disorder and misused as a cognitive enhancer and recreationally. In contrast to MDMA, methylphenidate only elevates the levels of DA and NE by inhibiting the DA transporter and NET [8]. Thus, both MDMA and methylphenidate share an enhancing effect on NE neurotransmission, resulting in sympathomimetic and psychostimulant effects [9], but they are otherwise indirect serotonergic or dopaminergic agonists, making them pharmacological tools to evaluate the role of 5-HT and DA as activators of the HPA axis.

Several studies evaluated the stimulant effects of MDMA on the HPA axis in humans [for reviews, see 10, 11]. Plasma cortisol has been shown to be increased after MDMA administration in many human laboratory studies [12–15] and in recreational ecstasy users following MDMA administration in a club setting [16, 17]. Small laboratory studies also previously reported MDMA-induced increases in ACTH [18] and dehydroepiandrosterone (DHEA) [12]. A trend toward an increase in testosterone was also found in subjects who used MDMA at a dance club [16]. However, the effects of MDMA on a wider range of corticosteroids have not yet been studied in humans. Therefore, we evaluated the acute effects of predominantly 5-HT activation using MDMA or predominantly DA activation using methylphenidate or MDMA + methylphenidate on changes in the plasma concentration of a series of steroids over 24 h in healthy subjects. Specifically, we measured the plasma levels of glucocorticoids (cortisol, cortisone, corticosterone, and 11-dehydrocorticosterone), mineralocorticoids (aldosterone and 11-deoxycorticosterone), and androgens (DHEA, DHEA sulfate (DHEAS), androstenedione, and testosterone). Cortisol is the main active glucocorticoid and a major stress hormone. It is converted to the inactive metabolite cortisone. Corticosterone is also a potent activator of glucocorticoid and mineralocorticoid receptors, but it is present at 10- to 20-times lower concentrations than cortisol in humans. 11-Deoxycorticosterone is a precursor of corticosterone and aldosterone and exhibits mineralocorticoid activity [19]. Mineralocorticoids increase renal sodium absorption and blood pressure. Androgens may modulate the addictive effects of drugs of abuse [12, 20, 21]. We hypothesized that methylphenidate and MDMA would differentially affect the plasma levels of these steroids based on their different pharmacological profiles.

Methods

Study Design

The study used a double-blind, placebo-controlled, cross-over design with four experimental test sessions (placebo-placebo, methylphenidate-placebo, placebo-MDMA, and methylphenidate-MDMA) performed in counterbalanced order according to a Latin square randomization scheme. All of the subjects received all of the study treatments in a within-subjects study design. The washout periods between sessions were at least 10 days. The study was conducted in accordance with the Declaration of Helsinki and International Conference on Harmonization Guidelines in Good Clinical Practice and approved by the local Ethics Committee and Swiss Agency for Therapeutic Products (Swissmedic). The study was registered at ClinicalTrials.gov: http://clinicaltrials.gov/ct2/show/NCT01465685. All of the subjects provided written informed consent.

Participants

Sixteen healthy subjects (8 men and 8 women; mean ± SD age 24.8 ± 2.6 years) were recruited from the University of Basel campus. The exclusion criteria were acute or chronic physical illness, psychiatric disorders, smoking, and a lifetime history of using illicit drugs more than 5 times, with the exception of past cannabis use. The use of any illicit drugs, including cannabis, within the past 2 months or during the study period was prohibited. We performed urine drug tests at screening and before each test session using Triage® 8 (Biosite, San Diego, Calif., USA). Female participants were investigated during the follicular phase of their men-

strual cycle (days 2–14) to account for cyclic changes in the reactivity to amphetamines. A detailed description of the participants has been previously published [9].

Study Procedures

Methylphenidate (60 mg, Ritalin®; Novartis, Bern, Switzerland) or placebo was administered orally at 08:00 h. MDMA (125 mg, racemic MDMA hydrochloride; Lipomed, Arlesheim, Switzerland) or placebo was administered orally at 09:00 h. A standardized lunch was served at 12:00 h, and the subjects were sent home at 18:00 h. The day following each test session, the participants returned to the research ward at 09:00 h for the collection of the 24-hour blood sample. The subjects did not engage in any physical activity and were resting in hospital beds during the test session. Blood samples for the analysis of plasma steroid hormone levels (cortisol, cortisone, corticosterone, 11-dehydrocorticosterone, 11-deoxycorticosterone, aldosterone, DHEA, DHEA-S, androstenedione, and testosterone) were collected 1 h prior to MDMA or placebo administration and 0, 0.33, 0.67, 1, 1.5, 2, 2.5, 3, 3.5, 4, 6, 8, and 24 h following the administration of MDMA or placebo. The psychotropic and autonomic effects of MDMA and methylphenidate from the present study have been presented elsewhere [9].

Steroid Quantification

A detailed description of the materials, procedure, and method validation is included in the see online supplementary material (for all online suppl. material, see www.karger.com/doi/10.1159/000364879). Briefly, plasma samples (1 ml) were mixed with 200 µl precipitation solution (0.8 M zinc sulfate in water/methanol and deuterium-labeled aldosterone, cortisol, corticosterone, and testosterone as internal standards), diluted with water to 2 ml and centrifuged again. The supernatants were subjected to Oasis HBL SPE cartridges for purification. The samples were reconstituted in 25 µl methanol. Steroids were separated and quantified by ultra-pressure liquid chromatography-tandem mass spectroscopy (UPLC-MS/MS) using an Agilent 1290 UPLC coupled to an Agilent 6490 triple quadrupole MS equipped with an electrospray ionization source (Agilent Technologies, Basel, Switzerland). The separation of analytes was achieved using a reverse-phase column (ACQUITY UPLC™ BEH C_{18}, 1.7 µm, 2.1, 150 mm; Waters, Wexford, Ireland). Mass Hunter software (Agilent Technologies) was used for data acquisition and analysis. For method validation, see online supplementary material.

Statistical Analyses

Peak concentration (C_{max}) values were determined for all repeated measures. Repeated-measures analyses of variance (ANOVAs) with the within-subject factors MDMA (MDMA vs. placebo) and methylphenidate (methylphenidate vs. placebo), followed by the Tukey post hoc tests based on significant main effects of interactions in the ANOVA were used to assess differences in the effect of the different treatment conditions. Associations were assessed using Spearman's rank correlations. One subject was excluded from the correlational analyses because of missing values. Because the effects of MDMA were similar regardless of whether MDMA was administered alone or combined with methylphenidate, the data were pooled for the correlational analyses (n = 30). The significance level was set to $p = 0.05$. The statistical analysis was performed using R project statistical packages (R Foundation for Statistical Computing, Vienna, Austria).

Results

The peak levels of plasma steroid hormone concentrations and statistics are shown in table 1. MDMA significantly increased the plasma levels of the glucocorticoids cortisol, corticosterone, and 11-dehydrocorticosterone and mineralocorticoid 11-deoxycorticosterone compared with placebo (fig. 1a, c–e) but not the glucocorticoid cortisone (fig. 1b). MDMA also significantly increased the sum of cortisol + cortisone and cortisol/cortisone ratio (table 1). The sum of corticosterone + 11-dehydrocorticosterone was also significantly elevated (data not shown), further supporting the increase in glucocorticoid production. The levels of the mineralocorticoid aldosterone were increased by MDMA (significant main effect) but this effect was only significant for the MDMA + methylphenidate condition compared with placebo (fig. 1f). MDMA did not significantly alter the circulating levels of the androgens DHEA, DHEAS, androstenedione, or testosterone (fig. 2a–e). For unknown reasons the absolute values obtained for DHEAS were lower than expected, allowing qualitative comparison only. Methylphenidate did not affect any of the measured glucocorticoid, mineralocorticoid, or androgen hormones compared with placebo (fig. 1, 2). Administration of MDMA + methylphenidate led to similar hormonal responses compared with MDMA alone (fig. 1, 2), with the exception of a more robust and significant increase in aldosterone. There were no interactive effects of MDMA and methylphenidate on steroid levels. As expected, testosterone levels were lower in women than in men. No sex differences were observed in the effects of the drugs on steroid levels. However, significant positive correlations were found between the MDMA-induced peak elevation of 11-deoxycorticosterone and aldosterone and the peak increase in systolic blood pressure ($R_s = 0.38$ and 0.40, respectively, both $p < 0.05$, $n = 30$) [9]. None of the steroid levels (peak or area under the concentration-time curve changes from baseline) correlated with the simultaneously recorded psychotropic effects of MDMA including 'good drug effects', 'drug liking', 'drug high', 'happy', and 'stimulated' that have been reported previously [9]. The time from MDMA administration to C_{max} for cortisol, corticosterone, 11-dehydrocorticosterone, 11-deoxycorticosterone, and aldosterone was 2.1 ± 0.8, 1.8 ± 0.6, 2.0 ± 0.6, 1.5 ± 0.5 h and 2.1 ± 1.5 h (mean ± SD), respectively. The time to C_{max} for MDMA was 2.4 ± 0.4 h [9]. The MDMA-induced acute increases in circulating steroids generally disappeared within 6 h after drug administration. The plasma levels of cortisol, determined by UPLC-MS/MS (present findings) or radioimmunoas-

Table 1. Absolute peak plasma steroid concentrations and statistics

	Placebo-placebo (mean ± SE)	Placebo-MDMA (mean ± SE)	Methylphenidate-placebo (mean ± SE)	Methylphenidate-MDMA (mean ± SE)	MDMA		Methylphenidate		Methylphenidate × MDMA	
					$F_{1,16}$	p value	$F_{1,16}$	p value	$F_{1,16}$	p value
Glucocorticoids										
Cortisol, nM	463±53	770±45***	556±54	765±43***	43.47	<0.001	3.05	0.10	2.39	0.14
Cortisone, nM	36.7±1.8	40.9±2.7	43.4±3.0	42.6±2.2	0.34	0.57	3.65	0.08	1.39	0.26
Corticosterone, nM	8.4±1.5	29.7±2.4***	12.8±2.4###	26.1±3.6***	46.35	<0.001	0.05	0.82	2.54	0.13
11-Dehydrocorticosterone, nM	2.0±0.3	5.1±0.4***	2.9±0.4###	5.2±0.5***	45.49	<0.001	4.75	0.05	1.65	0.22
Cortisol + cortisone	499±52	796±45***	582±54###	802±43***	43.47	<0.001	3.05	0.10	1.46	0.25
Cortisol/cortisone ratio	15.8±1.7	24.8±1.5***	16.6±1.5###	23.21±1.46***	26.77	<0.001	0.29	0.60	1.24	0.28
Mineralocorticoids										
Aldosterone, nM	0.16±0.04	0.25±0.06	0.17±0.04	0.33±0.11*	5.56	0.03	1.02	0.33	1.14	0.30
11-Deoxycorticosterone, nM	0.21±0.06	0.42±0.08**	0.26±0.07#	0.44±0.08***	14.57	0.002	0.86	0.37	0.16	0.69
Androgens										
DHEA, nM	24.7±6.6	24.6±3.5	19.7±2.4	23.7±3.4	0.69	0.42	0.95	0.35	0.27	0.61
DHEAS, nM	787±75	1.036±103	954±140	1,032±98	2.81	0.11	1.74	0.21	1.28	0.28
Androstenedione, nM	6.0±1.1	7.5±1.0	6.4±0.8	7.3±0.9	3.69	0.07	0.13	0.73	0.78	0.39
Testosterone in women, nM	0.59±0.25	0.55±0.14	0.45±0.19	0.57±0.10	0.07[a]	0.80	0.65[a]	0.45	0.45[a]	0.53
Testosterone in men, nM	11.8±4.4	13.0±3.9	14.0±4.3	13.0±4.0	0.00[a]	0.97	2.35[a]	0.17	3.03[a]	0.13

Values are peak concentrations (mean ± SEM) of 16 subjects. * For $p < 0.05$, ** for $p < 0.01$, and *** for $p < 0.001$ compared to placebo-placebo. # For $p < 0.05$, and ### for $p < 0.001$ compared to placebo-MDMA (Tukey post hoc tests based on significant main effects in the ANOVAs).

[a] $F_{1,7}$ (8 instead of 16 subjects).

say [9], at the 2 h time point after MDMA administration were significantly correlated across all measurements ($R_s = 0.77$, $p < 0.001$, respectively, $n = 64$).

Discussion

The present study provides insights into the acute effects of two sympathomimetic drugs or pharmacological stressors on the plasma levels of a series of steroids in healthy humans. MDMA increased the plasma levels of the glucocorticoid cortisol. MDMA also increased the plasma levels of corticosterone and the inactive steroid 11-dehydrocorticosterone, which is known to change in parallel with cortisol [22]. Although circulating concentrations of corticosterone are lower than those of cortisol, a significantly increased ratio of corticosterone to cortisol was observed in the brain as a result of differential transport by the P-glycoprotein at the blood-brain barrier [23]. MDMA had no effect on the inactive cortisol metabolite cortisone, which is produced by 11β-hydroxysteroid dehydrogenase (11β-HSD) type 2, mainly in the kidney, and the reverse reaction is catalyzed by 11β-HSD1 [24]. Notably, MDMA increased both the sum of cortisol + cortisone levels and cortisol/cortisone ratio, suggesting an increase in HPA axis stimulation and possibly reduced or saturated 11β-HSD2 enzyme function [25]. A high cortisol/cortisone ratio has also been observed after acute ACTH administration and in patients with chronic ACTH hypersecretion [25]. In contrast, a low cortisol/cortisone ratio characterizes adrenal insufficiency [26]. MDMA also increased the levels of the mineralocorticoids 11-deoxycorticosterone and aldosterone, an effect that reached significance for the latter only when MDMA was co-administered with methylphenidate. The mineralocorticoids, including aldosterone and 11-deoxycorticosterone, physiologically increase renal sodium absorption and blood pressure. We observed a significant association between MDMA-induced increases in mineralocorticoids and increases in systolic blood pressure. However, MDMA does not alter plasma sodium levels or plasma osmolality as shown in a previous study [27]. This finding would be well explained by the fact that MDMA also increases plasma arginine vasopressin [27, 28], which increases water retention and therefore has similar effects on blood pressure as aldosterone but opposite effects on plasma sodium levels. In fact, MDMA tended to increase urine osmolality [27]. In the present study, MDMA did not affect the concentrations of the androgens DHEA, DHEAS, androstenedione, or testosterone. Methylphenidate alone did not increase

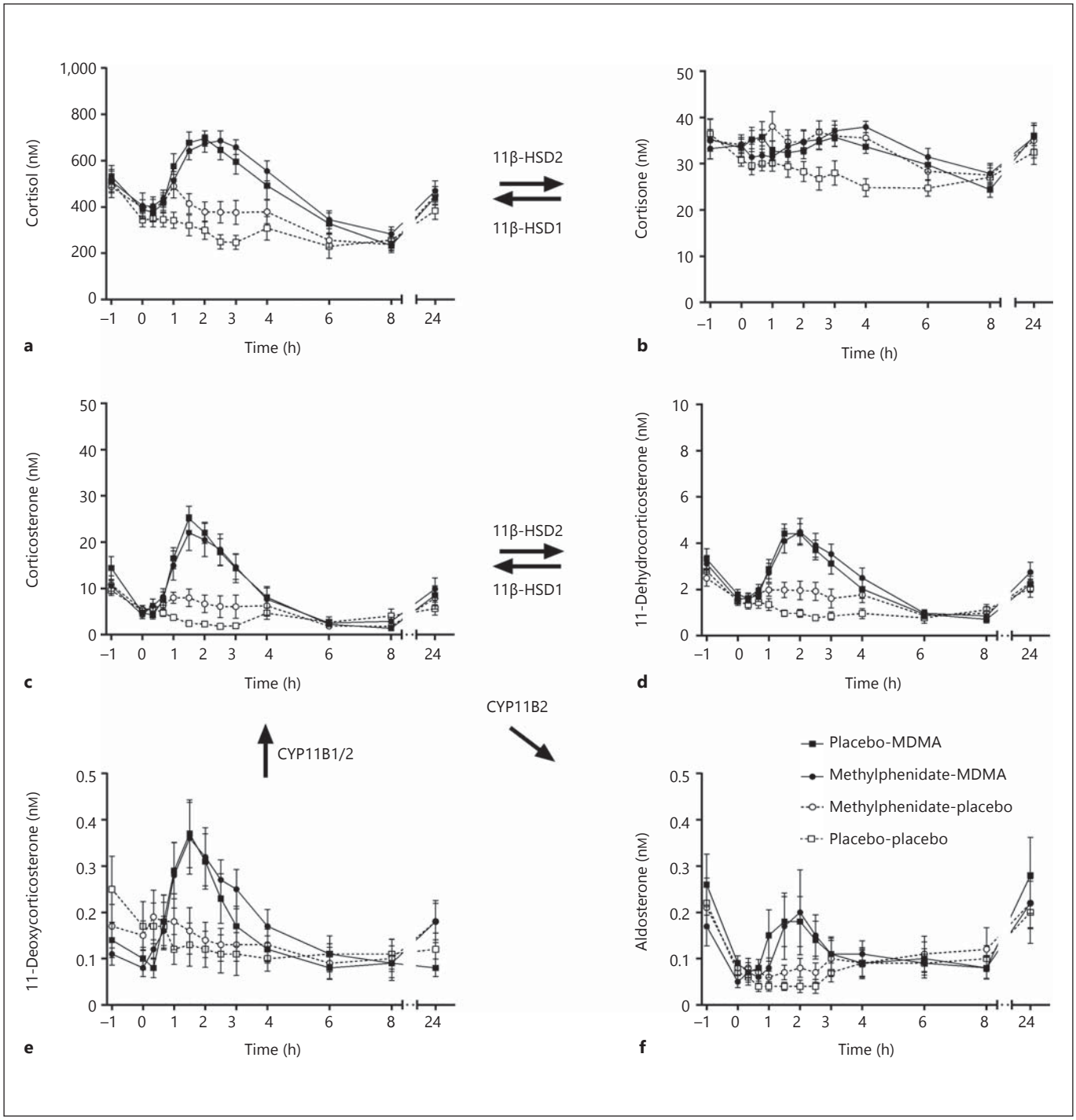

Fig. 1. a–f Effects of MDMA and methylphenidate on plasma concentration-time profiles of glucocorticoids and mineralocorticoids. The values are expressed as mean ± SEM in 16 subjects. MDMA was administered at t = 0 h. Methylphenidate was administered at t = –1 h. MDMA significantly increased the plasma concentrations of cortisol (**a**), corticosterone (**c**), 11-dehydrocorticosterone (**d**), and weak mineralocorticoid 11-deoxycorticosterone (**e**) but not the non-bioactive glucocorticoid cortisone (**b**). MDMA also tended to moderately increase the plasma levels of the mineralocorticoid aldosterone (**f**). Similar changes in plasma steroid levels were induced regardless of whether MDMA was administered alone or combined with methylphenidate (**a–f**). In contrast to MDMA, methylphenidate did not alter the plasma levels of any of the steroids (**a–f**). CYP = Cytochrome P450.

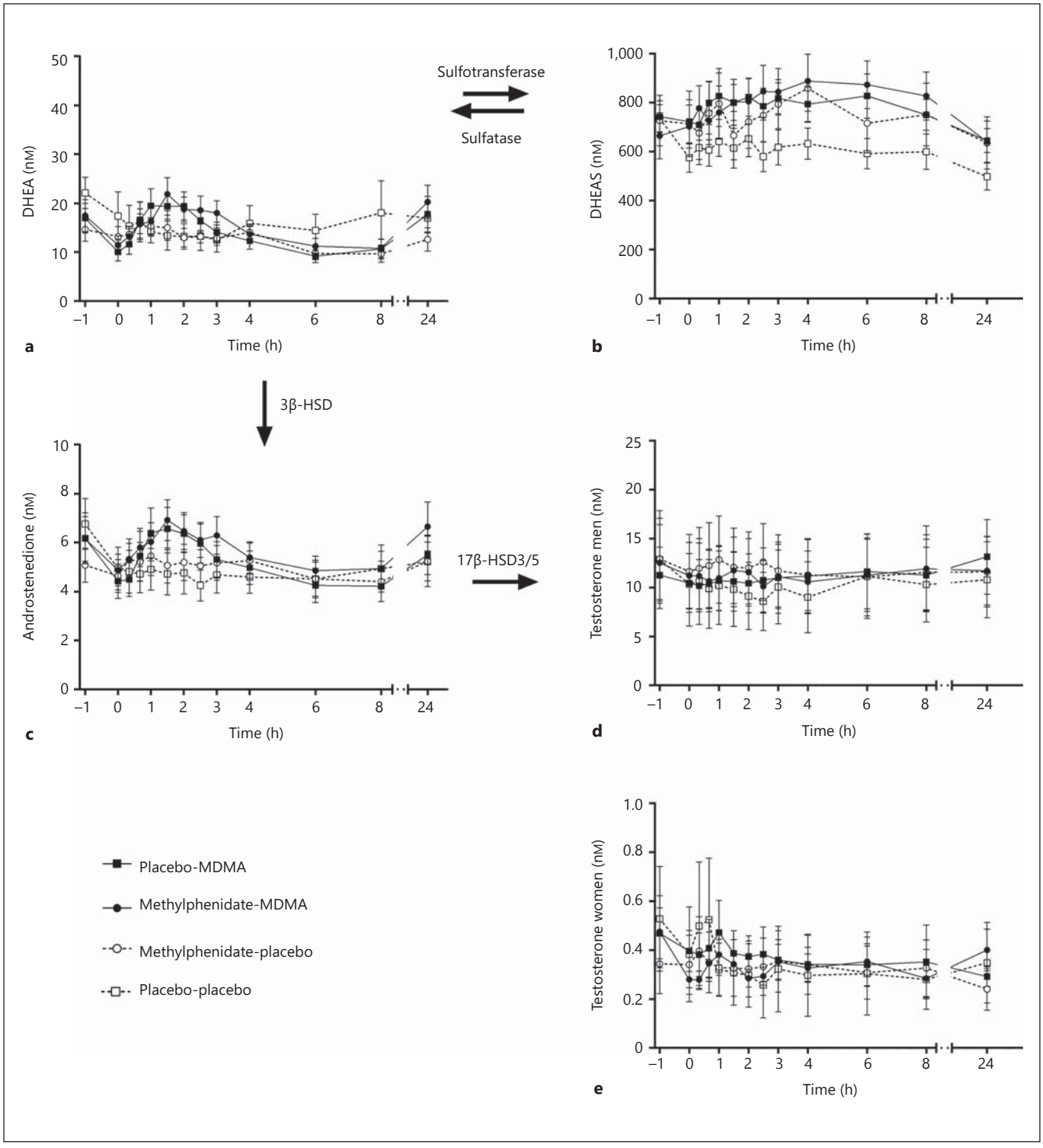

Fig. 2. Effects of MDMA and methylphenidate on plasma concentration-time profiles of androgens. The values are expressed as the mean ± SEM in 16 subjects (8 subjects for testosterone). MDMA was administered at t = 0 h. Methylphenidate was administered at t = –1 h. MDMA did not significantly alter the plasma concentrations of DHEA (**a**), DHEAS (**b**), androstenedione (**c**), or testosterone in men (**d**) or women (**e**). Similar changes in plasma androgen levels were induced regardless of whether MDMA was administered alone or combined with methylphenidate (**a–e**). Similarly, methylphenidate did not alter the plasma levels of any of the androgens (**a–e**). 17β-HSD = 17β-Hydroxysteroid dehydrogenase.

the concentrations of any of the steroids measured. Co-administration of MDMA + methylphenidate produced a similar hormonal response to MDMA alone.

Several previous laboratory studies have documented similar and maximal 2-fold (50–100%) increases in plasma cortisol levels in response to comparable doses of MDMA [12–15]. In contrast, 2- to 8-fold increases in cortisol levels were observed in dance clubbers who used MDMA while physically active [16, 17, 29]. Moderate MDMA-induced elevations of DHEA were seen in a previous laboratory study [12]. The effects of MDMA on all of the other steroids reported herein have not been previously described in a placebo-controlled setting. A non-significant trend toward an increase in plasma testosterone levels has been reported in healthy subjects who used MDMA at a dance club [16]. In contrast, we did not observe any effects of MDMA on testosterone levels in our placebo-controlled study.

Methylphenidate at an oral dose of 60 mg did not affect steroid levels in the present study. Similarly, oral methylphenidate at a dose of 20 mg did not alter plasma cortisol levels in healthy subjects [30, 31]. In contrast, intravenous methylphenidate at doses of 10 mg (0.12–0.15 mg/kg) or 0.3 mg/kg significantly increased cortisol levels in healthy subjects [32]. Related catecholaminergic substances, such as amphetamine and methamphetamine, have also been shown to elevate cortisol levels in some studies [33–36] but not others [14]. A single dose of the NET inhibitor reboxetine also increased cortisol levels [37], particularly in subjects who scored high on subclinical depression [38]. Chronic treatment with methylphenidate increased the levels of DHEA and DHEAS but not cortisol in children with attention-deficit/hyperactivity disorder [39]. There are several possible explanations why methylphenidate at a relatively high single oral dose of 60 mg [40, 41] did not affect steroid levels in the present study. For example, cortisol levels are typically highest in the morning, which is when methylphenidate was administered in our study. In contrast, in studies that reported significant increases in cortisol, methylphenidate was administered in the evening, when cortisol levels are typically low [32]. Additionally, physical activity may have enhanced the response to stimulant drugs in some previous studies [29], whereas our subjects were resting. Finally, a significant response was observed with intravenous but not oral administration, possibly because of faster changes associated with the mode of drug exposure.

Pharmacologically, MDMA activates the 5-HT system, and methylphenidate does not [7]. MDMA but not methylphenidate increased plasma prolactin levels [9], which is a clinical marker of serotonergic activity [42]. The present study, therefore, indicates that 5-HT plays a crucial role in mediating activation of the HPA axis. In rats, the MDMA-induced release of ACTH or corticosterone has been shown to involve 5-HT release and 5-HT_1 and 5-HT_2 receptor stimulation [43, 44]. We previously showed that MDMA-induced increases in plasma cortisol in humans were blocked by the SERT/NET inhibitor duloxetine [13], which blocks the interaction of MDMA with the SERT and NET and the resulting MDMA-induced transporter-mediated release of 5-HT and NE [7], but were not blocked by the NET inhibitor reboxetine [13], which only blocks the MDMA-induced release of NE [45].

Additionally, MDMA and the 5-HT releaser metachlorophenylpiperazine increased plasma cortisol levels, whereas amphetamine, which activates catecholamines more similarly to methylphenidate, did not [14]. Selective activation of the 5-HT system by acute administration of the SERT inhibitor citalopram also increased plasma and salivary cortisol levels [46]. Six-day treatment with citalopram but not the NET inhibitor reboxetine also increased waking salivary cortisol levels [47]. Finally, significant associations have been reported between polymorphisms in the genes that encode the SERT and HPA axis reactivity [48]. Thus, these findings indicate a role for 5-HT in the mediation of MDMA-induced HPA axis stimulation in humans but little or no role for NE. Additionally, MDMA releases 5-HT from peripheral non-neuronal tissues directly into the blood plasma [49] and 5-HT has been shown to directly stimulate aldosterone secretion by glomerulosa cells [50].

One important issue is the clinical relevance of MDMA's effects on corticosteroids. Steroids are involved in a wide range of central and peripheral physiological functions related to mood, cognition, adaptation to stress, immune function, and others. In the context of recreational drug use, cortisol, DHEA, and testosterone may contribute to or modulate substance-induced acute psychotropic and reinforcing effects [12, 20, 21]. For example, MDMA-induced increases in plasma cortisol levels have previously been shown to correlate with subjective drug liking in response to MDMA in a laboratory study [12]. Stress-induced increases in cortisol were also correlated with positive mood responses to amphetamine [51]. Nonetheless, we found no associations between plasma steroid levels and any of the previously reported psychotropic effects of MDMA in the present study [9] or in our previous work [13]. It is possible that we missed a true association because of the small study size. It is also possible that the subjective and some endocrine responses were maximal

and therefore similar in most subjects (low between-subject variability). For example, such a lack of between-subjects correlations has previously been documented for correlations between MDMA plasma levels and autonomic effects [52]. The pleasurable effects of amphetamine and methamphetamine in humans also did not change when cortisol levels were increased pharmacologically [53] or lowered by metyrapone administration prior to methamphetamine administration [33]. As noted above, MDMA-induced elevations of mineralocorticoids may also contribute to regulation of the hypertensive effects of MDMA. Corticosteroids may also facilitate the development of hyperthermia associated with amphetamines, a potentially fatal complication of recreational ecstasy use [54, 55]. In rats, adrenalectomy or administration of a glucocorticoid receptor antagonist suppressed methamphetamine- and MDMA-induced increases in body temperature [56–58]. Human data are lacking, but MDMA-induced elevations of steroids may contribute to the clinical toxicity of ecstasy [16, 29]. Finally, repeated HPA axis stimulation by MDMA may contribute to chronic toxicity [11, 17, 29], including the deficits in neurocognitive function described in heavy ecstasy users [59].

The present study has several limitations. First, we used only single doses of the drugs. However, the selected doses were high and produced pronounced and comparable sympathomimetic and drug-typical psychotropic effects [9]. Second, we did not assess corticotropin-releasing factor or ACTH levels to describe the drugs' effects on other mediators within the HPA axis. Instead, we provided the full profiles of ten steroids. Specifically, we included corticosterone, which is the biologically relevant glucocorticoid in rodents, the mineralocorticoid aldosterone, and androgens, which may play a role in mood regulation.

In conclusion, the MDMA- but not methylphenidate-induced effects on plasma steroids are consistent with a role for 5-HT in drug-induced HPA axis stimulation in the absence of other (psychosocial) stressors. Remaining to be investigated are whether and how the different steroids contribute to the acute and chronic effects of these psychoactive drugs.

Acknowledgements

This study was supported by the Swiss Centre of Applied Human Toxicology (to A. Odermatt), Swiss National Science Foundation (31003A_140961 to A. Odermatt and 32323B_144996 and 320030_149493 to M.E. Liechti), and University of Basel (DPH 2064 to C.M. Hysek). We thank Nathalie Schillinger and Nicole Meyer for study management and M. Arends for manuscript editing.

References

1 Armario A: Activation of the hypothalamic-pituitary-adrenal axis by addictive drugs: different pathways, common outcome. Trends Pharmacol Sci 2010;31:318–325.
2 Swerdlow NR, Koob GF, Cador M, Lorang M, Hauger RL: Pituitary-adrenal axis responses to acute amphetamine in the rat. Pharmacol Biochem Behav 1993;45:629–637.
3 Rivier C, Lee S: Stimulatory effect of cocaine on ACTH secretion: role of the hypothalamus. Mol Cell Neurosci 1994;5:189–195.
4 Sarnyai Z, Biro E, Telegdy G: Cocaine-induced elevation of plasma corticosterone is mediated by different neurotransmitter systems in rats. Pharmacol Biochem Behav 1993;45:209–214.
5 Borowsky B, Kuhn CM: Monoamine mediation of cocaine-induced hypothalamo-pituitary-adrenal activation. J Pharmacol Exp Ther 1991;256:204–210.
6 Zhou Y, Spangler R, Yuferov VP, Schlussmann SD, Ho A, Kreek MJ: Effects of selective D1- or D2-like dopamine receptor antagonists with acute 'binge' pattern cocaine on corticotropin-releasing hormone and proopiomelanocortin mRNA levels in the hypothalamus. Brain Res Mol Brain Res 2004;130:61–67.
7 Hysek CM, Simmler LD, Nicola V, Vischer N, Donzelli M, Krähenbühl S, et al: Duloxetine inhibits effects of MDMA ('ecstasy') in vitro and in humans in a randomized placebo-controlled laboratory study. PLoS One 2012;7:e36476.
8 Han DD, Gu HH: Comparison of the monoamine transporters from human and mouse in their sensitivities to psychostimulant drugs. BMC Pharmacol 2006;6:6.
9 Hysek CM, Simmler LD, Schillinger N, Meyer N, Schmid Y, Donzelli M, et al: Pharmacokinetic and pharmacodynamic effects of methylphenidate and MDMA administered alone and in combination. Int J Neuropsychopharmacol 2014;17:371–381.
10 Dumont GJ, Verkes RJ: A review of acute effects of 3,4-methylenedioxymethamphetamine in healthy volunteers. J Psychopharmacol 2006;20:176–187.
11 Parrott AC: Cortisol and 3,4-methylenedioxymethamphetamine: neurohormonal aspects of bioenergetic stress in ecstasy users. Neuropsychobiology 2009;60:148–158.
12 Harris DS, Baggott M, Mendelson JH, Mendelson JE, Jones RT: Subjective and hormonal effects of 3,4-methylenedioxymethamphetamine (MDMA) in humans. Psychopharmacology (Berl) 2002;162:396–405.
13 Hysek CM, Domes G, Liechti ME: MDMA enhances 'mind reading' of positive emotions and impairs 'mind reading' of negative emotions. Psychopharmacology (Berl) 2012;222:293–302.
14 Tancer M, Johanson CE: Reinforcing, subjective, and physiological effects of MDMA in humans: a comparison with D-amphetamine and mCPP. Drug Alcohol Depend 2003;72:33–44.
15 Mas M, Farre M, de la Torre R, Roset PN, Ortuno J, Segura J, et al: Cardiovascular and neuroendocrine effects and pharmacokinetics of 3,4-methylenedioxymethamphetamine in humans. J Pharmacol Exp Ther 1999;290:136–145.
16 Parrott AC, Lock J, Conner AC, Kissling C, Thome J: Dance clubbing on MDMA and during abstinence from ecstasy/MDMA: prospective neuroendocrine and psychobiological changes. Neuropsychobiology 2008;57:165–180.
17 Wolff K, Tsapakis EM, Pariante CM, Kerwin RW, Forsling ML, Aitchison KJ: Pharmacogenetic studies of change in cortisol on ecstasy (MDMA) consumption. J Psychopharmacol 2012;26:419–428.
18 Grob CS, Poland RE, Chang L, Ernst T: Psychobiologic effects of 3,4-methylenedioxymethamphetamine in humans: methodological considerations and preliminary observations. Behav Brain Res 1996;73:103–107.

19 Oddie CJ, Coghlan JP, Scoggins BA: Plasma desoxycorticosterone levels in man with simultaneous measurement of aldosterone, corticosterone, cortisol and 11-deoxycortisol. J Clin Endocrinol Metab 1972;34:1039–1054.
20 Mendelson JH, Mello NK, Sholar MB, Siegel AJ, Mutschler N, Halpern J: Temporal concordance of cocaine effects on mood states and neuroendocrine hormones. Psychoneuroendocrinology 2002;27:71–82.
21 Mello NK, Knudson IM, Kelly M, Fivel PA, Mendelson JH: Effects of progesterone and testosterone on cocaine self-administration and cocaine discrimination by female rhesus monkeys. Neuropsychopharmacology 2011; 36:2187–2199.
22 West CD, Mahajan DK, Chavre VJ, Nabors CJ, Tyler FH: Simultaneous measurement of multiple plasma steroids by radioimmunoassay demonstrating episodic secretion. J Clin Endocrinol Metab 1973;36:1230–1236.
23 Karssen AM, Meijer OC, van der Sandt IC, Lucassen PJ, de Lange EC, de Boer AG, et al: Multidrug resistance P-glycoprotein hampers the access of cortisol but not of corticosterone to mouse and human brain. Endocrinology 2001;142:2686–2694.
24 Odermatt A, Kratschmar DV: Tissue-specific modulation of mineralocorticoid receptor function by 11β-hydroxysteroid dehydrogenases: an overview. Mol Cell Endocrinol 2012; 350:168–186.
25 Dotsch J, Dorr HG, Stalla GK, Sippell WG: Effect of glucocorticoid excess on the cortisol/cortisone ratio. Steroids 2001;66:817–820.
26 Nomura S, Fujitaka M, Jinno K, Sakura N, Ueda K: Clinical significance of cortisone and cortisone/cortisol ratio in evaluating children with adrenal diseases. Clin Chim Acta 1996; 256:1–11.
27 Simmler LD, Hysek CM, Liechti ME: Sex differences in the effects of MDMA (ecstasy) on plasma copeptin in healthy subjects. J Clin Endocrinol Metab 2011;96:2844–2850.
28 Henry JA, Fallon JK, Kicman AT, Hutt AJ, Cowan DA, Forsling M: Low-dose MDMA ('ecstasy') induces vasopressin secretion. Lancet 1998;351:1784.
29 Parrott A, Lock J, Adnum L, Thome J: MDMA can increase cortisol levels by 800% in dance clubbers. J Psychopharmacol 2013;27:113–114.
30 Brown WA, Corriveau DP, Ebert MH: Acute psychologic and neuroendocrine effects of dextroamphetamine and methylphenidate. Psychopharmacology (Berl) 1978;58:189–195.
31 Van Kempen GM, Goekoop JG, Jong HB, Edelbroek PM, de Wolff FA: The plasma level of methylphenidate in the single-dose oral methylphenidate test. Biol Psychiatry 1990; 28:638–640.
32 Joyce PR, Donald RA, Nicholls MG, Livesey JH, Abbott RM: Endocrine and behavioral responses to methylphenidate in normal subjects. Biol Psychiatry 1986;21:1015–1023.
33 Harris DS, Reus VI, Wolkowitz OM, Mendelson JE, Jones RT: Altering cortisol level does not change the pleasurable effects of methamphetamine in humans. Neuropsychopharmacology 2003;28:1677–1684.
34 Jayaram-Lindstrom N, Konstenius M, Eksborg S, Beck O, Hammarberg A, Franck J: Naltrexone attenuates the subjective effects of amphetamine in patients with amphetamine dependence. Neuropsychopharmacology 2008;33:1856–1863.
35 Sofuoglu M, Poling J, Hill K, Kosten T: Atomoxetine attenuates dextroamphetamine effects in humans. Am J Drug Alcohol Abuse 2009;35:412–416.
36 White TL, Grover VK, de Wit H: Cortisol effects of D-amphetamine relate to traits of fearlessness and aggression but not anxiety in healthy humans. Pharmacol Biochem Behav 2006;85:123–131.
37 Hill SA, Taylor MJ, Harmer CJ, Cowen PJ: Acute reboxetine administration increases plasma and salivary cortisol. J Psychopharmacol 2003;17:273–275.
38 Hennig J, Lange N, Haag A, Rohrmann S, Netter P: Reboxetine in a neuroendocrine challenge paradigm: evidence for high cortisol responses in healthy volunteers scoring high on subclinical depression. Int J Neuropsychopharmacol 2000;3:193–201.
39 Maayan R, Yoran-Hegesh R, Strous R, Nechmad A, Averbuch E, Weizman A, et al: Three-month treatment course of methylphenidate increases plasma levels of dehydroepiandrosterone (DHEA) and dehydroepiandrosterone-sulfate (DHEA-S) in attention deficit hyperactivity disorder. Neuropsychobiology 2003;48:111–115.
40 Martin WR, Sloan JW, Sapira JD, Jasinski DR: Physiologic, subjective, and behavioral effects of amphetamine, methamphetamine, ephedrine, phenmetrazine, and methylphenidate in man. Clin Pharmacol Ther 1971;12:245–258.
41 Rush CR, Essman WD, Simpson CA, Baker RW: Reinforcing and subject-rated effects of methylphenidate and D-amphetamine in non-drug-abusing humans. J Clin Psychopharmacol 2001;21:273–286.
42 Sommers DK, van Wyk M, Snyman JR: Dexfenfluramine-induced prolactin release as an index of central synaptosomal 5-hydroxytryptamine during treatment with fluoxetine. Eur J Clin Pharmacol 1994;46:441–444.
43 Nash JF Jr, Meltzer HY, Gudelsky GA: Elevation of serum prolactin and corticosterone concentrations in the rat after the administration of 3,4-methylenedioxymethamphetamine. J Pharmacol Exp Ther 1988;245:873–879.
44 Zaretsky DV, Zaretskaia MV, Dimicco JA, Durant PJ, Ross CT, Rusyniak DE: Independent of 5-HT1A receptors, neurons in the paraventricular hypothalamus mediate ACTH responses from MDMA. Neurosci Lett 2013;555:42–46.
45 Hysek CM, Simmler LD, Ineichen M, Grouzmann E, Hoener MC, Brenneisen R, et al: The norepinephrine transporter inhibitor reboxetine reduces stimulant effects of MDMA ('ecstasy') in humans. Clin Pharmacol Ther 2011;90:246–255.
46 Bhagwagar Z, Hafizi S, Cowen PJ: Acute citalopram administration produces correlated increases in plasma and salivary cortisol. Psychopharmacology (Berl) 2002;163:118–120.
47 Harmer CJ, Bhagwagar Z, Shelley N, Cowen PJ: Contrasting effects of citalopram and reboxetine on waking salivary cortisol. Psychopharmacology (Berl) 2003;167:112–114.
48 Miller R, Wankerl M, Stalder T, Kirschbaum C, Alexander N: The serotonin transporter gene-linked polymorphic region (5-HTTLPR) and cortisol stress reactivity: a meta-analysis. Mol Psychiatry 2013;18:1018–1024.
49 Yubero-Lahoz S, Ayestas MA Jr, Blough BE, Partilla JS, Rothman RB, de la Torre R, et al: Effects of MDMA and related analogs on plasma 5-HT: relevance to 5-HT transporters in blood and brain. Eur J Pharmacol 2012;674:337–344.
50 Shenker Y, Gross MD, Grekin RJ: Central serotonergic stimulation of aldosterone secretion. J Clin Invest 1985;76:1485–1490.
51 Hamidovic A, Childs E, Conrad M, King A, de Wit H: Stress-induced changes in mood and cortisol release predict mood effects of amphetamine. Drug Alcohol Depend 2010; 109:175–180.
52 Hysek CM, Liechti ME: Effects of MDMA alone and after pretreatment with reboxetine, duloxetine, clonidine, carvedilol, and doxazosin on pupillary light reflex. Psychopharmacology (Berl) 2012;224:363–376.
53 Wachtel SR, Charnot A, de Wit H: Acute hydrocortisone administration does not affect subjective responses to D-amphetamine in humans. Psychopharmacology (Berl) 2001; 153:380–388.
54 Henry JA, Jeffreys KJ, Dawling S: Toxicity and deaths from 3,4-methylenedioxymethamphetamine ('ecstasy'). Lancet 1992;340:384–387.
55 Liechti ME, Kunz I, Kupferschmidt H: Acute medical problems due to ecstasy use. Case-series of emergency department visits. Swiss Med Wkly 2005;135:652–657.
56 Herring NR, Gudelsky GA, Vorhees CV, Williams MT: (+)-Methamphetamine-induced monoamine reductions and impaired egocentric learning in adrenalectomized rats is independent of hyperthermia. Synapse 2010; 64:773–785.
57 Makisumi T, Yoshida K, Watanabe T, Tan N, Murakami N, Morimoto A: Sympatho-adrenal involvement in methamphetamine-induced hyperthermia through skeletal muscle hypermetabolism. Eur J Pharmacol 1998;363: 107–112.
58 Fernandez F, Aguerre S, Mormede P, Chaouloff F: Influences of the corticotropic axis and sympathetic activity on neurochemical consequences of 3,4-methylenedioxymethamphetamine (MDMA) administration in Fischer 344 rats. Eur J Neurosci 2002;16:607–618.
59 Rogers G, Elston J, Garside R, Roome C, Taylor R, Younger P, et al: The harmful health effects of recreational ecstasy: a systematic review of observational evidence. Health Technol Assess 2009;13:iii–iv, ix–xii, 1–315.

5. Chapter 3: The role of the short-chain dehydrogenase/reductase (SDR) DHRS7 in prostate and breast cancer

Introduction

The SDRs are a class of enzymes known to be involved in metabolic functions and their impaired expression and activities have been associated with metabolic disorders, degenerative diseases and cancer [7]. Amongst others, the major physiological function of SDR enzymes, namely their ability to control the cellular availability of hormone receptor ligand, makes some members interesting therapeutic drug targets. 11β-HSD1 inhibition, for example, shows promise in the treatment of metabolic syndrome, atherosclerosis and osteoporosis [73]. On the other hand, inhibition of 17β-HSDs, which control sex hormone metabolism, may be important targets in breast and prostate cancer treatment [8, 74]. Uncharacterized SDRs may be potential candidates to treat monogenic and multifactorial diseases including cancer. The identification and subsequent functional characterization of new SDRs may help identifying novel targets for drug development [75]. There is evidence that several "orphan" enzymes may be involved in cancer processes, such as the "orphan" prostate SDR 1 (PSDR1) (also called retinol dehydrogenase 11 and known under the nomenclature name SDR7C1). PSDR1 is an androgen receptor regulated member of the SDR family, which was found to be highly expressed in healthy and neoplastic prostate tissue compared to tumor tissue, suggesting it may play a role in pathogenesis of prostate cancer (PCa) [76]. SDRO, also known under the nomenclature name SDR9C7, is another novel SDR. The expression of SDRO was closely correlated with metastasis and it was suggested to be a prognostic marker for cancer patients [77]. Furthermore, "orphan" 11βHSD3 (SCDR10B) showed increased expression in human cancerous lung compared to healthy lung tissue, suggesting a possible role in cancer progression [78]. Even though many "orphan" SDRs seem to play a role in complex cancer processes, the endogenous mechanisms of action remains unknown and one of the major challenges facing researchers is to identify and characterize the endogenous substrates of these enzymes [79].

Dehydrogenase/Reductase SDR Family Member 7 (DHRS7) (also known as retSDR4 and under the nomenclature name SDR34C1), is an "orphan" SDR expressed in various tissues including the liver, kidney, skeletal muscle and prostate [80, 81]. To date, little is known about DHRS7's catalytic activity. However, a recent publication by Stambergova et al. showed that DHRS7 metabolizes endogenous substrates with a steroid structure (estrone, cortisone, 4-androstene-3,17-dion) and exogenous substances bearing a carbonyl group (1,2-naphtoquinone, 9,10-phenantrenequinone, benzoquinone, nitrosamine 4-(methyl-nitrosamino)-1-(3-pyridyl)-1-butanone) *in vitro*, using NADP(H) as a cofactor with preference [82]. In another study, DHRS7 showed increased mRNA expression levels in goose hepatocytes treated with free fatty acid mixtures, indicating a possible role in the metabolism of

these compounds [83]. Interestingly, microarray data of a recent study showed elevated DHRS7 expression in wild type mice fed a low fat, high caloric diet compared to a normal diet, an observation abolished in the stearoyl-CoA desaturase-1 (SCD1) knockout animals [84]. This data suggests that SCD1 might be involved in DHRS7 regulation and since SCD1 is a key regulator of fatty acid metabolism, this finding suggests also a possible role of DHRS7 in fatty acid metabolism. Previously it was reported that mRNA expression levels of DHRS7 increased in rats following a 2/3 hepatectomy, indicating a possible function of this "orphan" enzyme in liver regeneration, entailing cell proliferation and differentiation processes [85]. Supporting the hypothesis of DHRS7 having a possible role in cell proliferation and differentiation, microarray expression data from three independent studies on human PCa tissue showed that DHRS7 levels are altered in this tumor [86-88]. A recent study in a novel hollow fibre mouse model setup, using the LNCaP PCa cells, showed that DHRS7 mRNA levels were significantly altered as the tumor develops into castration resistant prostate cancer (CRPC) [89]. DHRS7 may therefore play a role in this disease by sustaining *de novo* androgen synthesis and/or metabolism in CRPC, eventually leading to the reactivation of androgen receptor (AR), thus promoting cancer progression, even in the absence of testicular androgens [89]. Interpretation of this data leads to the assumption that DHRS7 may play a role in PCa progression.

Sites	**Estimated new cases**	**Estimated deaths**	**% of new cases**
Prostate	233000	29480	12.7
Lung	116000	86930	74.9
Urinary bladder	56390	11170	23.1
Colon	48450	26270	59.9
Skin (Melanoma)	43890	6470	11.5
Kidney	39140	8900	22.7
Non-Hodgekin Lymphoma	38270	10470	27.4
Liver	24600	15870	64.5
Pancreas	23530	20170	85.7
Rectum	23380		0.0

Table 2: US statistics of cancer in male 2014. Modified after: Siegel et al., *Cancer statistics 2014 [90]*

PCa is one of the most common malignancies worldwide and the second leading cause of cancer-related death among males in Europe and the United States (Table 2). Clinically, PCa manifests as a heterogeneous multifocal disease with rising incidence [90, 91]. The mechanisms underlying the initiation and progression of PCa are complex. Initial, pre-malignant lesions, which are attributed to genetic alterations in one or more cells, arise. The accumulation of genetic alterations in pre-malignant cells drives them into malignant growth and into the production of a primary tumor. Cells in a primary tumor express heterogeneous phenotypic and biological characteristics, which are caused by the differences in

the genes altered. Therefore, some highly metastatic cells, possessing invasive and metastatic ability, might occur. Such cells selectively are able to produce a metastatic tumor in a distant organ (Figure 6) [92].

In addition to environmental factors, age and familial inheritance, steroid hormone receptor signaling is mainly involved in all stages of prostate carcinogenesis. The early development of PCa, as well as the progression to CRPC can be driven by AR signaling pathway. Hence, the progression of PCa to CRPC can be initiated by several mechanisms, including hypersensitivity of the AR signaling pathway to androgens, enrichment or accumulation of androgen-insensitive stem cells, and the activation of intratumoral steroidogenesis. In addition to the AR, specific genes and signaling pathways such as Wnt/β-catenin signaling, proto-oncogenes MET and MYC, vascular endothelial growth factor receptor (VEGFR) signaling, phosphatase and tensin homolog (PTEN), ERBB2 encoding human epidermal growth factor receptor 2 (HER2), B-cell CLL/lymphoma 2 (BCL2) and many others have been suggested to play a role in PCas development and progression [93-95]. Furthermore, evidence suggested that the process of epithelial to mesenchymal transition (EMT) plays a pivotal role in the development of metastatic CRPC. EMT is a process by which epithelial cells lose their characteristics and acquire mesenchymal properties, which allows cancer cells to detach from the tumor mass and translocate to other tissues. At the molecular level, EMT is characterized by the loss of the epithelial cell adhesion molecule E-cadherin (CDH1), which enables cells to increase motility and invasiveness through the disruption of intercellular contacts [96, 97].

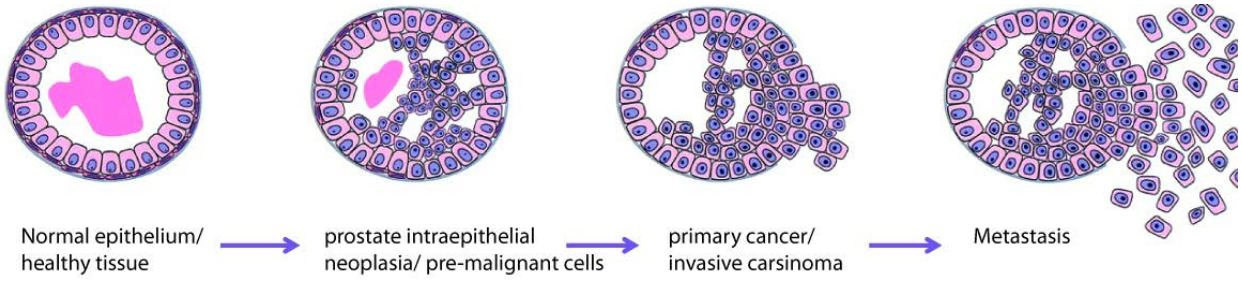

Figure 6: PCa progression. Modified after: Abate-Shen et al.; *Molecular genetics of prostate cancer* [98]

Although the survival rate of PCa is high due to recent advances in current therapeutic and screening methods, many patients still develop post-operative disease relapse and endure significant treatment-associated complications. The current standard for the treatment of PCa is either medical or surgical castration. However, after castration, PCa can progress to CRPC and patients may develop metastases in lymph nodes, liver and bone. To provide better strategies for the prevention and treatment of PCa it is important to further investigate the molecular mechanisms underlying the initiation and progression of the disease [99, 100].

Given that DHRS7s may play a role in PCa, we carried out tissue microarray (TMA) and immuno detection of DHRS7 in clinical human prostate tissue samples of different tumor stages in collaboration with Prof. Dr. L. Terracciano and co-workers. To expand on the findings in the clinical samples, I conducted an *in*

vitro study to evaluate the functional effects of the enzymes in cancer progression. To determine the effects of DHRS7 on the metastatic potential of cells *in vitro*, I evaluated cell proliferation, migration and adhesion after siRNA mediated knockdown of DHRS7 in three prostate cell lines, namely LNCaP, BPH1 and PC3. Additionally, I performed a microarray in LNCaP cells treated with siRNA against DHRS7 to identify pathways involved in DHRS7 action.

In addition to PCa, I also investigated the role of DHRS7s in breast cancer (BC). BC is also a heterogeneous disease and presents a leading cause of cancer death in females worldwide. [90] The development of BC involves the progression through an intermediate complex process, beginning with ductal hyperproliferation, followed by development of a local carcinoma and finally metastases [101]. Comparable to PCa, steroid signaling, specifically the estrogen receptor (ER) pathway, plays a critical role in the development of BC and its progression and continuing exposure to endogenous or exogenous estrogen is a well characterized cause of BC. For this reason, the use of selective estrogen receptor modulators, such as tamoxifen, is the most common treatment for BC. However, the efficacy of tamoxifen is limited by intrinsic and acquired resistance, since it requires functional ER signaling to work [102]. Possible mechanisms for endocrine resistance include the deregulation of the ER pathway itself, comprising loss of ER expression, post-translational modification of ER and the deregulation of ER co-activators. Besides altered estrogen signaling, other mechanisms also influence tumor cell proliferation and survival and can therefore cause resistance. For instance, increased receptor tyrosine kinase signaling also leads to the activation of various intracellular pathways involved in signaling transduction, proliferation and cell survival. Alterations in cell cycle and apoptosis, as well as epigenetic modification and altered expression of specific microRNAs are other possible mechanisms leading to BC progression [103]. EMT, which increases motility, invasiveness and metastatic capabilities of BC cells is suggested to be a mechanism for endocrine therapy resistance and cancer progression [104].

Given the high degree of diversity between and within tumors as well as among patients suffering from BC the determination of the risk of disease progression and therapeutic resistance is challenging. Molecular classification, using immunohistochemistry to characterize the hormone receptor expression of the tumors and other cell markers has become useful for diagnosis and treatment of BC. Three major subtypes can be distinguished within BC: luminal A (ER+ and/or PR+; HER2−) or B (ER+ and/or PR+; HER2+), the HER-2 amplified (ER−, PR−, and HER2+), and the basal-like (ER−, PR−, and HER2−) also called triple-negative cancer (TNBC). The characteristics and risk factors of each of these subtypes are different, such as their response and resistance to treatment, the risk of disease progression or the propensity to spread metastatic cells to a particular organ [105]. Thus, when compared with other BC subtypes, TNBC is an aggressive neoplasia strongly associated with distant recurrence, metastases and death. Hence, understanding and characterizing biomarkers, including their role in cancer progression and drug resistance as well as their use for diagnosis and treatment is important for BC treatment [106]. My recent findings in PCa and evidence of altered DHRS7 expression from several microarrays in different stages of BC suggests that DHRS7 may also play a role in BC progression [107-109]. To identify DHRS7s role in

BC I first selected a panel of cell lines based on the enzymes mRNA and protein levels. Subsequently, I performed proliferation and migration assay in ZR-75-1 cells.

Previous studies showed an increase in DHRS7 gene expression in regenerating rat liver following 2/3 hepatectomy [85]. Additionally, the assessment of microarray data derived from pathology group in patients suffering from hepatocellular carcinoma (HCC) also showed altered DHRS7 levels [85]. Taking these results into account, I hypothesized that DHRS7 may play a role in liver regeneration. We obtained mouse liver samples from regenerating liver following 2/3 hepatectomy from Prof. Dr. Dufour. Additional work on molecular regulation of DHRS7 by factors involved in liver regeneration has been examined by the master student P. Marbet whom I supervised [110].

To date, several steroid hormones and xenobiotics have been tested by me, to see if they are metabolized by DHRS7 using different *in vitro* setups such as activity assays in cells expressing recombinant DHRS7. The first results presented in the third chapter of my thesis provide evidence that the “orphan” enzyme DHRS7 acts as a tumor suppressor and that its loss of function promotes PCa and BC cell aggressiveness. Additionally, I characterized, using qPCR and transactivation methods, the molecular regulation of DHRS7 by sex steroids in LNCaP cells.

Finally, based on data from several microarrays, I tested if diet plays a role in the expression of DHRS7 in high fat versus low fat fed animals [111-113].

Results and Discussion

The role of DHRS7 in prostate cancer

The first study on DHRS7 conducted in this thesis focused on the role of DHRS7 in different PCa grades. In collaboration with Prof. Dr. L. Terraccianos Molecular Pathology, University of Basel, DHRS7 protein levels were analysed by immunohistochemistry in a large collection of human prostate specimens using TMA (Figure 1A in the submitted manuscript). This analysis determined DHRS7 to be highly expressed in normal prostate and samples scored as benign (Figure 1B in the submitted manuscript). Conversely, most of the PCa specimens showed lower levels of DHRS7 protein expression. Importantly, this study reports for the first time, that DHRS7 protein levels are decreased in human PCa tissues and negatively correlate with Gleason levels. However, Kaplan-Meier analysis did not show a significant association between DHRS7 expression and the survival of PCa patients (Figure 1C in the submitted manuscript). Other important tumor suppressor genes, like p53, also fail to serve as prognostic markers for survival although their partial loss of expression in PCa is correlated with increased tumor aggressiveness. This may be due to heterogeneity within the tumor and small TMA cohorts with low statistical power [114]. Therefore, it remains to be established whether low DHRS7 levels serve as a possible biomarker to predict a poor prognosis of PCa patients. To support the TMA findings, the impact of DHRS7 on prostate cancer cell

aggressiveness was tested *in vitro*. I identified three cell lines expressing DHRS7 on an endogenous level. MRNA and protein levels of DHRS7 in the selected cell lines, namely LNCaP, BPH1 and PC3, were highly diverse (Figure 7A and Figure 2 in the submitted manuscript). From the panel of cell lines, LNCaP showed the highest expression of DHRS7 on the protein and mRNA level. A recent study suggested highly elevated DHRS7 levels in the LNCaP cell line in a novel hollow fibre mouse model setup [89]. LNCaP is a PCa cell line established from a metastatic lesion of human prostatic adenocarcinoma. High specific expression of ARs and ERs and its hormone responsiveness rank among the main characteristics of this cell line; thus 5α-dihydrotestosterone modulates cell growth and stimulates acid phosphatase production in LNCaP *in vitro*. The mean population doubling time of these androgen-dependent cells is approximately 60 hours [115]. In contrast, BPH1, an immortalized but non-transformed human prostate epithelial cell line displayed the lowest amount of DHRS7 protein expression close to the limit of detection using immunoblotting. This cell line expresses a relatively low mRNA level in qPCR analysis when compared to the other cell lines. BPH1 cells do not express AR or the secretory markers, prostate specific antigen (PSA) and prostatic acid phosphatase [116]. Another cell line, PC3, showed a lower endogenous expression of DHRS7 protein compared to the LNCaP cells. PC3 cells are derived from human lumbar vertebral metastasis. Similar to BPH1, PC3 cells do not express AR and PSA. The doubling time of PC3 cells is approximately 33 hours, the lowest of all the tested models [117]. Additionally, I assessed the endogenous expression of DHRS7 in DU145 cells, another PCa cell line commonly used in other studies. Neither the mRNA nor protein levels of DHRS7 could be detected in this cell model.

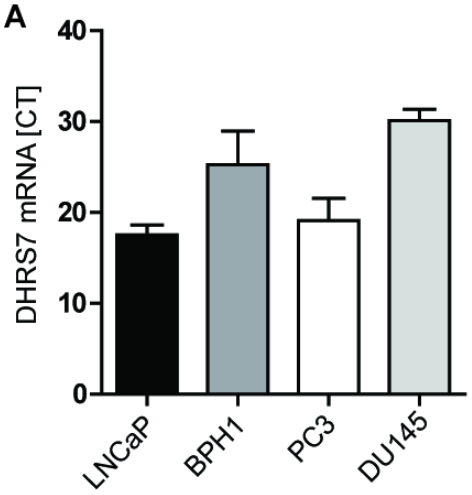

B

	LNCaP	BPH1	PC3	DU-145
Androgen sensitive	Yes	No	No	No
Approximate doubling time (hrs)	60	45	33	34
Express:				
AR	RNA + protein	No	No	No
PSA	RNA + protein	No	No	No
prostatic acid phosphatase	RNA + protein	No	No	No

Figure 7: (A) Endogenous expression of DHRS7 mRNA in different prostate cell lines, (B) main characteristics of the prostate cell models (modified after *Sobel et al.* [117])

Following the selection of the prostate cell model panel, I characterized the effects of siRNA-mediated DHRS7 knockdown. First I selected one DHRS7 targeted siRNA from a panel of four. The selected molecule clearly showed lower expression of DHRS7 mRNA levels compared to the other siRNAs after 72 hours of knockdown in the LNCaP cells (Supplementary Figure 1 in the submitted manuscript). To exclude

off-target siRNA mediated effects, the proliferation experiments in the LNCaP cells were performed using an additional siRNA molecule targeting DHRS7 (Supplementary Figure 2 in the submitted manuscript). Subsequently, proliferation, migration and adhesion assays in LNCaP, BPH1 and PC3 cells were performed. XCelligence measurement as well as Ki-67 immunostaining showed increased cell proliferation in LNCaP cells but not in BPH1 and PC3 cells following DHRS7 knockdown (Figure 2 in the submitted manuscript). The significantly lower endogenous expression of DHRS7 in BPH1 and PC3 cells compared to LNCaP cells is one possible explanation for the different growth response in these cell models. Furthermore, LNCaP cells differ extensively in their characteristics from the other models, as androgen-dependent proliferation might promote DHRS7 knockdown effects. The basal proliferation rate of LNCaP cells is additionally much lower (approximately 60 h doubling time) compared to the doubling time of PC3 and BPH1 cells (approximately 30-45 hrs), hence might account for the more pronounced proliferation effects in LNCaP cells. The heterogeneity of the cell models used in this study and the fact that many other studies reported differences in growth response in different prostate cell lines like the LNCaP and PC3 explain the variable results [118-120]. Migration and adhesion were found to be altered in all three cell lines after siRNA controlled knockdown of DHRS7 (Figure 4 in the submitted manuscript). However, in a transwell migration setup, LNCaP cells showed the most pronounced increase in migrating cells when compared to the two other models. Again, the low endogenous expression of DHRS7 in BPH1 and PC3 cells as well as the variance in characteristics of the cell models might account for the observed differences. Nevertheless, adhesion was affected to a similar degree in all the cell lines.

To understand the mechanisms underlying the effects of DHRS7 depletion and to further support the previous findings, I performed a microarray study using cells treated with siRNA targeting DHRS7 and compared the gene expression with that of cells transfected with a non-targeted RNA control. Given the high endogenous expression level and the most pronounced changes after DHRS7 knockdown, LNCaP cells were chosen for this experiment. Several genes involved in cell proliferation and adhesion pathways were found to be altered in DHRS7 depleted LNCaP cells. Specifically, expression of genes belonging to the BRCA1/2 pathway as well as the major EMT regulator CDH1 decreased following DHRS7 knockdown (Figure 5 in the submitted manuscript). Loss of CDH1 promotes the transition of epithelial cells to the mesenchymal state (EMT), which is linked to PCa progression [121]. Decreased CDH1 expression could additionally be linked to the observed increase in migration and altered adhesion in the prostate cell lines [122, 123].

Another possible mechanism for the DHRS7-mediated regulation of PCa progression could involve the BRCA1/2 pathway, which is a key player in repairing DNA double-strand breaks or directing cells into apoptosis if DNA cannot be repaired. BRCA1 and BRCA2, are both breast and prostate tumor suppressors and their loss is associated with enhanced cell proliferation and cancer progression [124, 125]. Other genes belonging to the BRCA pathway changed expression following DHRS7 knockdown, including BRCA1 associated ring domain protein 1 (BARD1), BRCA1 interacting protein C-terminal helicase 1 (BRIP), cell cycle checkpoint kinase 1/2 (CHEK1/2), fanconi anemia complementation group D2 protein, isoform 1 (FANCD2) and DNA repair protein, *S.cerevisiae* homolog (RAD51). There are

numerous DNA repair pathways directed by the BRCA pathway to specific types of DNA damage (Figure 8). Following DNA damage, activation of BRCA1 occurs via phosphorylation directly or indirectly through CHEK2. BRCA1 then can activate several pathways involved in different repair mechanisms. For example, homologous recombination repair is directed by interaction of BRCA1 and BRCA2 with RAD51 and FANCD2. Moreover, BRCA1 can activate BRIP1, which is also able to trigger homologous recombinational repair [126]. Another repair mechanism includes the interaction of BRCA1 with BARD1, which forms a heterodimeric ubiquitin E3 ligase complex that is required for the accumulation of ubiquitin conjugates at sites of DNA damage and for silencing at DNA satellite repeat regions [127]. Detected down-regulation of these genes was found in the microarray analysis, which leads to the assumption that DHRS7 may play a role in the BRCA pathway. However, the changes in the BRCA pathway genes were most pronounced 72 hours following the knockdown and might therefore be secondary effects. Consequently, the microarray helped to generate new hypothesis, but the identification of the mechanism of DHRS7 and its role in cancer progression warrants further research.

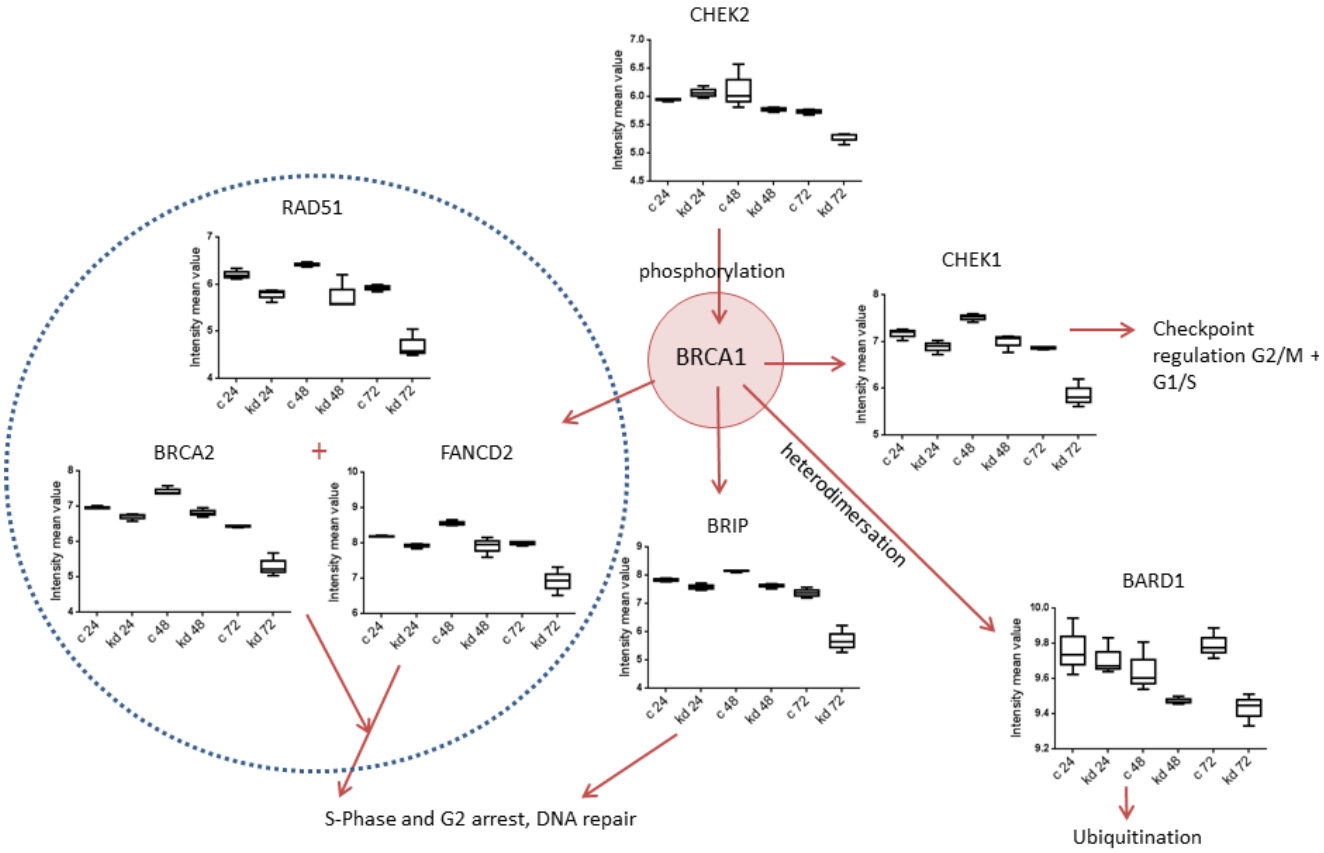

Figure 8: Microarray results: BRCA1 pathway. Boxplot represents median, 75th confidence interval and whiskers represent 95th of three independent replicates

In conclusion, the results of this study provide the first evidence that DHRS7 may be a tumor suppressor and that its loss of function promotes PCa cell aggressiveness. Further studies are required to

characterize the function of DHRS7 and to uncover its regulation. Additional evidence for the tumor-suppressive role of DHRS7 may help to evaluate this enzyme as a novel therapeutic PCa target and/or as a diagnostic biomarker.

The role of DHRS7 in breast cancer

The findings regarding the role of DHRS7 in PCa and the effects on the BRCA1/2 pathway that also play a crucial role in breast cancer, led me to examine the role of DHRS7 in BC *in vitro*. First, it was necessary to identify cell models endogenously expressing DHRS7 on the mRNA and protein level. All tested BC cell lines, namely MDA-MB-231, MDA-MB-453, HCC1569, T47D, MCF7, ZR-75-1, SUM159 and MDA-MB-468 expressed comparable DHRS7 mRNA levels, but the protein levels did not correlate (Figure 9). This may be explained by the substantial role for regulatory processes, which occur after mRNA is transcribed including post-transcriptional, translational modifications and protein degradation regulation in controlling steady-state protein abundances [128]. Compared to LNCaP cells, the protein expression of DHRS7 in all the examined BC cell lines is much lower. The cell line SUM159 showed only background levels of protein expression. Since BC is highly heterogeneous, the different cell lines used in this study differ not only in DHRS7 expression but also vary in their properties (Table 3) [129].

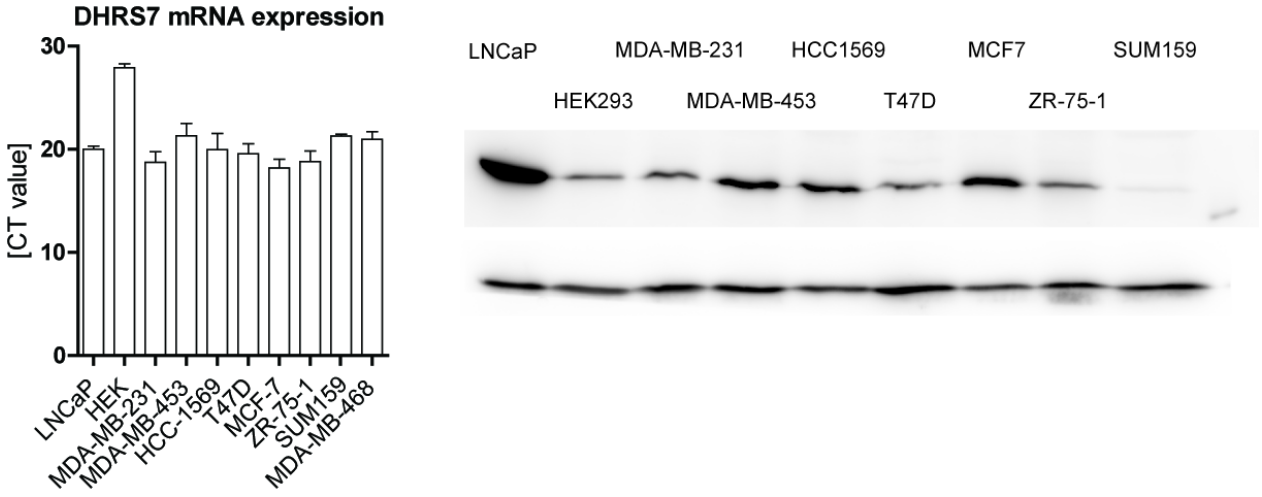

Figure 9: Endogenous mRNA and protein expression of DHRS7 in different BC cell lines. LNCaP served as a positive and HEK as a negative control

Almost all of the examined cell lines were established from malignant effusions and thus are derived from patients with an advanced stage of the disease. Nevertheless, each BC cell line possessed distinct differences in their morphological characteristics and ploidy, immunohistochemical expression of the ERs, progesterone receptors (PR), and ERBB2 amplification. Hence their proliferation behavior as well as their migration and invasive potential are different. Cell lines, for example MDA-MB-231 and SUM159 with

stellate morphology for example are reported to be highly metastatic and invasive, therefore may share similar characteristics to the PCa cell line PC3 and may no longer respond to effects mediated by DHRS7 knockdown [130]. Since variable proliferation effects were shown in the prostate cells, the heterogeneity of the BC cell lines may similarly lead to variable results. Because of their slow growth rate ZR-75-1 cells were used as the first model in this study. Other cell lines, with moderate growth rates that could be valid to tested for siRNA mediated knockdown effects of DHRS7 are the hormone-dependent MCF7 and T47D as well as the ERBB2 amplifying MDA-MB-453 and the basal-like cell line MDA-MB-468. ZR-75-1 cultures were derived from a malignant ascetic effusion of a 63-year-old female [131].

Morphology	Cell line	ER	PR	ERBB2 amp	Mutation status	Tumor type	Tumor source	Tumor classification	Doubling time [hrs]
Mass	HCC1569	neg	neg	pos	PTEN, TP53	metaplastic carcinoma	primary	ERBB2 amplified	40
	MCF7	pos	pos	pos	CDKN2A, PIK3CA	invasive ductal carcinoma	metastasis (pleural effusion)	Luminal	38
	T47D	pos	pos	neg	PIK3CA, TP53	invasive ductal carcinoma	metastasis (pleural effusion)	Luminal	50
Grape like	MDA-MB-468	neg	neg	neg	MADH4, PTEN, RB1, TP53	adenocarcinoma	metastasis (pleural effusion)	Basal-like	47
	MDA-MB-453	neg	neg	pos	CDH1, PIK3CA	adenocarcinoma	metastasis (pleural effusion)	ERBB2 amplified	50
	ZR-75-1	pos	pos	pos	N/A	invasive ductal carcinoma	metastasis (ascites)	Luminal	80
Stellate	MDA-MB-231	neg	neg	neg	BRAF, CDKN2A, KRAS, TP53	adenocarcinoma	metastasis (pleural effusion)	Basal-like	24
	SUM159	neg	neg	pos	N/A	anaplastic carcinoma	primary	ERBB2 amplified	20

Table 3: Relevant characteristics of malignant breast cell lines used are organized by morphology and summarized here. ER, PR, ERBB2 amplification status, primary tumor type, tissue source and tumor classification (modified after *Kenny et al.*)

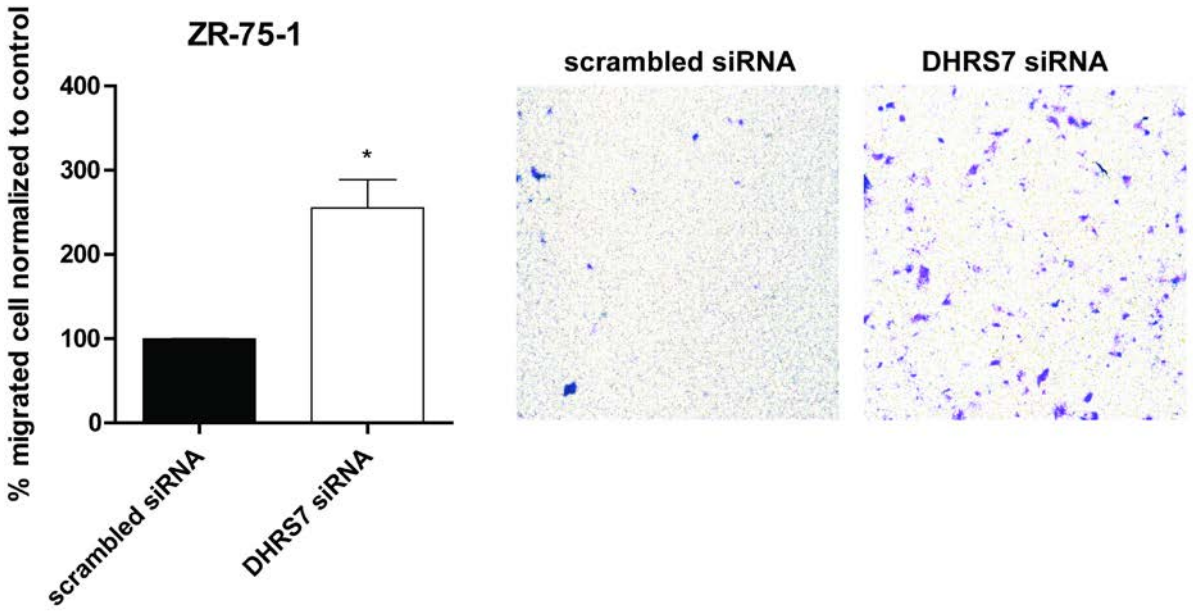

Figure 10: Migration of ZR-75-1 cells after knockdown of DHRS7 assessed by the transwell migration assay. Cells transfected with siRNA against DHRS7 or scrambled non-targeted control siRNA were seeded on transwell inserts at 24 h post-transfection, followed by crystal violet staining after another 24 h. Stained cells in 5 fields scanned at 10x magnification setting were analysed using ImageJ. Representative pictures of migration assays are shown. Data represents mean ± SD from three independent experiments conducted in triplicate. Statistical analysis was performed using the Student's t-test; *p ≤ 0.0001 compared to the non-targeted control.

They have a very high cell-doubling time of approximately 80 hours and their growth can be stimulated by estrogen and inhibited by tamoxifen [131]. The MCF7 cells originate from pleural effusion of a patient with metastatic mammary carcinoma [132]. This cell line has characteristics of a differentiated mammary epithelium, including the expression of cytoplasmic ER and the capability of forming domes. Its growth is moderate with a doubling time of approximately 38 hours [132]. T47D also express a functional ER response [133]. Doubling time of this model is about 50 hours. The MDA-MB-453 BC cell line was obtained from a malignant pleural effusion of a 48-year-old female and has been suggested as a model for the molecular apocrine breast subtype since it exhibits as characteristic apocrine carcinoma steroid receptor profile: ER-α-negative, PR-negative and AR-positive. Increased proliferation in response to androgens is the key feature of MDA-MB-453, which can be blocked by anti-androgens, such as flutamid. Her-2/neu activity has been well documented in this model, as well as the existence of a functional cross-talk between AR and Her-2/neu, involving the MAPK/ERK1/2 pathway. These features also tend to characterize a substantial proportion of

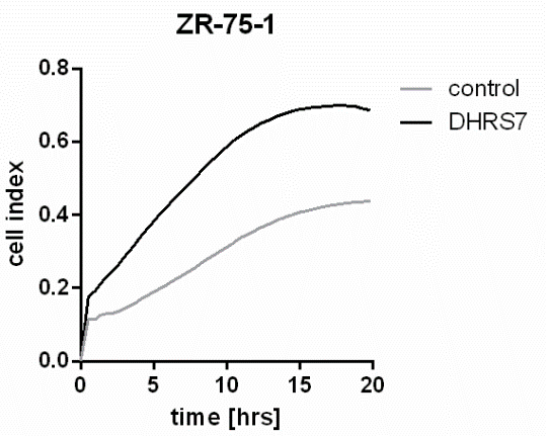

Figure 11: proliferation of ZR-75-1 cells after DHRS7 knockdown with siRNA. (n=1)

invasive apocrine carcinomas of the breast. Doubling time of MDA-MB-453 cells is approximately 50 hours [134]. The cell line MDA-MB-468 originates from the same female patient, but belongs to the basal-like group and exhibits a doubling time of 47 hours.

Following the characterization of BC cell models, the first experiments using siRNA to knockdown DHRS7 were carried out in ZR-75-1 cells. Comparable to the prostate cell lines in the first study described in this thesis, this BC model showed an increase in the migration rate following 24 hour DHRS7 knockdown (Figure 10). Additionally, preliminary xCelligence data shows an increase in the cell proliferation in the ZR-75-1 cells following DHRS7 knockdown (Figure 11). These first results give a hint that DHRS7 not only plays a role in prostate, but also in BC progression. However, disclosing the role of DHRS7 in breast cancer warrants further research in the ZR-75-1 cells as well as other BC cell lines. To expand this study in the future, in addition to the assays we used in the PCa project, I would like to establish methods to assess cancer progression such as an invasion assay and the use of -omics methodologies such as proteomics as well as interactomics to study the mechanism of DHRS7 action in cancer progression on molecular level.

The role of DHRS7 in liver regeneration, metabolism and its regulation on molecular level

In addition, to the role of DHRS7 in cancer, the “orphan” enzyme was previously linked to liver regeneration. In an earlier publication the mRNA expression of DHRS7 was shown to be elevate in rats following a 2/3 hepatectomy, indicating that DHRS7 may play a functional role in liver regeneration [85]. To further investigate these findings, I obtained liver tissue samples from 9 mice as a kind gift from Prof. Dr. JF. Dufour and co-workers from the Inselspital in Bern. The samples consisted of regenerating liver taken 24, 72 and 120 hours following 2/3 hepatectomy. Tissue obtained from the same animals during the hepatectomy surgery at time point 0 was used as a control. The qPCR analysis showed no significant differences in DHRS7 gene expression in regenerating liver following hepatectomy compared to control (Figure 12). In contrast, I observed a trend for a reduction in DHRS7 mRNA levels following hepatectomy. Interspecies differences may be a possible explanation for this finding, since other publications also highlight interspecies phenotypic discrepancies, for example, stem cell-mediated liver regeneration was different between rats and mice. Therefore it is important to take into account the differences of individual species when extrapolating data [135]. Furthermore, the two studies followed different experimental protocols. The control samples I assessed were derived from the same animal at time point 0 during the 2/3 hepatectomy surgery,

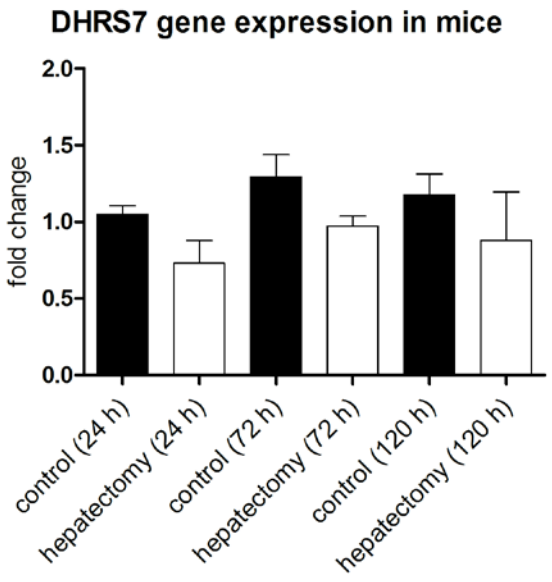

Figure 12:DHRS7 gene expression in mice24, 72 and 120 h following 2/3 hepatectomy compared to control

whereas Wang et al. performed an operation control in additional animals [85, 136]. Other studies also show variable results in the liver under different stresses and pathologies [112, 137, 138]. To further investigate the role of DHRS7 in liver regeneration, DNA expression levels of patients exposed to different causes, leading to liver damage, were analyzed. Microarray data derived from patients suffering from hepatocellular carcinoma (HCC), performed in Prof. Dr. L. Terracianos group showed decreased levels of DHRS7 mRNA in HCC caused by Hepatitis C Virus (HCV) (Figure 13). Previous data generated in our lab by Dr. A. Meyer showed elevated DHRS7 mRNA following ethanol (4% in drinking water) administration to rats for three month (data not shown).

Microarray data from a recent publication showed patients with alcoholic hepatitis had elevated gene expression compared to normal tissue [137]. However, comparisons between species as well as between cause and stage of liver damage, seems to be complex, since specific pathways might be triggered and therefore DHRS7 might be regulated in different ways [139, 140]. The levels of DHRS7 are clearly altered in the liver under specific conditions and warrant further research to understand its role.

To determine the possible mechanisms underlying transcriptional regulation of DHRS7 following liver damage, the impact of several factors involved in hepatocyte proliferation during liver regeneration has been assessed in different hepatic cell lines by the master student P. Marbet, under my supervision. None of the tested factors, namely epidermal growth factor, tumor necrosis factor alpha, insulin and transforming growth factor beta 1 impacted significantly on DHRS7 mRNA levels in any of the evaluated cell lines [110].

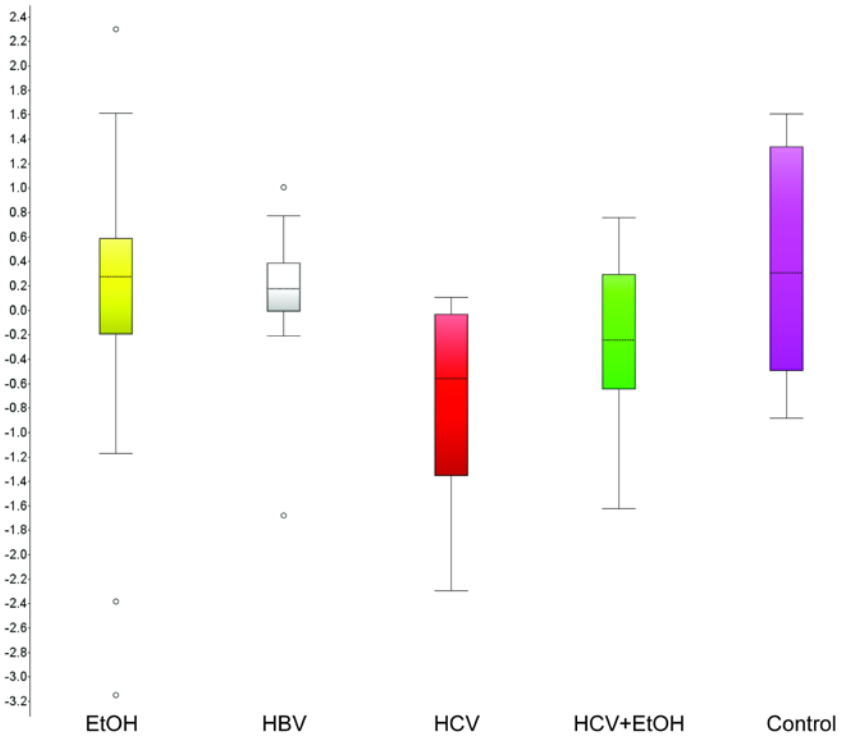

Figure 13:DHRS7 mRNA expression in human liver of patients suffering from HCC cause by alcohol (EtOH), Hepatits B or C virus (HBV, HBC) or combinations compared to normal liver. The data is derived from microarray data

Besides, defining the role of DHRS7 in different disease states, I also focussed on characterizing the enzymes metabolic properties and gene regulation. Therefore, experiments were designed to attempt to "deorphanize" DHRS7 by finding its possible substrates. I used LC-MS/MS as well as assessing the gene expression of DHRS7 following steroid hormone treatments *in vitro*. To date, the substrate(s) of DHRS7 remain unknown. Although a recent study suggested that DHRS7 might catalyze the reduction of several steroid hormones such

as cortisone, 4-androstene-3, 17-dione and xenobiotics like 1, 2-naphtoquinone, 9,10-phenantrenequinone, this evidence was derived from indirect activity measurements of NADP and needs to be verified [82]. Treating HEK-293 cells expressing recombinant human DHRS7 with radiolabeled substrates, cortisone/cortisol and 4-androstenedione/testosterone, I was unable to detect any activity (Figure 14). I also performed LC-MS/MS measurements (method described in the second project of this thesis) with HEK-293 cells transfected with DHRS7 and assessed the metabolism of 12 steroid hormones, namely cortisol, cortisone, corticosterone, 11-dehydrocorticosterone, aldosterone, DOC, DHEA, DHEAS, androstenedione and testosterone compared to HEK-293 cells transfected with pcDNA3 as a control. None of these steroid hormones could be confirmed as a substrate of DHRS7 (data not shown). In addition to the steroid hormones, several xenobiotics, such as bupropion, climbazol, metyrapone, menadione, triadimefon and triadimenol and metabolites of arachidonic acids including 5-HETE, 5-oxo-ETE, 12 HETE, 12-oxo-ETE, 15 HETE and 15-oxo-ETE were also assessed for their potential as possible substrates for DHRS7. Again none of the tested compounds was metabolized after incubation with HEK-293 cells expressing recombinant DHRS7 (data not shown). However, further experiments using the LNCaP cells knocked-down DHRS7 need to be performed to ensure that the previous findings have not been biased by transient expression of DHRS7 in HEK-293 cells with resulting inactivity of the enzyme or absence of interaction partners. Furthermore, it remains to be investigated whether DHRS7 might play a role in the production of androgens via the backdoor pathway or whether it indirectly stimulates androgen-dependent cancer cell proliferation. Therefore experiments using “untargeted” steroidomics are ongoing.

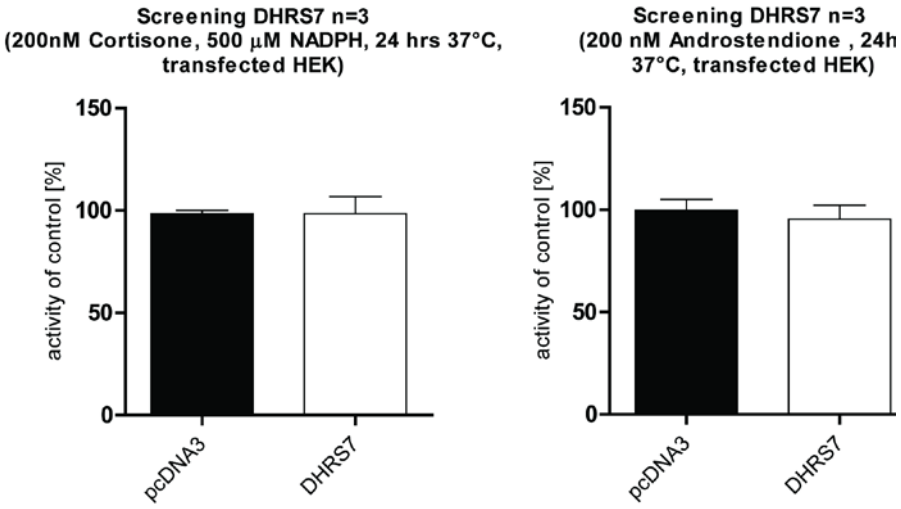

Figure 14: Activity assay in intact cells. HEK cells transfected with pcDNA3 or DHRS7 were incubated with radiolabeled androstenedione or cortisone and conversion was measured. Results display mean±SD of three independent replicates.

The regulation of DHRS7 gene expression in LNCaP cells treated with steroid hormones has been analyzed (Figure 15A). Treatment of LNCaP cells with testosterone and estradiol elevated expression of DHRS7 mRNA after 48 and 72 h, respectively. However, the results in these experiments were highly

variable and therefore no significance was found, possibly depending on cell characteristics such as growth, passage and viability. Evaluation of regulatory effects of steroid hormones on DHRS7 protein levels warrants therefore additional assessment by immunoblotting. Furthermore, the effect of DHRS7 expression on AR transactivation was examined (Figure 15B). HEK-293 cells expressing recombinant DHRS7 as well as a reporter gene under control of AR were treated with either vehicle control (DMSO 0.01%), testosterone (10 nM) or the combination of testosterone (10 nM) with the AR antagonist Flutamide (1 μM) for 24 h. Testosterone increased the expression of the reporter gene via activation of AR, whereby the antagonist Flutamide was able to reverse this effect. The expression of DHRS7 did not affect the observed effects when compared to pcDNA3 transfection control.

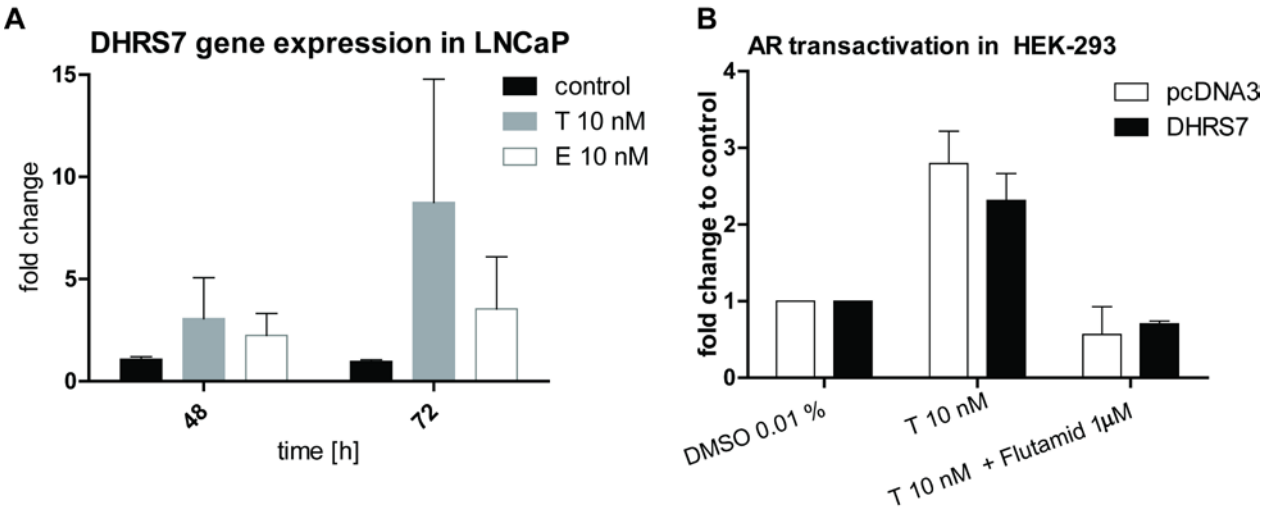

Figure 15: DHRS7 gene expression regulated by testosterone and estradiol and AR transactivation. (A) DHRS7 mRNA expression in LNCaP cells after treatment with 10 nM testosterone (T) and 10 nM estradiol (E) for 48 and 72 h. (B) AR transactivation in HEK-293 expressing DHRS7 and pcDNA3 as a control. Data represents mean ± SD from three independent experiments. Statistical analysis was performed using the Student's t-test; *p ≤ 0.0001 compared to the control.

Recent studies indicated altered expression of DHRS7 gene expression in animals receiving low and high fat diets compared to controls [111-113]. Thus, special diets might influence DHRS7 on the molecular level. To test this hypothesis DHRS7 mRNA expression was assessed in rat liver samples from animals fed with either a high fat or standard chow diet obtained from Prof. Dr. JP. Montani, University of Fribourg. DHRS7 gene expression was found to be decreased in rats fed with a high fat diet when compared to a standard chow control. In addition, microarray data of a previous study showed that DHRS7 gene expression was decreased in wild type mice obtaining a high fat diet. In comparison, this effect was abolished in the SCD1 knockout animals, suggesting this enzyme may play a role in the regulation of DHRS7 following high fat diet [84]. Interestingly a recent study performed in obese women found the opposite trend, increased DHRS7 levels during a short term low fat, hypocaloric diet [138]. Further research needs to be performed to disclose the function and regulation of DHRS7 during different nutrition availabilities in animals and humans.

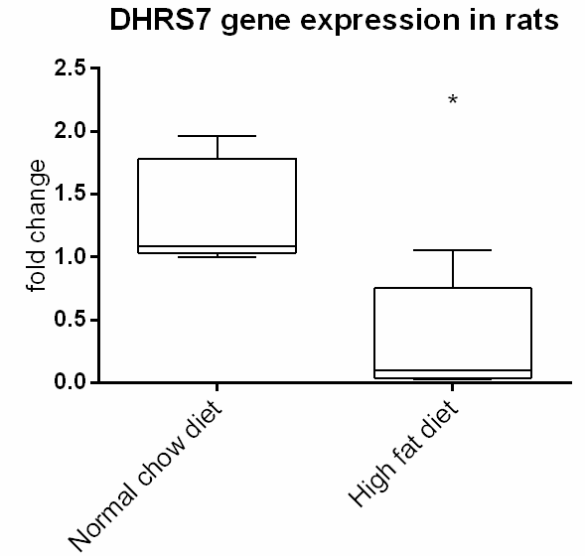

Figure 16: Gene expression of DHRS7 in liver in rats receiving high or low fat diet. Data displays 5 animals in each group. Statistical analysis was performed using the Mann-Whitney U test *p ≤ 0.0001 compared to high fat diet rats.

In summary, the work described in this thesis suggests that DHRS7 functions as a tumor suppressor. DHRS7 protein was found to be decreased with human prostate cancer progression in a TMA. Knockdown of the "orphan" enzyme led to increased cell proliferation and migration as well as decreased cell adhesion in several prostate and breast cancer cell lines *in vitro*. Microarray data suggested EMT and/ or BRCA pathway as possible mechanisms for DHRS7 effects. Furthermore, a possible role of DHRS7 in liver regeneration was identified. The substrate of DHRS7 still remains unknown. However, some steroid hormones can be excluded as possible substrates based on the results of this thesis. Regulation of DHRS7 gene expression may be influenced by sex steroid hormones such as testosterone or estradiol and by different diets and toxicants such as alcohol. Further research needs to be performed to define the function and regulation of DHRS7. In addition to following up on some of the targeted hypothesis generated with the help of the results in this thesis, untargeted omics approaches, such as metabolomics, (phospho)proteomics and interactomics, could be used to help support our current hypothesis and generate new ideas.

Outlook

More than 70 SDRs have been identified in the human genome so far and almost half of them are not at all characterized. Thus, characterization of "orphan" SDRs may be beneficial, since they may serve as novel diagnostic tools or therapeutic targets in several diseases, including cancer. "Orphan" SDRs share substantial structural similarity with others, characterized SDRs, such as 11βHSD1. Pharmaceutical inhibitors of 11βHSD1 may cause adverse effects by cross-reacting with other SDRs, including "orphan" SDRs. Therefore, the characterization of "orphan" enzymes is not only crucial for the assessment of their physiological roles, but also for the evaluation and understanding of potential adverse drug effects. This thesis characterized DHRS7 as a potential tumor suppressor and possible marker for breast and prostate cancer. Therefore, pharmaceuticals cross-reacting with DHRS7 may cause highly undesirable off-target effects, since they potentially promote cancer. In future experiments, a screening method to assess DHRS7 activity should be developed in order to study the physiological role of this enzyme and to use it as counter screen to avoid adverse effects. Furthermore, DHRS7 may serve as a useful tumor marker, since we found altered expression of the protein in early grades of prostate tumors. However, to understand the mechanism and function of DHRS7 its substrate(s) need to be identified. An untargeted metabolomics approach or a large compound screening could be used to help to "deorphanize" DHRS7.

In addition, structural modelling in combination with compound library screening may aid the identification of DHRS7 substrate(s).

Submitted manuscript: A role for the dehydrogenase DHRS7 (SDR34C1) in prostate cancer

A role for the dehydrogenase DHRS7 (SDR34C1) in prostate cancer

Julia K. Seibert[a], Luca Quagliata[b], Cristina Quintavalle[b], Thomas G. Hammond[a], Luigi Terracciano[b], Alex Odermatt[a]

[a] Division of Molecular and Systems Toxicology, Department of Pharmaceutical Sciences, University of Basel, Klingelbergstrasse 50, CH-4056 Basel, Switzerland
[b] Molecular Pathology Division, Institute of Pathology, University Hospital and University of Basel, Schönbeinstrasse 40, CH-4003 Basel, Switzerland

C**orresponding author**:
Dr. Alex Odermatt, Division of Molecular and Systems Toxicology, Department of Pharmaceutical Sciences, University of Basel, Klingelbergstrasse 50, CH-4056 Basel, Switzerland
Phone: +41 61 267 1530, Fax: +41 61 267 1515, E-mail: alex.odermatt@unibas.ch

ABSTRACT

Several microarray studies of prostate cancer (PCa) samples have suggested altered expression of the 'orphan' enzyme short-chain dehydrogenase/reductase *DHRS7* (retSDR4, SDR34C1). However, the role of DHRS7 in prostate cancer is largely unknown and the impact of DHRS7 modulation on cancer cell properties has not yet been studied. Here, we investigated DHRS7 expression in normal human prostate and PCa tissue samples at different tumor grade using tissue-microarray (TMA) and immuno-visualization. Moreover, we characterized the effects of siRNA-mediated DHRS7 knockdown on the properties of three distinct human prostate cell lines. We found that DHRS7 protein expression decreases alongside tumor grade, as judged by the Gleason level, in PCa tissue samples. Additionally, siRNA-mediated knockdown of DHRS7 expression in the human prostate cancer cell lines LNCaP, BPH1 and PC3 significantly increased cell proliferation in LNCaP cells as well as cell migration in all of the investigated cell lines. Furthermore, cell adhesion was decreased upon DHRS7 knockdown in all three cell lines. To begin to understand the mechanisms underlying the effects of DHRS7 depletion, we performed a microarray study with samples from LNCaP cells treated with *DHRS7*-specific siRNA. Several genes involved in cell proliferation and adhesion pathways were found to be altered in DHRS7 depleted LNCaP cells. Additionally, genes of the BRCA1/2 pathway and the epithelial to mesenchymal transition regulator E-cadherin were altered following DHRS7 knockdown. Based on these results, further research is needed to evaluate the potential role of DHRS7 as a tumor suppressor and whether its loss-of-function promotes PCa progression and metastasis.

Key words

SDR34C1, DHRS7, prostate cancer, gene expression, proliferation, tumor suppressor

INTRODUCTION

Prostate cancer (PCa) is one of the most common malignancies worldwide, with its incidence continually rising. It is also the second leading cause of cancer-related death among men. [1] Clinically, PCa manifests as a heterogeneous, multifocal disease. [2, 3] The mechanisms underlying the initiation and progression of PCa are complex. Initially, pre-malignant lesions, which are attributed to genetic alterations in one or more cells, arise. Subsequently, genetic alterations can occur in one or a few of the pre-malignant cells, resulting in changes of signaling pathways and resulting in malignant growth and the formation of a primary tumor. Cells in a primary tumor are heterogeneous regarding their phenotypic and biological characteristics, caused by the differences in the genes that were affected, thus making therapeutic interventions challenging.

Besides environmental factors, age and familial inherited susceptibility factors, steroid hormone receptor signaling plays a pivotal role in all stages of prostate carcinogenesis. The androgen receptor (AR) signaling pathway is thought to promote the early development of PCa, and it also has an important role in the development of castration resistant prostate cancer (CRPC), which fails to respond to hormone deprivation therapies. Several mechanisms have been suggested to cause the progression of PCa to CRPC, including hypersensitivity of the AR signaling pathway to androgens, enrichment or accumulation of androgen-insensitive stem cells, and activation of intratumoral steroidogenesis. [4] Furthermore, there is evidence for a pivotal role of the process of epithelial-mesenchymal transition (EMT) in the development of metastatic CRPC. [5]

In its initial stages, PCa is often curable; however, despite recent advances in current therapeutic methods, many patients develop post-operative disease relapse and suffer from significant treatment-associated complications. The current standard for the treatment of PCa is either medical or surgical castration. Nevertheless, following castration, PCa can progress to CRPC and patients may develop metastases in various organs such as lymph nodes, liver and bone. [6, 7] Besides the androgen-dependent growth stimulation, a comprehensive understanding of the molecular mechanisms underlying PCa progression is largely incomplete, with further research warranted. Thus, it is important to investigate new players in prostate cancer to understand disease progression and develop improved strategies for the prevention and therapy.

In this context, analyses of the transcriptome of PCa samples can provide hints to genes involved in cancer development and progression. Microarray expression data from three independent studies on human prostate cancer tissues suggested that the levels of the short-chain dehydrogenase/reductase (SDR) enzyme DHRS7 (also known as retSDR4 and under the nomenclature name SDR34C1) [8] are frequently altered in this tumor. [9-11] A recent study of the transcriptome of human LNCaP prostate cancer cells hypothesized that DHRS7, among several other genes, may play a role in sustaining *de novo* androgen synthesis and/or metabolism in CRPC, eventually leading to the reactivation of androgen receptor (AR), thus promoting cancer progression even upon ablation of testicular androgen production. [12]

DHRS7 was initially cloned from retinal pigment epithelium cells; [13] however, it is expressed in various tissues including the prostate. [14, 15] Little is known on the catalytic activity and physiological role of

DHRS7 and this enzyme has therefore to be considered as an “orphan” SDR. A recent study by Stambergova *et al.* suggested that DHRS7 possesses NADP(H) cofactor preference and enzymatic reducing activity towards endogenous substrates with a steroid structure (estrone, cortisone, 4-androstene-3,17-dione) and exogenous substances bearing a carbonyl group (1,2-naphtoquinone, 9,10-phenantrenequinone, benzoquinone, nitrosamine 4-(methyl-nitrosamino)-1-(3-pyridyl)-1-butanone). [16] However, the evidence for a role of DHRS7 in the metabolism of these compounds was based on indirect measurements of NADPH consumption. Other investigators did not observe any activity towards steroids and retinoids.[13] Nevertheless, some of the closest relatives of DHRS7, *i.e.* 11β-HSD and 17β-HSD enzymes, have been associated with cancer. Especially, the fact that 17β-HSDs are involved in the control of sex steroid metabolism and that their expression levels are altered in tumors, emphasized the importance of these SDRs in breast and prostate cancer. [17-19]

Based on the preliminary observations from microarray studies and the relation of DHRS7 to SDRs involved in PCa, we investigated the role of DHRS7 in PCa, taking advantage of a combination of human data obtained on a large cohort (n=348) of samples and *in vitro* experiments comprising modulation of DHRS7 expression by knockdown. To determine the effects of DHRS7 on the aggressiveness of prostate cells *in vitro* we evaluated cell proliferation, migration and adhesion after siRNA-mediated knockdown in three prostate cell lines, namely LNCaP, BPH1 and PC3. Furthermore, we performed a microarray experiment using LNCaP cells treated with siRNA against DHRS7 in order to obtain initial insights into pathways involved in its action.

MATERIAL AND METHODS

Tissue-microarray (TMA) construction and clinical pathology data

The use of clinical specimens for the construction of tissue-microarrays (TMAs) was approved by the ethical committee of the University Hospital of Basel, Switzerland. The TMAs were manufactured as previously described. [20, 21] Briefly, the PCa progression TMAs consist of formalin-fixed and paraffin-embedded (FFPE) specimens obtained from 551 prostate cancer patients plus 68 normal prostate tissues. To evaluate DHRS7 protein expression the TMAs were stained with an anti-DHRS7 antibody (rabbit anti-human DHRS7 polyclonal antibody, HPA031121**,** Sigma, St. Louis, USA, 1:200 dilution) and analyzed by an experienced pathologist (L.T.). Immunoreactivity was scored semi-quantitatively (0=negative and 3=highest intensity) by evaluating the staining intensity as described by Allred *et al*. [22]

Cell lines and cell culture

The human prostate carcinoma cell line LNCaP was newly purchased from ATCC (LGC Standards GmbH, Wesel, Germany). PC3 cells and the benign prostate hyperplastic cell line BPH1 were available in-house and originally purchased from ATCC. The identity of the cell lines was verified by the multiplex human cell line authentication test (Multiplexion, Immenstaad, Germany). All cell lines were maintained in RPMI 1640 (R8758, Sigma) supplemented with 10% fetal calf serum (FCS) and penicillin (100 U/mL)/streptomycin (100 µg/mL). Cells were cultured at 37°C in a 5% CO_2 atmosphere.

Immunohistochemical staining

LNCaP, PC3 and BPH1 cells were seeded in 6-well plates containing a 18 mm round glass slide (Menzal-Glaser, Braunschweig, Germany) at 3 x 10^5 cells per well. For indirect immunofluorescence experiments, culture medium was removed and cells were washed twice with PBS, fixed with 4% paraformaldehyde for 15 min and washed three times with PBS. Cells were permeabilized with 0.1% Triton X-100 for 10 min and blocked with 1% BSA for 20 min at room temperature. Blocking was followed by incubation with a primary antibody against DHRS7 (rabbit anti-human DHRS7 polyclonal antibody; 1:500 dilution in 1% BSA, HPA031121**,** Sigma) for 1 h at room temperature. After three washes with PBS, Hoechst-33342 (5 µg/ml, H3570, Invitrogen Life Technologies, Zug, Switzerland) and goat anti-rabbit HiLyte™ Fluor 488-labeled (1:2000, AS-61056-1-H488, Anaspec, Fremont, USA) secondary antibody was applied for 30 min at room temperature. Cells were washed three times with PBS, mounted in Mowiol 4-88 and slides were analyzed under a laser scanning confocal microscope (Fluoview 1000, Olympus, Shinjuku, Japan).

Transfection with siRNA

LNCaP, PC3 and BPH1 cells (3 x 10^5) were reverse transfected on a 6-well plate using Lipofectamine RNAiMax reagent with 10 nM of siRNA targeting *DHRS7* (D-009573-02, Thermo Scientific, Waltham, USA) or a non-targeting siRNA negative control (D-001810-03-20, Thermo Scientific). Effective knockdown was verified by qPCR as well as western blot and immunodetection. To choose the siRNA for the main experiments, we performed preliminary knockdown experiments with four different siRNAs and a pool of all of them (MQ-009573-00, Thermo Scientific), and determined the most effective knockdown by qPCR after 24 h, 48 h and 72 h (Supplementary Figure 1).

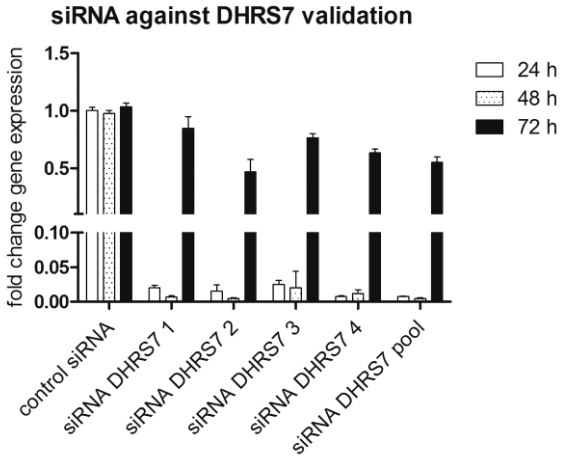

Supplementary Figure 1: Comparison of the knockdown efficiency of four different siRNAs against DHRS7 mRNA levels. Four siRNAs against DHRS7 were assessed by single application and as pooled siRNA mixture at a concentration of 15 nM for gene silencing in LNCaP cells after 24 h, 48 h and 72 h. As a control, non-targeted siRNA was used. DHRS7 mRNA expression was normalized to the housekeeping gene for cyclophillin A (PPIA).

To ensure that the siRNA effects observed for the specific siRNA (D-009573-02) were due to DHRS7 knockdown and not off-target effects, we additionally performed the proliferation assay in LNCaP with another DHRS7-specific siRNA (D-009573-04) (Supplementary Figure 2). The results obtained were similar for both tested siRNAs. For the functional assays cells were used at 24 h post-transfection.

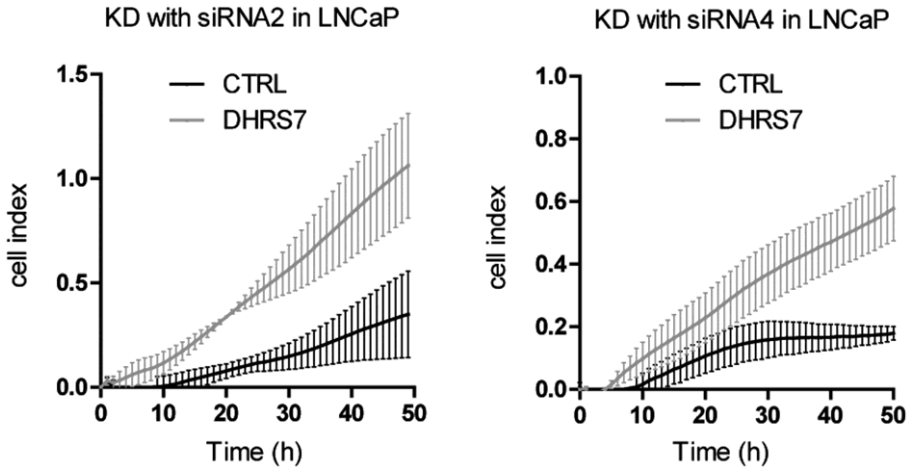

Supplementary Figure 2: Comparison of cell proliferation in LNCaP cells after knockdown of DHRS7 with two different siRNAs. The xCELLigence system was used to monitor dynamic cell proliferation in real-time. Following 24 h of transfection with siRNA No.2 or No.4 against DHRS7 or non-targeted control siRNA, respectively, LNCaP cells were seeded in E-plates of the xCELLigene RTCA instrument and monitored for a further 48 h.

Real-time qPCR

Total RNA was isolated from cultured cells using TRI-reagent (T9424, Sigma) according to the manufacturer`s instructions. RNA quality and quantity was measured using a ND-1000 spectrometer (Nano-drop, Wilmington, USA). Reverse transcription was performed using the M-MLV Reverse Transcriptase Kit (M368B, Promega, Wallisellen, Switzerland) according to the manufacturer`s instructions. Relative quantification of mRNA expression levels was performed by real-time qPCR. Briefly, cDNA (10 ng), gene-specific oligonucleotide primers (Supplementary Table 1) (200 nM) and KAPA SYBR FAST qPCR reagent (KK4600, Kapa systems, Wilmington, USA) (5 µL), in a final volume of 10 µL, were analyzed by qPCR in a rotor-gene 3000A (Corbett Research, Sydney, Australia).

Gene	Primer	
	forward (5'-3')	**reverse (5'-3')**
BRCA1	GAAACCGTGCCAAAAGACTTC	CCAAGGTTAGAGAGTTGGACAC
BRCA2	CACCCACCCTTAGTTCTACTGT	CCAATGTGGTCTTTGCAGCTAT
CDH1	CGAGAGACTACACGTTCACGG	GGGTGTCGAGGGGAAAAATAGG
CHEK1	ATATGAAGCGTGCCGTAGACT	TGCCTATGTCTGGCTCTATTCTG
CHEK2	TCTCGGGACTCGGATGTTGAG	CCTGAGTGGACACTGTCTCTAA
DHRS7	GAGTTTGGTAGAATCGACTTTCTG	GAAAGAGGTACAGATATGATACCC
FANCD2	AAAACGGGAGAGAGTCAGAATCA	ACGCTCACAAGACAAAAGGCA
PPIA	CATCTGCACTGCCAAGACTGA	TGCAATCCAGCTAGGCATG
RAD51	CAACCCATTTCACGGTTAGAGC	TTCTTTGGCGCATAGGCAACA

Supplementary Table 1: Human oligonucleotide primers used for qPCR

Thermal cycler parameters were as follows: denaturation for 15 min at 95°C, followed by amplification of cDNA for 40 cycles with melting for 15 s at 94°C, annealing for 30 s at 56°C and extension for 30 s at 72°C. Relative gene expression normalized to the internal control gene coding for cyclophillin A (PPIA) was obtained by the $2^{-\Delta\Delta Ct}$ method [23].

Western Blot

Cells were lysed using RIPA buffer (R0278, Sigma) and centrifuged at 12,000 x g for 10 min at 4°C. The supernatant was collected and protein concentration quantified using the Pierce® biocinchonic acid protein assay kit (23225, Thermo Scientific). Samples were heated at 95°C for 5 min in Laemmli buffer (5 mM Tris HCl, pH 6.8, 10% glycerol (v/v), 0.2% sodium dodecyl sulfate (SDS) (w/v), 1% bromophenol blue (w/v)) and stored at -20°C until used. Lysates were separated by a 12.5% Tris-glycine SDS-polyacrylamide gel, and transferred to Immun-Blot® polyvinylidene difluoride (PVDF) membranes (162-0177, Bio-Rad Laboratories, Hercules, USA) at constant 230 mA for 1 h. For detection of DHRS7 the membrane was blocked using 2% milk (v/v) for 1 h at room temperature, followed by incubation with the mouse anti-human DHRS7 polyclonal antibody (ab69348, abcam, Cambridge, UK) at a dilution of 1:500 (v/v) in 2% milk (v/v), overnight at 4°C. After washing with Tris-buffered saline (20 mM Tris-base, 140 mM NaCl) containing 0.1% Tween-20 (v/v) (TBS-T), the membrane was subsequently incubated with horseradish peroxidase-conjugated goat anti-mouse secondary antibody (Jackson Immuno Research, Suffolk, UK) for 1 h at room temperature. For cyclophilin-A detection, the membrane was blocked using 10% milk (v/v) overnight at 4°C, followed by incubation with the rabbit anti-human cyclophilin A polyclonal antibody (ab41684, abcam) at a dilution of 1:2,000 (v/v) in 2% milk for 1 h at room temperature. After washing with TBS-T, the membrane was subsequently incubated with horseradish peroxidase-conjugated goat anti-rabbit secondary antibody (Santa Cruz Biotechnology, Santa Cruz, USA) at a dilution of 1:1,000 (v/v) in 2% milk (v/v). After washing the membranes in TBS-T, images were visualized using the Immobilon Western Chemiluminescent HRP substrate kit (Millipore, Schaffhausen, Switzerland), and a FujiFilm ImageQuant™ LAS-4000 detector (GE Healthcare, Glattbrugg, Switzerland) using the chemiluminescence detection setting.

xCELLigence cell proliferation assay

The xCELLigence DP device (ACEA Biosciences, San Diego, USA) was used to monitor cell proliferation in real-time. LNCaP, PC3 and BPH1 cells were seeded in E-plates (E-Plate View™; ACEA) at 1×10^4, 5×10^3 and 5×10^3 cells per well, respectively. Proliferation was determined kinetically over 48 h using the xCELLigence system according to the manufacturer's protocol. Cell proliferation measurements were performed in triplicates with programmed signal detection every 15 min. Data acquisition and analyses were performed using the RTCA software (version 1.2, ACEA).

Ki-67 cell proliferation assay

Following 24 h after DHRS7 siRNA transfection, cells were detached, diluted to 10,000 cells in 100 µL and placed onto a Superfrost™ microscope slide using a Cytospin™ centrifuge (Thermo Scientific).

The slides were fixed in delaune for 2 min and then left to dry at room temperature for 5 min. Ki-67 staining was performed with a BenchMark Ultra platform automated IHC/ISH staining system (Roche, Rotkreuz, Switzerland). Ki-67 index was determined by ascertaining the percentage of Ki-67 positively stained cells in 5 fields scanned at 20x magnifications using ImageJ software (http://imagej.nih.gov/ij/).

Transwell migration assay

LNCaP, PC3 and BPH1 cells were re-seeded 24 h post-transfection into the top chamber of a 24-well non-coated insert (pore size 8 µm, Corning Inc., Lowell, MA, USA) at 1 x 10^5, 0.5 x 10^5 and 1 x 10^5 cells per well respectively. The upper chamber contained RPMI media supplemented with 1% FBS, whereas the bottom chamber contained 10% FBS as a chemoattractant. Following 24 h of incubation, cells were stained with 0.1% crystal violet (w/v) (C3886, Sigma) in 25% methanol (v/v). Non-migrated cells in the upper chamber were removed using a cotton swab. Images of migrated cells which adhered to the bottom of the filter were captured at 10x magnification using a light microscope (Zeiss Axiovert 100; Carl Zeiss Microscopy GmbH, Feldbach, Switzerland) and relative areas of staining were assessed using the threshold setting on Image J.

Cell adhesion

96-well plates were coated with 50 µg/mL fibronectin and blocked with 0.5% BSA in RPMI medium for 45 min at room temperature. LNCaP, PC3 and BPH1 cells were seeded at 1 × 10^5 cells per well and allowed to adhere for 60 min. Wells were then washed twice with PBS. The number of adherent cells in each well was quantified through staining with 0.1% crystal violet (w/v) in 25% methanol (v/v), followed by OD measurement.

cRNA target synthesis and gene chip hybridization

Total RNA for the microarray was isolated with Direct-Zol RNA MiniPrep Kit (Zymo Research, Irvine, USA) including on-column DNAse treatment. RNA concentration was assessed using a NanoDrop ND 1000 (Nanodrop) and RNA integrity was monitored on a Bioanalyzer RNA 6000 Chip (Agilent, Basel, Switzerland). 270 ng of DNAse-treated total RNA was subjected to target synthesis using the WT Expression kit (Life Technologies), following the manufacturer`s recommendations. Fragmentation and labeling of amplified cDNA was performed using the WT Terminal Labeling Kit (Affymetrix, Santa Clara, USA). Synthesis reactions were carried out using a PCR machine (TProfessionnalTrio, Biometra, Goettingen, Germany) in 0.2 mL tubes. 85 µL of cocktail containing 23.4 ng/µL labeled DNA was loaded on a Affimetrix GeneChip Human Gene 2.0 ST Array (Cat# 902499) and hybridized for 17 h (45°C, 60 rpm) in a hybridization oven 645 (Affymetrix). These gene chips have the particularity of interrogating all well-established annotation RefSeq coding transcripts (26,191) and in addition many well-established annotation RefSeq non-coding transcripts (3,391). The arrays were washed and stained on a Fluidics Stations 450 (Affymetrix), using the Hybridization Wash and Stain Kit according to the FS450_0002 protocol (Affymetrix). The gene chips were scanned with an Affymetrix GeneChip Scanner 3000 7G. DAT images and CEL files of the microarrays were generated using Affymetrix GeneChip Command Control software (version 4.0). Afterwards, CEL files were imported into Qlucore

software and Robust Multichip Average (RMA) normalized. Subsequently, principal component analysis to discriminate between engineered and control cells was performed. Quantile normalization and data processing were performed using the GeneSpringGXv11.5.1 software package (Agilent). The gene signature value was assessed using the BRB-ArrayTool (v4.3.2, NIH). Ingenuity software (Qiagen, Venlo, Netherlands) was use to perform pathways analysis.

Statistics

For the statistical analysis, the Chi-square test and the Fisher's exact test for non-parametric variables and ANOVA or Student's t-test for parametric variables were used, with all probabilities reported as two-tailed. Differences in patient survival were assessed using the Kaplan-Meier method and analyzed using the log-rank test in univariate analysis. All tests were two sided and p values < 0.05 considered being statistically significant. Cut-off scores were selected by evaluating the receiver- operating characteristic (ROC) curves. The point on the curve with the shortest distance to the coordinate (0, 1) was selected as the threshold value to classify cases as 'positive/overexpressing' or 'negative/down regulated'. Analyses were performed using the SPSS software (IBM, Armonk, USA).

RESULTS

DHRS7 expression is down regulated in human prostate cancer with increasing tumor grade To evaluate a potential role of DHRS7 in PCa, DHRS7 protein levels were analyzed by immunohistochemistry with a rabbit polyclonal anti-human DHRS7 antibody in a large collection of human prostate specimens using a set of TMAs. Representative pictures of DHRS7 staining are shown in Figure 1A and Supplementary Figure 3. Of the 491 stained tissue punches of PCa, 326 were suitable for analysis and 31 out of the 68 tissue punches from normal prostate could be used for this study. Tissues were excluded either as a consequence of poor staining quality or loss of the section from the slide. These analyses revealed DHRS7 to be highly expressed in normal prostate, with the vast majority of analyzed samples (80.6%) classified as benign with intensity 3 (scoring system: 0=negative for DHRS7 and 3=highest intensity of DHRS7, as described under Materials and Methods). Conversely, most of the PCa specimens were scored having either score 2 or 1, 39% and 34.4%, respectively (Figure 1B).

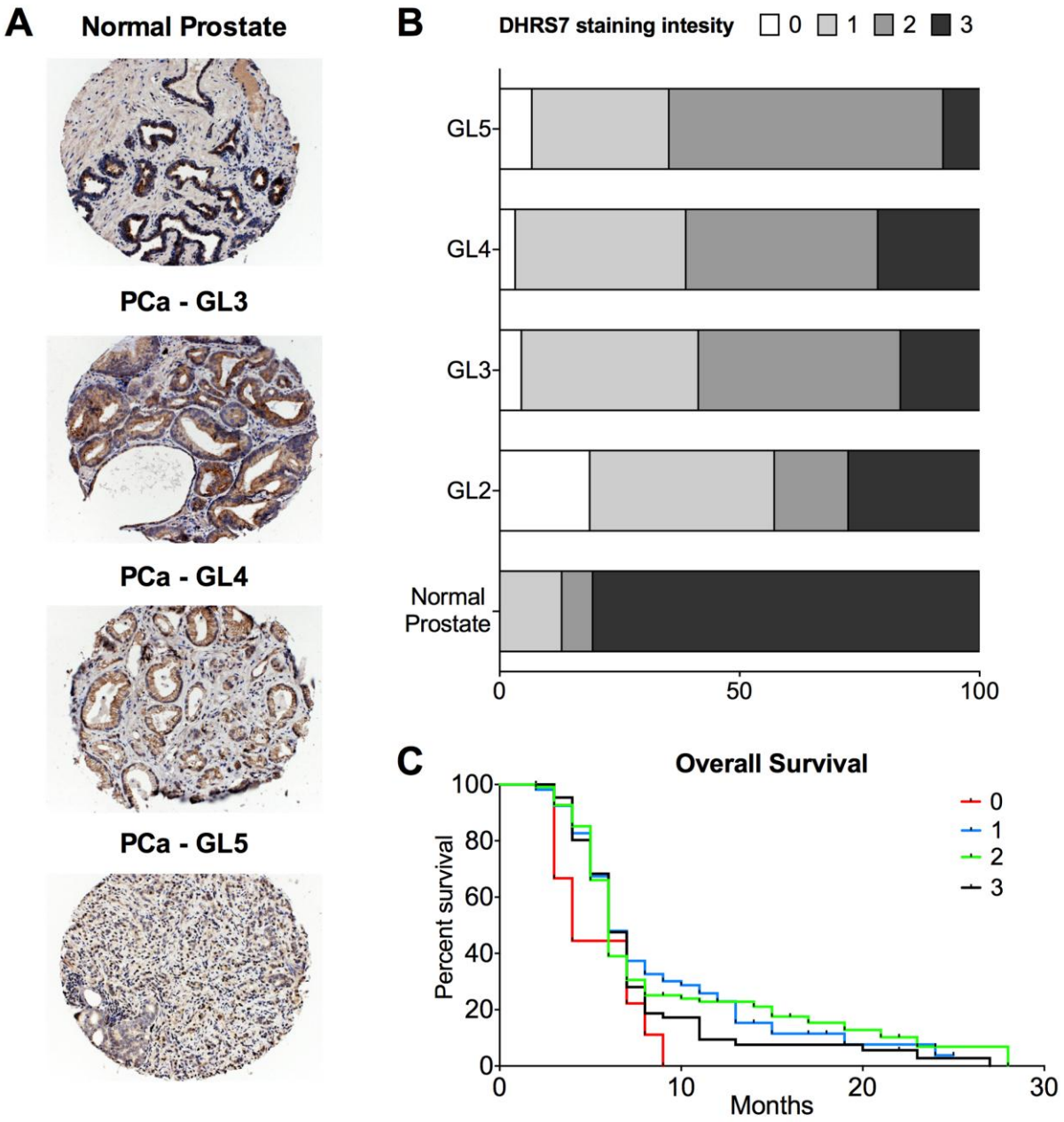

Figure 1: DHRS7 expression in human prostate samples. (A) Representative pictures of DHRS7 staining intensity in normal prostate versus PCa with different Gleason levels (GL). Formalin-fixed and paraffin-embedded prostate specimens were analyzed using a rabbit polyclonal anti-human DHRS7 antibody. (B) DHRS7 staining intensity distribution plots highlight that DHRS7 expression is reduced in PCa compared with normal prostate. (C) Kaplan-Meier curves based on DHRS7 expression levels suggest no major impact on the survival of PCa patients.

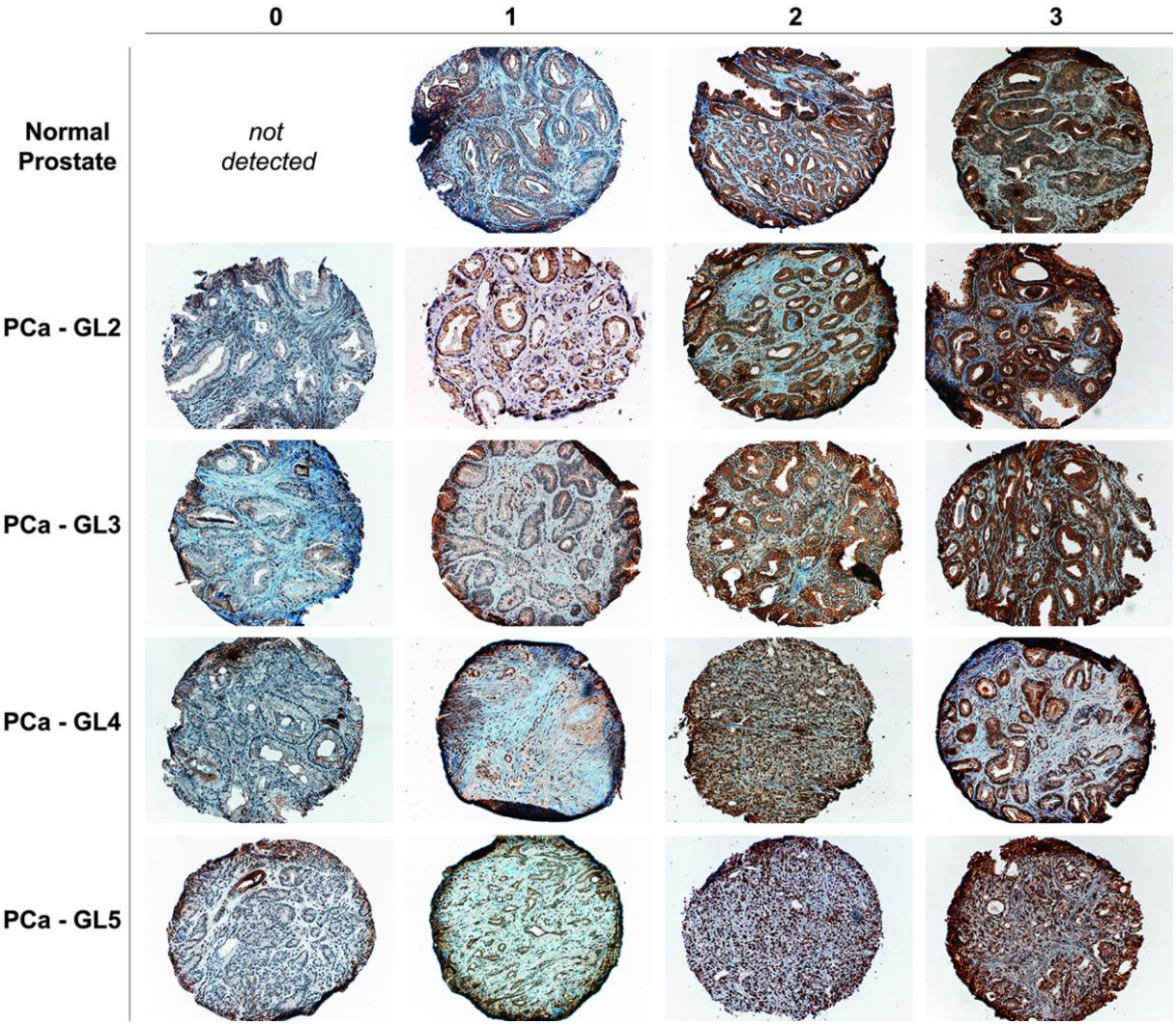

Supplementary Figure 3: DHRS7 representative staining in human normal prostate and PCa samples. The spectrum of DHRS7 staining intensity ranges from absent/low (0) to very high/strong (3), from left to right side respectively, in tested samples. Normal prostate to PCa GL5 specimens are reported, going from up to down side respectively.

Complete loss of DHRS7 was never observed in normal prostate tissue samples, while this was the case in 6.1% of PCa samples. Further stratification of PCa samples, based on their Gleason level (GL), outlined that the group of patients with the highest GL, namely GL5, presented with the lowest percentage of score 3 DHRS7 specimens (22.2%) (Table 1). These results suggest that the loss of DHRS7 is associated with PCa and tumor grade. Nevertheless, Kaplan-Meier plots did not reveal a significant association between DHRS7 expression and the survival of PCa patients (Figure 1C).

Impact of DHRS7 knockdown on the proliferation of PCa cells

Since DHRS7 expression decreases significantly as the tumor grade increases, we investigated the functional effects of silencing DHRS7 expression in prostate cell lines endogenously expressing DHRS7 at different amounts, as determined by real-time PCR, Western blotting and immunovisualisation, namely LNCaP (high), PC3 (moderate) and BPH1 (low) (Figure 2).

Tissue type	DHRS7 intensity n				χ^2	*P*
	0	**1**	**2**	**3**		
Normal Prostate	0	4	2	25		
PCa - GL2	3	5	2	6	11.10	**0.01**
PCa - GL3	9	70	80	40	49.90	**< 0.0001**
PCa - GL4	3	32	36	22	32.52	**< 0.0001**
PCa - GL5	4	4	8	2	25.54	**< 0.0001**

Table 1: Summary of observed DHRS7 protein levels in normal prostate and PCa samples. Stratification of PCa samples based on their Gleason level (GL) was performed by semi-quantitatively evaluating the immunostaining intensity as described by Allred et al. 22 Normal prostate (n=31), PCa - GL2 (n=16), PCa - GL3 (n=199), PCa - GL4 (n=93), PCa - GL5 (n=18). Results were analyzed using Chi-square test (χ2 test).

SiRNA-mediated targeting efficiently depleted *DHRS7* mRNA expression by more than 90% at all investigated time points (Figure 3A). The impact of siRNA-mediated knockdown of *DHRS7* gene expression on protein levels was assessed by western blotting (Figure 3B). Although the mouse anti-human DHRS7 polyclonal antibody used showed limited sensitivity in western blots, it was preferable over the rabbit anti-human DHRS7 polyclonal antibody and allowed qualitative assessment of protein expression. Protein levels were reduced to approximately 30-50% after 24 h and to below 10-20% after 48 h and 72 h in siRNA treated LNCaP cells. Knockdown of DHRS7 protein expression was also demonstrated in PC3 and BHP1 cells, whereby a very faint band was still detectable after 24 h but no longer after 48 h and 72 h. No morphological changes were observed following depletion of DHRS7 in these prostate cell lines (data not shown)

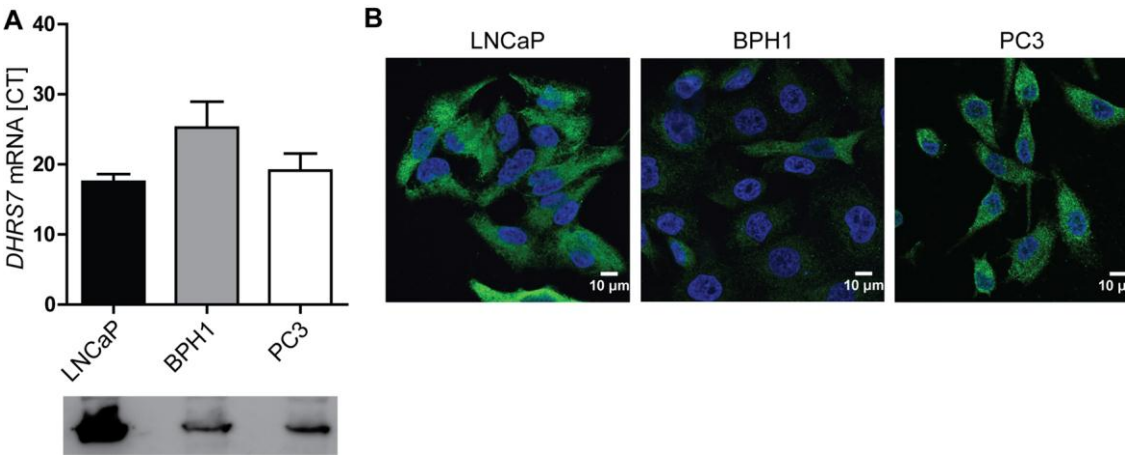

Figure 2: Endogenous expression of DHRS7 in LNCaP, BPH1 and PC3 cells as assessed by qPCR, Western blot and immunovisualisation. (A) For qPCR 10 ng cDNA was used and data was normalized to cyclophilin A (PPIA) control. For western blotting an amount of 40 µg of total protein was separated by SDS-PAGE, proteins were transferred onto PVDF membranes, followed by detection using a mouse polyclonal anti-human DHRS7 antibody. (B) Immunofluorescence staining was performed using a rabbit polyclonal anti-human DHRS7 antibody. Nuclei were stained with Hoechst-33342.

.

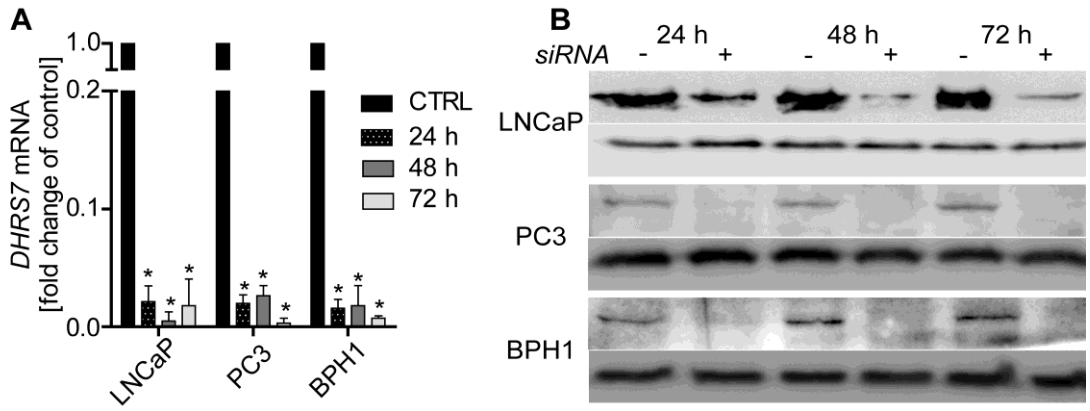

Figure 3: Knockdown of DHRS7 in prostate cell lines. Real-time qPCR (A) and western blot (B) showed the efficacy of siRNA against DHRS7 compared with that of control siRNA after 24 h, 48 h and 72 h in LNCaP, BPH1 and PC3 cells. (A) For real-time PCR 10 ng cDNA was used. Cyclophilin A (PPIA) served as a house-keeping control. Results are expressed as fold change of control and represent mean ± SD from three independent experiments conducted in triplicates. Statistical analysis was determined using the Student's t-test. *p ≤ 0.0001. (B) For western blot 10 µg of total protein for LNCaP and 30 µg for BPH1 and 37 µg for PC3 were subjected to SDS-PAGE and western blotting using a mouse polyclonal anti-human DHRS7 antibody. Representative experiments are shown.

The impact of DHRS7 knockdown on cell proliferation was assessed using the xCELLigence system. Depletion of DHRS7 resulted in a 3-fold increase in LNCaP cell proliferation, which was supported by an enhanced Ki-67 staining (Figure 4A-C). The effect on cell proliferation upon knockdown of DHRS7 was verified by using an independent siRNA molecule (Supplementary Figure 2).

In contrast to LNCaP, no significant changes in cell proliferation following DHRS7 depletion could be observed for PC3 and BPH1 cells, and also Ki-67 staining was not different between control and knockdown. Interestingly, depletion of DHRS7 had no effect on the cell cycle as detected by flow cytometric analysis (Supplementary Figure 4). These results suggest that knockdown of DHRS7 impairs cell proliferation, dependent on their basal proliferation rate and/or DHRS7 expression levels.

Depletion of DHRS7 promotes cell migration and adhesion in PCa cells

To study the effects of DHRS7 down regulation on the migratory and adhesive capabilities of LNCaP, PC3 and BPH1 cells transwell cell migration and fibronectin adhesion assays were performed. Cell migration was significantly enhanced in cells treated with siRNA against DHRS7 compared with cells treated with non-targeted control siRNA ($p<0.05$, Figures 4D and 4E). The effect was most pronounced in LNCaP cells where migration was increased 3-fold upon DHRS7 knockdown. The number of adherent cells following DHRS7 depletion was significantly reduced compared with controls ($p<0.05$, Figure 4F). These results suggest that loss of DHRS7 promotes cell migration and decreases adhesion in all three cell lines tested.

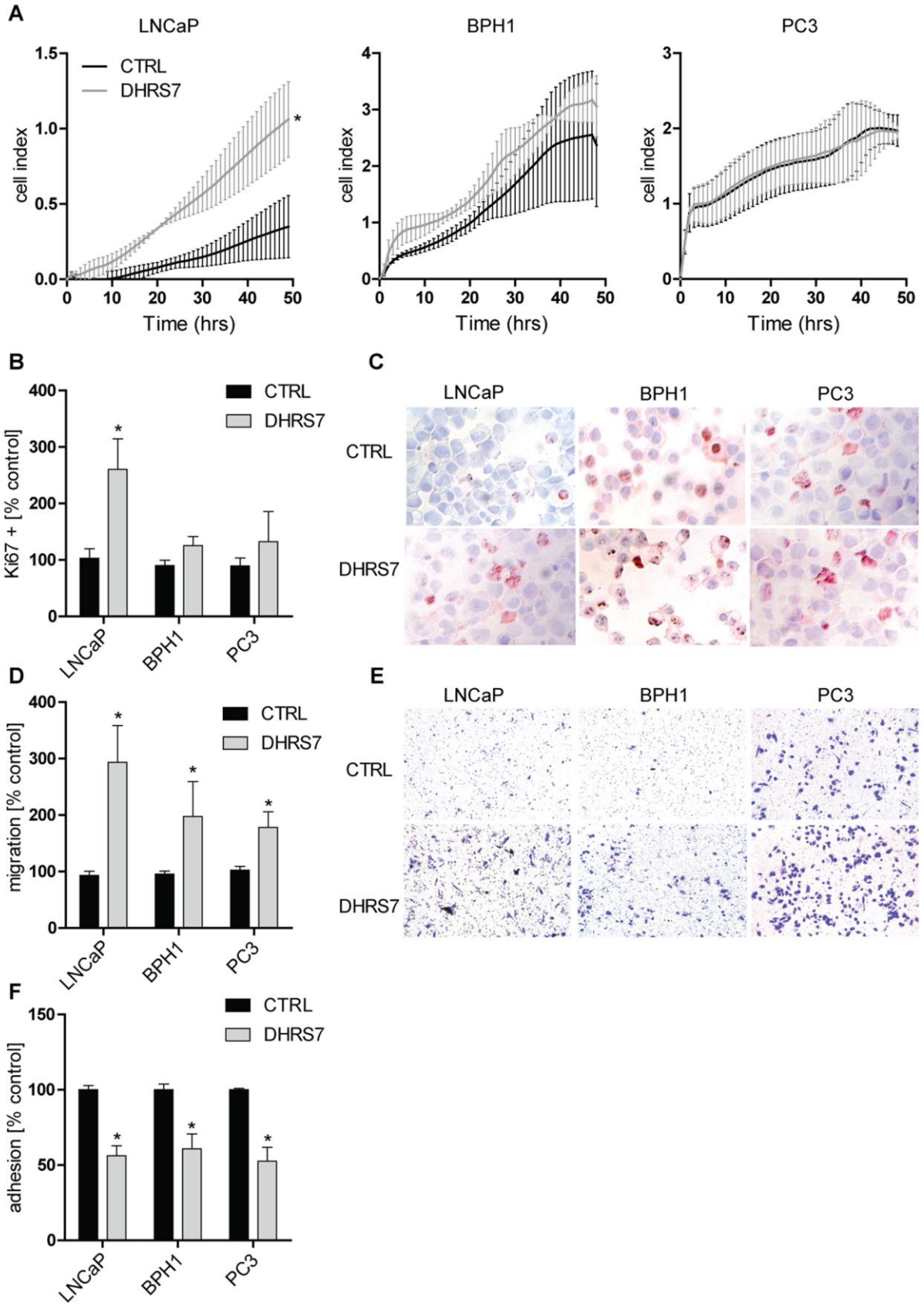

Figure 4: Influence of DHRS7 knockdown on proliferation, migration and adhesion in LNCaP, BPH1 and PC3 cells. (A) The xCELLigence system was used to monitor dynamic cell proliferation in real-time. 24 h after transfection with siRNA against DHRS7 or non-targeted control siRNA, LNCaP, BPH1 and PC3 cells

were seeded in E-plates of the xCELLigene RTCA instrument and monitored for a further 48 h. Cell index refers to a relative change in electrical impedance representing the number of cells detected on the microelectrodes on the bottom of the plate. (B,C) Immunohistochemical staining of Ki-67 expression in LNCaP, BPH and PC3 cells 48 h after knockdown of DHRS7, normalized to cells treated with control siRNA. Ki-67 index was determined by detecting the fraction of Ki-67 positively stained cells in 5 fields, scanned at 20x magnification using ImageJ. Representative images are shown. (D, E) Migration of LNCaP, BPH1 and PC3 cells after knockdown of DHRS7 assessed by the transwell migration assay. Cells transfected with siRNA against DHRS7 or scrambled non-targeted control siRNA were seeded on Boyden chamber transwell inserts at 24 h post-transfection, followed by crystal violet staining after another 24 h. Stained cells in 5 fields scanned at 10x magnification setting were analysed using ImageJ. Representative pictures of Boyden chamber assays are shown. (F) Cell adhesion assay using fibronectin as an extracellular matrix (ECM) in LNCaP, BPH1 and PC3 cells. At 24 h post-transfection with siRNA against DHRS7 or scrambled non-targeted control siRNA cells were seeded in fibronectin coated plates. Adherent cells were quantified after 60 min by crystal violet staining. All data represent mean ± SD from at least three independent experiments conducted in triplicate. Statistical analysis was performed using the Student's t-test; *p ≤ 0.0001 compared to the non-targeted control.

The impact of DHRS7 knockdown on the gene expression profile of LNCaP cells

Based on these *in vitro* findings, we investigated whether ablation of DHRS7 expression may impair the expression of genes involved in proliferation, migration and adhesion. For this purpose we used LNCaP cells, due to their high endogenous expression level and the pronounced effects of siRNA-mediated knockdown, and conducted a microarray study using the Affymetrix GeneChip Human Gene 2.0 ST Array. RNA was prepared at 24 h, 48 h and 72 h post-transfection with siRNA against *DHRS7*. Non-targeting siRNA was used as control. First, we assured that *DHRS7* expression was efficiently decreased (Figure 5A). Following this, the transcriptome data was examined, revealing that DHRS7 knockdown altered the global gene expression profile of LNCaP cells as early as 24 h after siRNA treatment, as shown by PCA analysis (Figure 5B) and hierarchical clustering (Figure 5C). The differences were more pronounced at 48 h and 72 h (Figure 5B). To validate our microarray data, we performed qPCR to confirm some of the expression changes observed in the microarray following DHRS7 knockdown. The target genes were selected based on the fold change between control and DHRS7 knockdown treatment and due to their potential role in cell proliferation or metastasis, namely: *CLSPN*, *EIF3I*, *H2AFV* and *CDH1* (Figure 5D). In order to determine whether the differentially expressed genes had functional relationships in similar signaling pathways, we employed the interactive pathway analysis (IPA) tool with Ingenuity software. IPA revealed enrichment of pathways involved in DNA replication, cellular growth and proliferation, cellular assembly and organization, migration and adhesion as well as cancer (Supplementary Figure 5).

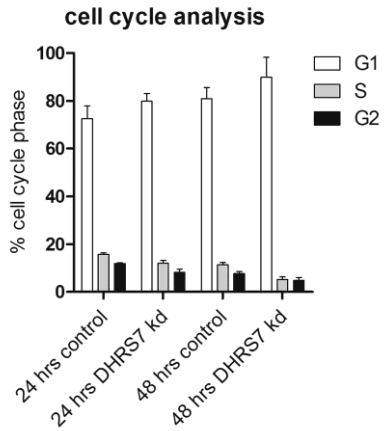

Supplementary Figure 4: Histogram showing the percentages of cells in each phase of the cell cycle after DHRS7 knockdown. LNCaP cells were treated with siRNA against DHRS7 and collected after 24 h or 48 h. Subsequently, cells were subjected to propidium iodide staining and analyzed for DNA content by flow cytometry.

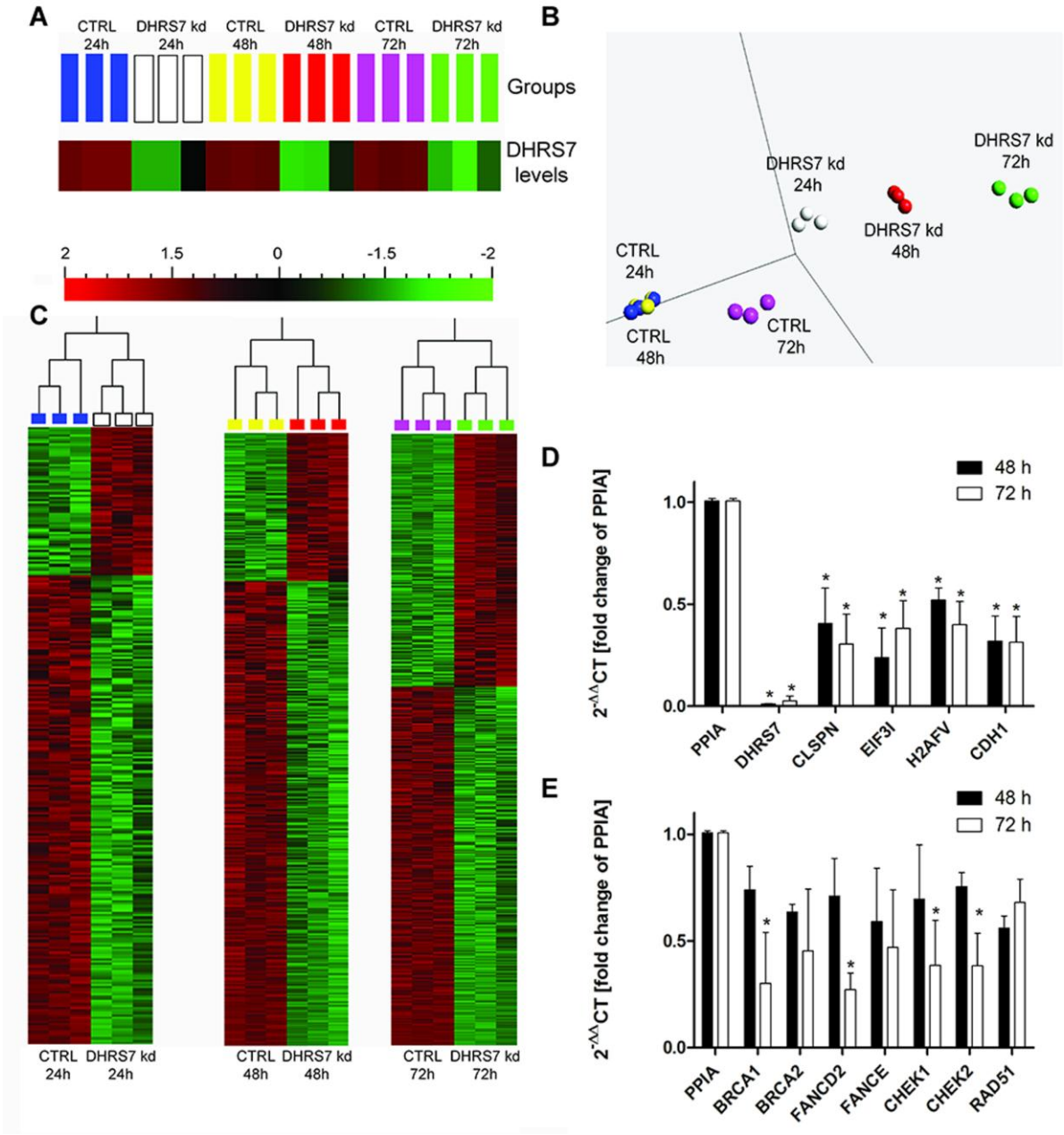

Figure 5: The impact of DHRS7 knockdown on the gene expression profile in LNCaP cells. (A) DHRS7 expression was efficiently decreased as early as 24 h after siRNA treatment. Color scheme representing normalized (-2 to 2) gene expression fold-change. (B) PCA analysis showing profound alterations in the global gene expression profile of LNCaP cells upon DHRS7 knockdown. Each sphere represents one of the three replicates used for the microarray. Replicates samples obtained from DHRS7 knockdown cells cluster to each other but far away from the CTRL cells. Most profound gene expression profile differences in DHRS7 knockdown cells compared to CTRL are observed at 72 h after siRNA treatment. (C) Hierarchical clustering of samples based on significant differentially expressed genes (normalized fold-change −2.0 to 2.0) with FDR (False discovery rate at p<0.05) highlights major differences in gene expression among analysed groups. (D) Validation of microarray data by qPCR on a selected pool of genes. (E) Genes involved in the BRCA1 pathway whose expression was altered in LNCaP cells upon DHRS7 knockdown.

Among the different pathways influenced by DHRS7 depletion, the BRCA1 pathway was one of the most affected. We also validated the expression of genes related to this pathway following DHRS7 knockdown by assessing the mRNA expression of *BRCA1*, *BRCA2*, *FANCD2*, *FANCE*, *CHEK1*, *CHEK2* and *RAD51* by qPCR (Figure 5E). Together, these results suggest that DHRS7 knockdown

alters the gene expression profile of LNCaP cells and supports our results described above concerning the effects on cell proliferation and migration.

Supplementary Figure 5: Interactive pathway analysis (IPA)-based gene enrichment analysis. Graphical representation of most alerted diseases and cell functions (A), toxicity function related pathways (B) and cell cycle associated genes (C) in DHRS7 knockdown cells.

DISCUSSION

Uncharacterized SDRs may play important physiological and pathological roles in multiple diseases, including cancer. Elucidation of their function is likely to provide an improved understanding of disease

mechanisms, which is essential for the development of novel diagnostic and therapeutic applications. [24] The “orphan” enzyme DHRS7 belongs to this enzyme family. Microarray-based gene expression profiling studies suggested that *DHRS7* expression is often decreased or even lost in PCa, [9-11] raising the question about its potential role in tumor progression, however its role in cancer has not been elucidated. Therefore, we decided to study the expression of DHRS7 in normal human prostate and in PCa tissue samples at different tumor stages. Furthermore, we assessed the effects of DHRS7 knockdown *in vitro* using different human prostate cell lines.

Through the analysis of hundreds of specimens from patients at different stages of disease, TMA technology has proven to serve as a powerful tool to promptly analyze clinical significance of new molecular markers in human tumors. Here, we took advantage of a prostate-specific TMA generated at our institution to asses DHRS7 expression in a large cohort of specimens (n=348). In line, with previously reported RNA-based microarray data, [9-11] we verified that DHRS7 expression is diminished in PCa compared with normal prostate tissue samples on the protein level using TMA. Importantly, we report for the first time that DHRS7 protein levels are decreased in PCa tissues and negatively correlate with the Gleason level. It remains to be established whether low DHRS7 expression levels in primary PCa tissue may predict a high subsequent risk of distant metastases, as such finding would have significant potential for diagnostic and therapeutic implications. To date, we have not observed a clear correlation between DHRS7 expression levels and the survival of patients. However, this is not surprising in the context of PCa since it is in line with the lack of predictive value of important tumor suppressor genes. For example, although frequently mutated in 5-20% of PCa, the p53 status also failed to serve as a prognostic marker for survival in localized prostate adenocarcinoma while it serves as a useful marker in locally advanced prostate cancer treated by androgen deprivation. [25-27]

We then sought to support the protein expression-based findings from analysis of human tissues with a set of *in vitro* experiments using different prostate-derived cell lines. First, DHRS7 expression levels in LNCaP, PC3 and BPH1 cells were evaluated and then the effect of DHRS7 knockdown on key characteristics of aggressive cancer phenotypes like cell proliferation, migration and adhesion was investigated. DHRS7 knockdown led to a dramatically increased proliferation rate of LNCaP cells; however, no significant increase in cell proliferation was observed for PC3 and BPH1 cells. This may be explained by the fact that the basal proliferation rate of LNCaP cells is much lower (approximately 60 h doubling time) compared with that of PC3 and BPH1 cells (approximately 30-45 h doubling time).[28] Furthermore, LNCaP show very high DHRS7 expression, whereas PC3 and BPH1 express only moderate to low levels. It should be noted that the proliferation of LNCaP cells is androgen-dependent, whereas that of PC3 and BPH1 cells has been shown to be androgen-independent. [29-31] Although the underlying mechanism remains unknown, it has been recently suggested that DHRS7 may promote *de novo* androgen synthesis, thus directly influencing the activation of the androgen receptor (AR), thereby stimulating cancer progression. [12]

Currently, the substrate(s) of DHRS7 remains unknown. Although a recent study suggested that DHRS7 might catalyze the reduction of several steroids, including 4-androstene-3, 17-dione, as well as quinone containing xenobiotics, this evidence stems from indirect activity measurements and need to be confirmed. Using recombinant human DHRS7 expressed in HEK-293 cells, we were unable to

detect any activity on estrone/estradiol, cortisone/cortisol and 4-androstene-3, 17-dione /testosterone, in contrast to the potent activities that we observed for 17β-HSD1, 11β-HSD1 and 17β-HSD3, respectively (data not shown). It remains to be investigated whether DHRS7 might play a role in the production of androgens via the backdoor pathway [32] or whether it indirectly stimulates androgen-dependent cancer cell proliferation.

To evaluate a possible influence of DHRS7 on cell cycle, LNCaP cells were analyzed by flow cytometry. Nevertheless, no significant changes could be detected, (Supplementary Figure 4), indicating that DHRS7 knockdown is increasing proliferation of LNCaP cells without affecting the cell cycle. In addition to the changes in LNCaP cell proliferation, increased cell migration as well as decreased cell adhesion was observed for all three cell lines tested. These results are further supported by our microarray data analysis that underlines the effect of DHRS7 depletion on the expression of genes involved in cell proliferation and cell adhesion pathways in LNCaP cells. Moreover, the transcriptome profiling of DHRS7 knockdown versus control LNCaP cells revealed a decreased expression of *CDH1* (also known as E-cadherin). Loss of E-cadherin promotes the transition of epithelial cells to the mesenchymal state (EMT), which is observed in metastasis. [33] E-cadherin is an important switch in EMT, which could explain the increased migration and adhesion observed in the prostate cell lines. Another possible mechanism for the DHRS7-mediated regulation of prostate cancer progression could involve the BRCA1/2 pathway that was also affected based on the data from our microarray analysis. BRCA1 and BRCA2 both are prostate tumor suppressors and their loss is associated with enhanced cell proliferation and overall cancer progression. [34, 35] Nevertheless, further research is needed to investigate the impact of DHRS7 function on these pathways.

In conclusion, our *in vitro* experiments provide compelling evidence for DHRS7 as a key regulator of PCa cancer cell properties. According to our results and those of others, DHRS7 possesses tumor suppressor functions in prostate cancer. Nevertheless, the mechanism underlying the effects of DHRS7 on cancer cell (and normal cell) behavior remains unknown and warrants further research. Future studies are required to identify the substrate(s) and product(s) of DHRS7 and to elucidate its regulation of expression. A better understanding of the tumor-suppressive role of DHRS7 may lead to the identification of a novel therapeutic prostate cancer target and/or the potential development of a diagnostic application.

ACKNOWLEDGEMENTS

We thank Dominik Witzigmann from the Institute of Pharmaceutical Technology, University of Basel, for the technical assistance in performing the flow cytometry experiments. This work was supported by the Swiss National Science Foundation (31003A_140961). Alex Odermatt has a Novartis Chair for Molecular and Systems Toxicology.

References

1. Siegel R, Ma J, Zou Z, Jemal A. Cancer statistics, 2014. *CA: a cancer journal for clinicians* 2014;64: 9-29.

2. Andreoiu M, Cheng L. Multifocal prostate cancer: biologic, prognostic, and therapeutic implications. *Hum Pathol* 2010;41: 781-93.

3. Ferlay J, Steliarova-Foucher E, Lortet-Tieulent J, Rosso S, Coebergh JWW, Comber H, Forman D, Bray F. Cancer incidence and mortality patterns in Europe: Estimates for 40 countries in 2012. *Eur J Cancer* 2013;49: 1374-403.

4. Yokota J. Tumor progression and metastasis. *Carcinogenesis* 2000;21: 497-503.

5. Matuszak EA, Kyprianou N. Androgen regulation of epithelial-mesenchymal transition in prostate tumorigenesis. *Expert review of endocrinology & metabolism* 2011;6: 469-82.

6. Suzman DL, Antonarakis ES. Castration-resistant prostate cancer: latest evidence and therapeutic implications. *Therapeutic advances in medical oncology* 2014;6: 167-79.

7. Schroeder FH, Hugosson J, Roobol MJ, Tammela TLJ, Ciatto S, Nelen V, Kwiatkowski M, Lujan M, Lilja H, Zappa M, Denis LJ, Recker F, et al. Screening and Prostate-Cancer Mortality in a Randomized European Study. *New Engl J Med* 2009;360: 1320-8.

8. Persson B, Kallberg Y, Bray JE, Bruford E, Dellaporta SL, Favia AD, Duarte RG, Jornvall H, Kavanagh KL, Kedishvili N, Kisiela M, Maser E, et al. The SDR (short-chain dehydrogenase/reductase and related enzymes) nomenclature initiative. *Chemico-biological interactions* 2009;178: 94-8.

9. Wong SY, Haack H, Kissil JL, Barry M, Bronson RT, Shent SS, Whittaker CA, Crowley D, Hynes RO. Protein 4.1B suppresses prostate cancer progression and metastasis. *P Natl Acad Sci USA* 2007;104: 12784-9.

10. Arredouani MS, Lu B, Bhasin M, Eljanne M, Yue W, Mosquera JM, Bubley GJ, Li V, Rubin MA, Libermann TA, Sanda MG. Identification of the Transcription Factor Single-Minded Homologue 2 as a Potential Biomarker and Immunotherapy Target in Prostate Cancer. *Clin Cancer Res* 2009;15: 5794-802.

11. Tomlins SA, Mehra R, Rhodes DR, Cao XH, Wang L, Dhanasekaran SM, Kalyana-Sundaram S, Wei JT, Rubin MA, Pienta KJ, Shah RB, Chinnaiyan AM. Integrative molecular concept modeling of prostate cancer progression. *Nat Genet* 2007;39: 41-51.

12. Romanuik TL, Wang G, Morozova O, Delaney A, Marra MA, Sadar MD. LNCaP Atlas: gene expression associated with in vivo progression to castration-recurrent prostate cancer. *BMC Med Genomics* 2010;3: 43.

13. Haeseleer F, Palczewski K. Short-chain dehydrogenases/reductases in retina. *Methods Enzymol* 2000;316: 372-83.

14. ArrayExpress. Body Map 2.0 qIE-M-c. *Available from: http://wwwebiacuk/arrayexpress* 2011.

15. ArrayExpress. RNA-seq of coding RNA from tissue samples of 95 human individuals representing 27 different tissues in order to determine tissue-specificity of all protein-coding genes qI. *Available from: http://wwwebiacuk/arrayexpress* 2013.

16. Stambergova H, Skarydova L, Dunford JE, Wsol V. Biochemical properties of human dehydrogenase/reductase (SDR family) member 7. *Chemico-biological interactions* 2014;207: 52-7.

17. Marchais-Oberwinkler S, Henn C, Moller G, Klein T, Negri M, Oster A, Spadaro A, Werth R, Wetzel M, Xu K, Frotscher M, Hartmann RW, et al. 17beta-Hydroxysteroid dehydrogenases (17beta-HSDs) as therapeutic targets: protein structures, functions, and recent progress in inhibitor development. *The Journal of steroid biochemistry and molecular biology* 2011;125: 66-82.

18. Rabbitt EH, Gittoes NJ, Stewart PM, Hewison M. 11beta-Hydroxysteroid dehydrogenases, cell proliferation and malignancy. *The Journal of steroid biochemistry and molecular biology* 2003;85: 415-21.

19. Day JM, Tutill HJ, Purohit A, Reed MJ. Design and validation of specific inhibitors of 17beta-hydroxysteroid dehydrogenases for therapeutic application in breast and prostate cancer, and in endometriosis. *Endocrine-related cancer* 2008;15: 665-92.

20. Kononen J, Bubendorf L, Kallioniemi A, Barlund M, Schraml P, Leighton S, Torhorst J, Mihatsch MJ, Sauter G, Kallioniemi OP. Tissue microarrays for high-throughput molecular profiling of tumor specimens. *Nat Med* 1998;4: 844-7.

21. Zellweger T, Ninck C, Mirlacher M, Annefeld M, Glass AG, Gasser TC, Mihatsch MJ, Gelmann EP, Bubendorf L. Tissue microarray analysis reveals prognostic significance of syndecan-1 expression in prostate cancer. *Prostate* 2003;55: 20-9.

22. Allred DC, Harvey JM, Berardo M, Clark GM. Prognostic and predictive factors in breast cancer by immunohistochemical analysis. *Mod Pathol* 1998;11: 155-68.

23. Livak KJ, Schmittgen TD. Analysis of relative gene expression data using real-time quantitative PCR and the 2(-Delta Delta C(T)) Method. *Methods* 2001;25: 402-8.

24. Keller B, Volkmann A, Wilckens T, Moeller G, Adamski J. Bioinformatic identification and characterization of new members of short-chain dehydrogenase/reductase superfamily. *Molecular and cellular endocrinology* 2006;248: 56-60.

25. Kluth M, Harasimowicz S, Burkhardt L, Grupp K, Krohn A, Prien K, Gjoni J, Hass T, Galal R, Graefen M, Haese A, Simon R, et al. Clinical significance of different types of p53

gene alteration in surgically treated prostate cancer. *International journal of cancer Journal international du cancer* 2014;135: 1369-80.

26. Abaza R, Diaz LK, Jr., Laskin WB, Pins MR. Prognostic value of DNA ploidy, bcl-2 and p53 in localized prostate adenocarcinoma incidentally discovered at transurethral prostatectomy. *The Journal of urology* 2006;176: 2701-5.

27. Che M, DeSilvio M, Pollack A, Grignon DJ, Venkatesan VM, Hanks GE, Sandler HM, Rtog. Prognostic value of abnormal p53 expression in locally advanced prostate cancer treated with androgen deprivation and radiotherapy: a study based on RTOG 9202. *International journal of radiation oncology, biology, physics* 2007;69: 1117-23.

28. Sobel RE, Sadar MD. Cell lines used in prostate cancer research: a compendium of old and new lines--part 1. *The Journal of urology* 2005;173: 342-59.

29. Horoszewicz JS, Leong SS, Kawinski E, Karr JP, Rosenthal H, Chu TM, Mirand EA, Murphy GP. LNCaP model of human prostatic carcinoma. *Cancer research* 1983;43: 1809-18.

30. Hayward SW, Dahiya R, Cunha GR, Bartek J, Deshpande N, Narayan P. Establishment and characterization of an immortalized but non-transformed human prostate epithelial cell line: BPH-1. *In vitro cellular & developmental biology Animal* 1995;31: 14-24.

31. Fu LJ, Ding YB, Wu LX, Wen CJ, Qu Q, Zhang X, Zhou HH. The Effects of Lycopene on the Methylation of the GSTP1 Promoter and Global Methylation in Prostatic Cancer Cell Lines PC3 and LNCaP. *International journal of endocrinology* 2014;2014: 620165.

32. Fiandalo MV, Wilton J, Mohler JL. Roles for the backdoor pathway of androgen metabolism in prostate cancer response to castration and drug treatment. *Int J Biol Sci* 2014;10: 596-601.

33. Semb H, Christofori G. The tumor-suppressor function of E-cadherin. *Am J Hum Genet* 1998;63: 1588-93.

34. Fan SJ, Wang JA, Yuan RQ, Ma YX, Meng QH, Erdos MR, Brody LC, Goldberg ID, Rosen EM. BRCA1 as a potential human prostate tumor suppressor: modulation of proliferation, damage responses and expression of cell regulatory proteins. *Oncogene* 1998;16: 3069-82.

35. Moro L, Arbini AA, Yao JL, di Sant'Agnese PA, Marra E, Greco M. Loss of BRCA2 promotes prostate cancer cell invasion through up-regulation of matrix metalloproteinase-9 (vol 99, pg 553, 2008). *Cancer Sci* 2014;105: 932-.

6. Acknowledgements

I would like to thank Prof. Alex Odermatt for his continuous support and stimulating discussions and for giving me the opportunity to develop this thesis in his laboratory. I also appreciate his understanding for my private problems appearing during the time of my PhD. Furthermore, I thank Prof. Michael Arand for being the co-advisor in my thesis committee.

Additional thanks go to my collaborators and colleagues, without them this whole thesis would not have been possible. Special thanks go to Dr. Luca Quagliata and Dr. Cristina Quintavalle from Luigi Terraccianos molecular pathology group who supported the DHRS7 project. I also want to thank my master student Philipp Marbet for his work and contribution of important data and Dr. Adam Lister for the stimulating discussions and suggestions concerning my projects and proofreading of my doctoral thesis.

In addition I want to thank all members from the Molecular and Systems Toxicology group for their support, the discussions and the nice time we had together.

Sincere thanks goes to my family and my friends for their continuous trust and support.

7. References

1. Kavanagh KL, Jornvall H, Persson B, Oppermann U: **Medium- and short-chain dehydrogenase/reductase gene and protein families : the SDR superfamily: functional and structural diversity within a family of metabolic and regulatory enzymes**. *Cellular and molecular life sciences : CMLS* 2008, **65**(24):3895-3906.
2. Bray JE, Marsden BD, Oppermann U: **The human short-chain dehydrogenase/reductase (SDR) superfamily: a bioinformatics summary**. *Chemico-biological interactions* 2009, **178**(1-3):99-109.
3. Filling C, Berndt KD, Benach J, Knapp S, Prozorovski T, Nordling E, Ladenstein R, Jornvall H, Oppermann U: **Critical residues for structure and catalysis in short-chain dehydrogenases/reductases**. *The Journal of biological chemistry* 2002, **277**(28):25677-25684.
4. Tang NT, Le L: **Comparative Study on Sequence-Structure-Function Relationship of the Human Short-chain Dehydrogenases/Reductases Protein Family**. *Evolutionary bioinformatics online* 2014, **10**:165-176.
5. Nobel S, Abrahmsen L, Oppermann U: **Metabolic conversion as a pre-receptor control mechanism for lipophilic hormones**. *European journal of biochemistry / FEBS* 2001, **268**(15):4113-4125.
6. Odermatt A, Nashev LG: **The glucocorticoid-activating enzyme 11beta-hydroxysteroid dehydrogenase type 1 has broad substrate specificity: Physiological and toxicological considerations**. *The Journal of steroid biochemistry and molecular biology* 2010, **119**(1-2):1-13.
7. Duax WL, Ghosh D: **Structure and function of steroid dehydrogenases involved in hypertension, fertility, and cancer**. *Steroids* 1997, **62**(1):95-100.

8. Vihko P, Herrala A, Harkonen P, Isomaa V, Kaija H, Kurkela R, Li Y, Patrikainen L, Pulkka A, Soronen P *et al*: **Enzymes as modulators in malignant transformation**. *The Journal of steroid biochemistry and molecular biology* 2005, **93**(2-5):277-283.
9. Oppermann UC, Salim S, Tjernberg LO, Terenius L, Jornvall H: **Binding of amyloid beta-peptide to mitochondrial hydroxyacyl-CoA dehydrogenase (ERAB): regulation of an SDR enzyme activity with implications for apoptosis in Alzheimer's disease**. *FEBS letters* 1999, **451**(3):238-242.
10. Masuzaki H, Paterson J, Shinyama H, Morton NM, Mullins JJ, Seckl JR, Flier JS: **A transgenic model of visceral obesity and the metabolic syndrome**. *Science* 2001, **294**(5549):2166-2170.
11. Odermatt A, Kratschmar DV: **Tissue-specific modulation of mineralocorticoid receptor function by 11beta-hydroxysteroid dehydrogenases: an overview**. *Molecular and cellular endocrinology* 2012, **350**(2):168-186.
12. Tomlinson JW, Walker EA, Bujalska IJ, Draper N, Lavery GG, Cooper MS, Hewison M, Stewart PM: **11beta-hydroxysteroid dehydrogenase type 1: a tissue-specific regulator of glucocorticoid response**. *Endocrine reviews* 2004, **25**(5):831-866.
13. Ricketts ML, Verhaeg JM, Bujalska I, Howie AJ, Rainey WE, Stewart PM: **Immunohistochemical localization of type 1 11beta-hydroxysteroid dehydrogenase in human tissues**. *The Journal of clinical endocrinology and metabolism* 1998, **83**(4):1325-1335.
14. Morgan SA, Tomlinson JW: **11beta-hydroxysteroid dehydrogenase type 1 inhibitors for the treatment of type 2 diabetes**. *Expert opinion on investigational drugs* 2010, **19**(9):1067-1076.
15. Adcock IM: **Molecular mechanisms of glucocorticosteroid actions**. *Pulmonary pharmacology & therapeutics* 2000, **13**(3):115-126.
16. Kumar R, Thompson EB: **Gene regulation by the glucocorticoid receptor: structure:function relationship**. *The Journal of steroid biochemistry and molecular biology* 2005, **94**(5):383-394.
17. Stewart PM: **Tissue-specific Cushing's syndrome uncovers a new target in treating the metabolic syndrome--11beta-hydroxysteroid dehydrogenase type 1**. *Clinical medicine* 2005, **5**(2):142-146.
18. Wang Y, Yan C, Liu L, Wang W, Du H, Fan W, Lutfy K, Jiang M, Friedman TC, Liu Y: **11beta-Hydroxysteroid dehydrogenase type 1 shRNA ameliorates glucocorticoid-induced insulin resistance and lipolysis in mouse abdominal adipose tissue**. *American journal of physiology Endocrinology and metabolism* 2015, **308**(1):E84-95.
19. Morgan SA, McCabe EL, Gathercole LL, Hassan-Smith ZK, Larner DP, Bujalska IJ, Stewart PM, Tomlinson JW, Lavery GG: **11beta-HSD1 is the major regulator of the tissue-specific effects of circulating glucocorticoid excess**. *Proceedings of the National Academy of Sciences of the United States of America* 2014, **111**(24):E2482-2491.
20. An G, Liu W, Katz DA, Marek GJ, Awni W, Dutta S: **Population pharmacokinetics of the 11beta-hydroxysteroid dehydrogenase type 1 inhibitor ABT-384 in healthy volunteers following single and multiple dose regimens**. *Biopharmaceutics & drug disposition* 2014, **35**(7):417-429.
21. Steward PM, Edwards CR: **Specificity of the mineralocorticoid receptor: crucial role of 11beta-hydroxysteroid dehydrogenase**. *Trends in endocrinology and metabolism: TEM* 1990, **1**(4):225-230.
22. Edwards CR, Stewart PM, Burt D, Brett L, McIntyre MA, Sutanto WS, de Kloet ER, Monder C: **Localisation of 11 beta-hydroxysteroid dehydrogenase--tissue specific protector of the mineralocorticoid receptor**. *Lancet* 1988, **2**(8618):986-989.
23. Dorrance AM: **Interfering with mineralocorticoid receptor activation: the past, present, and future**. *F1000prime reports* 2014, **6**:61.
24. Bertocchio JP, Warnock DG, Jaisser F: **Mineralocorticoid receptor activation and blockade: an emerging paradigm in chronic kidney disease**. *Kidney international* 2011, **79**(10):1051-1060.
25. van der Pas R, van Esch JH, de Bruin C, Danser AH, Pereira AM, Zelissen PM, Netea-Maier R, Sprij-Mooij DM, van den Berg-Garrelds IM, van Schaik RH *et al*: **Cushing's disease and hypertension:**

in vivo and in vitro study of the role of the renin-angiotensin-aldosterone system and effects of medical therapy. *European journal of endocrinology / European Federation of Endocrine Societies* 2014, **170**(2):181-191.

26. Farese S, Kruse A, Pasch A, Dick B, Frey BM, Uehlinger DE, Frey FJ: **Glycyrrhetinic acid food supplementation lowers serum potassium concentration in chronic hemodialysis patients**. *Kidney international* 2009, **76**(8):877-884.
27. Zhang MZ, Xu J, Yao B, Yin H, Cai Q, Shrubsole MJ, Chen X, Kon V, Zheng W, Pozzi A *et al*: **Inhibition of 11beta-hydroxysteroid dehydrogenase type II selectively blocks the tumor COX-2 pathway and suppresses colon carcinogenesis in mice and humans**. *The Journal of clinical investigation* 2009, **119**(4):876-885.
28. Stewart PM, Prescott SM: **Can licorice lick colon cancer?** *The Journal of clinical investigation* 2009, **119**(4):760-763.
29. Paraschos S, Mitakou S, Skaltsounis AL: **Chios gum mastic: A review of its biological activities**. *Current medicinal chemistry* 2012, **19**(14):2292-2302.
30. Dimas KS, Pantazis P, Ramanujam R: **Review: Chios mastic gum: a plant-produced resin exhibiting numerous diverse pharmaceutical and biomedical properties**. *In vivo* 2012, **26**(5):777-785.
31. Georgiadis I, Karatzas T, Korou LM, Agrogiannis G, Vlachos IS, Pantopoulou A, Tzanetakou IP, Katsilambros N, Perrea DN: **Evaluation of Chios mastic gum on lipid and glucose metabolism in diabetic mice**. *Journal of medicinal food* 2014, **17**(3):393-399.
32. Georgiadis I, Karatzas T, Korou LM, Katsilambros N, Perrea D: **Beneficial health effects of chios gum mastic and peroxisome proliferator-activated receptors: indications of common mechanisms**. *Journal of medicinal food* 2015, **18**(1):1-10.
33. Souness GW, Latif SA, Laurenzo JL, Morris DJ: **11 alpha- and 11 beta-hydroxyprogesterone, potent inhibitors of 11 beta-hydroxysteroid dehydrogenase (isoforms 1 and 2), confer marked mineralocorticoid activity on corticosterone in the ADX rat**. *Endocrinology* 1995, **136**(4):1809-1812.
34. Rafestin-Oblin ME, Fagart J, Souque A, Seguin C, Bens M, Vandewalle A: **11beta-hydroxyprogesterone acts as a mineralocorticoid agonist in stimulating Na+ absorption in mammalian principal cortical collecting duct cells**. *Molecular pharmacology* 2002, **62**(6):1306-1313.
35. Wang GM, Ge RS, Latif SA, Morris DJ, Hardy MP: **Expression of 11beta-hydroxylase in rat Leydig cells**. *Endocrinology* 2002, **143**(2):621-626.
36. Bujalska I, Shimojo M, Howie A, Stewart PM: **Human 11 beta-hydroxysteroid dehydrogenase: studies on the stably transfected isoforms and localization of the type 2 isozyme within renal tissue**. *Steroids* 1997, **62**(1):77-82.
37. Salunke DB, Hazra BG, Pore VS: **Steroidal conjugates and their pharmacological applications**. *Current medicinal chemistry* 2006, **13**(7):813-847.
38. Vincze I, Hackler L, Szendi Z, Schneider G: **Steroids 54. Amino acylamidosteroids**. *Steroids* 1996, **61**(12):697-702.
39. Giaginis C, Theocharis S: **Current evidence on the anticancer potential of Chios mastic gum**. *Nutrition and cancer* 2011, **63**(8):1174-1184.
40. Zhou L, Satoh K, Takahashi K, Watanabe S, Nakamura W, Maki J, Hatano H, Takekawa F, Shimada C, Sakagami H: **Re-evaluation of anti-inflammatory activity of mastic using activated macrophages**. *In vivo* 2009, **23**(4):583-589.
41. Gathercole LL, Lavery GG, Morgan SA, Cooper MS, Sinclair AJ, Tomlinson JW, Stewart PM: **11beta-Hydroxysteroid dehydrogenase 1: translational and therapeutic aspects**. *Endocrine reviews* 2013, **34**(4):525-555.

42. Wakelin SH: **Allergic contact dermatitis from mastic in compound mastic paint**. *Contact dermatitis* 2001, **45**(2):118.
43. Kang JS, Wanibuchi H, Salim EI, Kinoshita A, Fukushima S: **Evaluation of the toxicity of mastic gum with 13 weeks dietary administration to F344 rats**. *Food and chemical toxicology : an international journal published for the British Industrial Biological Research Association* 2007, **45**(3):494-501.
44. Anderson A, Walker BR: **11beta-HSD1 inhibitors for the treatment of type 2 diabetes and cardiovascular disease**. *Drugs* 2013, **73**(13):1385-1393.
45. Joharapurkar A, Dhanesha N, Shah G, Kharul R, Jain M: **11beta-Hydroxysteroid dehydrogenase type 1: potential therapeutic target for metabolic syndrome**. *Pharmacological reports : PR* 2012, **64**(5):1055-1065.
46. Schweizer RA, Atanasov AG, Frey BM, Odermatt A: **A rapid screening assay for inhibitors of 11beta-hydroxysteroid dehydrogenases (11beta-HSD): flavanone selectively inhibits 11beta-HSD1 reductase activity**. *Molecular and cellular endocrinology* 2003, **212**(1-2):41-49.
47. Parrott AC: **Human psychopharmacology of Ecstasy (MDMA): a review of 15 years of empirical research**. *Hum Psychopharmacol* 2001, **16**(8):557-577.
48. White C, Edwards M, Brown J, Bell J: **The impact of recreational MDMA 'ecstasy' use on global form processing**. *Journal of psychopharmacology* 2014, **28**(11):1018-1029.
49. Doblin R: **A clinical plan for MDMA (Ecstasy) in the treatment of posttraumatic stress disorder (PTSD): partnering with the FDA**. *Journal of psychoactive drugs* 2002, **34**(2):185-194.
50. Parrott AC: **The potential dangers of using MDMA for psychotherapy**. *Journal of psychoactive drugs* 2014, **46**(1):37-43.
51. Ricaurte GA, Yuan J, McCann UD: **(+/-)3,4-Methylenedioxymethamphetamine ('Ecstasy')-induced serotonin neurotoxicity: studies in animals**. *Neuropsychobiology* 2000, **42**(1):5-10.
52. Parrott A, Lock J, Adnum L, Thome J: **MDMA can increase cortisol levels by 800% in dance clubbers**. *Journal of psychopharmacology* 2013, **27**(1):113-114.
53. Parrott AC: **Cortisol and 3,4-methylenedioxymethamphetamine: neurohormonal aspects of bioenergetic stress in ecstasy users**. *Neuropsychobiology* 2009, **60**(3-4):148-158.
54. Parrott AC, Montgomery C, Wetherell MA, Downey LA, Stough C, Scholey AB: **MDMA, cortisol, and heightened stress in recreational ecstasy users**. *Behavioural pharmacology* 2014, **25**(5-6):458-472.
55. Parrott AC, Rodgers J, Buchanan T, Ling J, Heffernan T, Scholey AB: **Dancing hot on Ecstasy: physical activity and thermal comfort ratings are associated with the memory and other psychobiological problems reported by recreational MDMA users**. *Hum Psychopharmacol* 2006, **21**(5):285-298.
56. Dickerson SM, Walker DM, Reveron ME, Duvauchelle CL, Gore AC: **The recreational drug ecstasy disrupts the hypothalamic-pituitary-gonadal reproductive axis in adult male rats**. *Neuroendocrinology* 2008, **88**(2):95-102.
57. Harris DS, Baggott M, Mendelson JH, Mendelson JE, Jones RT: **Subjective and hormonal effects of 3,4-methylenedioxymethamphetamine (MDMA) in humans**. *Psychopharmacology (Berl)* 2002, **162**(4):396-405.
58. Burns N, Olverman HJ, Kelly PA, Williams BC: **Effects of ecstasy on aldosterone secretion in the rat in vivo and in vitro**. *Endocrine research* 1996, **22**(4):601-606.
59. Wang LJ, Hsiao CC, Huang YS, Chiang YL, Ree SC, Chen YC, Wu YW, Wu CC, Shang ZY, Chen CK: **Association of salivary dehydroepiandrosterone levels and symptoms in patients with attention deficit hyperactivity disorder during six months of treatment with methylphenidate**. *Psychoneuroendocrinology* 2011, **36**(8):1209-1216.
60. Maayan R, Yoran-Hegesh R, Strous R, Nechmad A, Averbuch E, Weizman A, Spivak B: **Three-month treatment course of methylphenidate increases plasma levels of**

dehydroepiandrosterone (DHEA) and dehydroepiandrosterone-sulfate (DHEA-S) in attention deficit hyperactivity disorder. *Neuropsychobiology* 2003, **48**(3):111-115.

61. Chen YH, Lin XX, Chen H, Liu YY, Lin GX, Wei LX, Hong YL: **The change of the cortisol levels in children with ADHD treated by methylphenidate or atomoxetine**. *Journal of psychiatric research* 2012, **46**(3):415-416.
62. Lee MS, Yang JW, Ko YH, Han C, Kim SH, Lee MS, Joe SH, Jung IK: **Effects of methylphenidate and bupropion on DHEA-S and cortisol plasma levels in attention-deficit hyperactivity disorder**. *Child psychiatry and human development* 2008, **39**(2):201-209.
63. Wang LJ, Wu CC, Lee SY, Tsai YF: **Salivary neurosteroid levels and behavioural profiles of children with attention-deficit/hyperactivity disorder during six months of methylphenidate treatment**. *Journal of child and adolescent psychopharmacology* 2014, **24**(6):336-340.
64. Bolanos CA, Barrot M, Berton O, Wallace-Black D, Nestler EJ: **Methylphenidate treatment during pre- and periadolescence alters behavioral responses to emotional stimuli at adulthood**. *Biol Psychiatry* 2003, **54**(12):1317-1329.
65. Avital A, Dolev T, Aga-Mizrachi S, Zubedat S: **Environmental enrichment preceding early adulthood methylphenidate treatment leads to long term increase of corticosterone and testosterone in the rat**. *PloS one* 2011, **6**(7):e22059.
66. Mattison DR, Plant TM, Lin HM, Chen HC, Chen JJ, Twaddle NC, Doerge D, Slikker W, Jr., Patton RE, Hotchkiss CE *et al*: **Pubertal delay in male nonhuman primates (Macaca mulatta) treated with methylphenidate**. *Proceedings of the National Academy of Sciences of the United States of America* 2011, **108**(39):16301-16306.
67. Hysek CM, Simmler LD, Schillinger N, Meyer N, Schmid Y, Donzelli M, Grouzmann E, Liechti ME: **Pharmacokinetic and pharmacodynamic effects of methylphenidate and MDMA administered alone or in combination**. *The international journal of neuropsychopharmacology / official scientific journal of the Collegium Internationale Neuropsychopharmacologicum* 2014, **17**(3):371-381.
68. Kanehisa L: **Steroid hormone biosynthesis - Homo sapiens (human)**. In. http://www.genome.jp/kegg-bin/show_pathway?hsa00140: KEGG; 2013.
69. Wolff K, Aitchison K: **Reply to 'MDMA can increase cortical levels by 800% in dance clubbers' Parrott et al**. *Journal of psychopharmacology* 2013, **27**(1):115-116.
70. Dotsch J, Dorr HG, Stalla GK, Sippell WG: **Effect of glucocorticoid excess on the cortisol/cortisone ratio**. *Steroids* 2001, **66**(11):817-820.
71. Mendelson JH, Mello NK, Sholar MB, Siegel AJ, Mutschler N, Halpern J: **Temporal concordance of cocaine effects on mood states and neuroendocrine hormones**. *Psychoneuroendocrinology* 2002, **27**(1-2):71-82.
72. Hamidovic A, Childs E, Conrad M, King A, de Wit H: **Stress-induced changes in mood and cortisol release predict mood effects of amphetamine**. *Drug and alcohol dependence* 2010, **109**(1-3):175-180.
73. Stojanovic OI, Lazovic M, Lazovic M, Vuceljic M: **Association between atherosclerosis and osteoporosis, the role of vitamin D**. *Archives of medical science : AMS* 2011, **7**(2):179-188.
74. Oppermann U, Filling C, Hult M, Shafqat N, Wu X, Lindh M, Shafqat J, Nordling E, Kallberg Y, Persson B *et al*: **Short-chain dehydrogenases/reductases (SDR): the 2002 update**. *Chemico-biological interactions* 2003, **143-144**:247-253.
75. Keller B, Volkmann A, Wilckens T, Moeller G, Adamski J: **Bioinformatic identification and characterization of new members of short-chain dehydrogenase/reductase superfamily**. *Molecular and cellular endocrinology* 2006, **248**(1-2):56-60.
76. Lin B, White JT, Ferguson C, Wang S, Vessella R, Bumgarner R, True LD, Hood L, Nelson PS: **Prostate short-chain dehydrogenase reductase 1 (PSDR1): a new member of the short-chain**

steroid dehydrogenase/reductase family highly expressed in normal and neoplastic prostate epithelium. *Cancer research* 2001, **61**(4):1611-1618.

77. Tang S, Gao L, Bi Q, Xu G, Wang S, Zhao G, Chen Z, Zheng X, Pan Y, Zhao L *et al*: **SDR9C7 promotes lymph node metastases in patients with esophageal squamous cell carcinoma**. *PloS one* 2013, **8**(1):e52184.
78. Huang C, Wan B, Gao B, Hexige S, Yu L: **Isolation and characterization of novel human short-chain dehydrogenase/reductase SCDR10B which is highly expressed in the brain and acts as hydroxysteroid dehydrogenase**. *Acta biochimica Polonica* 2009, **56**(2):279-289.
79. Kowalik D, Haller F, Adamski J, Moeller G: **In search for function of two human orphan SDR enzymes: hydroxysteroid dehydrogenase like 2 (HSDL2) and short-chain dehydrogenase/reductase-orphan (SDR-O)**. *The Journal of steroid biochemistry and molecular biology* 2009, **117**(4-5):117-124.
80. ArrayExpress. Body Map 2.0 qIE-M-c: *Available from: http://wwwebiacuk/arrayexpress* 2011.
81. ArrayExpress. RNA-seq of coding RNA from tissue samples of 95 human individuals representing 27 different tissues in order to determine tissue-specificity of all protein-coding genes qI: *Available from: http://wwwebiacuk/arrayexpress* 2013.
82. Stambergova H, Skarydova L, Dunford JE, Wsol V: **Biochemical properties of human dehydrogenase/reductase (SDR family) member 7**. *Chemico-biological interactions* 2014, **207**:52-57.
83. Pan Z, Wang J, Kang B, Lu L, Han C, Tang H, Li L, Xu F, Zhou Z, Lv J: **Screening and identification of differentially expressed genes in goose hepatocytes exposed to free fatty acid**. *Journal of cellular biochemistry* 2010, **111**(6):1482-1492.
84. Flowers MT, Groen AK, Oler AT, Keller MP, Choi Y, Schueler KL, Richards OC, Lan H, Miyazaki M, Kuipers F *et al*: **Cholestasis and hypercholesterolemia in SCD1-deficient mice fed a low-fat, high-carbohydrate diet**. *Journal of lipid research* 2006, **47**(12):2668-2680.
85. Wang WB, Fan JM, Zhang XL, Xu J, Yao W: **Serial expression analysis of liver regeneration-related genes in rat regenerating liver**. *Molecular biotechnology* 2009, **43**(3):221-231.
86. Wong SY, Haack H, Kissil JL, Barry M, Bronson RT, Shent SS, Whittaker CA, Crowley D, Hynes RO: **Protein 4.1B suppresses prostate cancer progression and metastasis**. *P Natl Acad Sci USA* 2007, **104**(31):12784-12789.
87. Arredouani MS, Lu B, Bhasin M, Eljanne M, Yue W, Mosquera JM, Bubley GJ, Li V, Rubin MA, Libermann TA *et al*: **Identification of the Transcription Factor Single-Minded Homologue 2 as a Potential Biomarker and Immunotherapy Target in Prostate Cancer**. *Clin Cancer Res* 2009, **15**(18):5794-5802.
88. Tomlins SA, Mehra R, Rhodes DR, Cao XH, Wang L, Dhanasekaran SM, Kalyana-Sundaram S, Wei JT, Rubin MA, Pienta KJ *et al*: **Integrative molecular concept modeling of prostate cancer progression**. *Nat Genet* 2007, **39**(1):41-51.
89. Romanuik TL, Wang G, Morozova O, Delaney A, Marra MA, Sadar MD: **LNCaP Atlas: gene expression associated with in vivo progression to castration-recurrent prostate cancer**. *BMC medical genomics* 2010, **3**:43.
90. Siegel R, Ma J, Zou Z, Jemal A: **Cancer statistics, 2014**. *CA: a cancer journal for clinicians* 2014, **64**(1):9-29.
91. Ferlay J, Steliarova-Foucher E, Lortet-Tieulent J, Rosso S, Coebergh JW, Comber H, Forman D, Bray F: **Cancer incidence and mortality patterns in Europe: estimates for 40 countries in 2012**. *European journal of cancer* 2013, **49**(6):1374-1403.
92. Yokota J: **Tumor progression and metastasis**. *Carcinogenesis* 2000, **21**(3):497-503.
93. Mazaris E, Tsiotras A: **Molecular pathways in prostate cancer**. *Nephro-urology monthly* 2013, **5**(3):792-800.

94. Andreoiu M, Cheng L: **Multifocal prostate cancer: biologic, prognostic, and therapeutic implications**. *Human pathology* 2010, **41**(6):781-793.
95. Nandana S, Chung LW: **Prostate cancer progression and metastasis: potential regulatory pathways for therapeutic targeting**. *American journal of clinical and experimental urology* 2014, **2**(2):92-101.
96. Matuszak EA, Kyprianou N: **Androgen regulation of epithelial-mesenchymal transition in prostate tumorigenesis**. *Expert review of endocrinology & metabolism* 2011, **6**(3):469-482.
97. Thiery JP, Acloque H, Huang RY, Nieto MA: **Epithelial-mesenchymal transitions in development and disease**. *Cell* 2009, **139**(5):871-890.
98. Abate-Shen C, Shen MM: **Molecular genetics of prostate cancer**. *Genes & development* 2000, **14**(19):2410-2434.
99. Suzman DL, Antonarakis ES: **Castration-resistant prostate cancer: latest evidence and therapeutic implications**. *Therapeutic advances in medical oncology* 2014, **6**(4):167-179.
100. Schroeder FH, Hugosson J, Roobol MJ, Tammela TLJ, Ciatto S, Nelen V, Kwiatkowski M, Lujan M, Lilja H, Zappa M *et al*: **Screening and Prostate-Cancer Mortality in a Randomized European Study**. *New Engl J Med* 2009, **360**(13):1320-1328.
101. Polyak K: **Breast cancer: origins and evolution**. *The Journal of clinical investigation* 2007, **117**(11):3155-3163.
102. Musgrove EA, Sutherland RL: **Biological determinants of endocrine resistance in breast cancer**. *Nature reviews Cancer* 2009, **9**(9):631-643.
103. Zhao M, Ramaswamy B: **Mechanisms and therapeutic advances in the management of endocrine-resistant breast cancer**. *World journal of clinical oncology* 2014, **5**(3):248-262.
104. Zielinska HA, Bahl A, Holly JM, Perks CM: **Epithelial-to-mesenchymal transition in breast cancer: a role for insulin-like growth factor I and insulin-like growth factor-binding protein 3?** *Breast cancer* 2015, **7**:9-19.
105. Higgins MJ, Baselga J: **Targeted therapies for breast cancer**. *The Journal of clinical investigation* 2011, **121**(10):3797-3803.
106. Byler S, Goldgar S, Heerboth S, Leary M, Housman G, Moulton K, Sarkar S: **Genetic and epigenetic aspects of breast cancer progression and therapy**. *Anticancer research* 2014, **34**(3):1071-1077.
107. Wu H, Chen Y, Liang J, Shi B, Wu G, Zhang Y, Wang D, Li R, Yi X, Zhang H *et al*: **Hypomethylation-linked activation of PAX2 mediates tamoxifen-stimulated endometrial carcinogenesis**. *Nature* 2005, **438**(7070):981-987.
108. Turashvili G, Bouchal J, Baumforth K, Wei W, Dziechciarkova M, Ehrmann J, Klein J, Fridman E, Skarda J, Srovnal J *et al*: **Novel markers for differentiation of lobular and ductal invasive breast carcinomas by laser microdissection and microarray analysis**. *BMC cancer* 2007, **7**:55.
109. Lee S, Medina D, Tsimelzon A, Mohsin SK, Mao S, Wu Y, Allred DC: **Alterations of gene expression in the development of early hyperplastic precursors of breast cancer**. *The American journal of pathology* 2007, **171**(1):252-262.
110. Marbet P: **Impact of xenobiotics on the transcriptional redulation of the short-chain dehydrogenase/reductase member 7 in hepatocytes**. University Basel; 2014.
111. Buettner R, Parhofer KG, Woenckhaus M, Wrede CE, Kunz-Schughart LA, Scholmerich J, Bollheimer LC: **Defining high-fat-diet rat models: metabolic and molecular effects of different fat types**. *Journal of molecular endocrinology* 2006, **36**(3):485-501.
112. Kennedy AR, Pissios P, Otu H, Roberson R, Xue B, Asakura K, Furukawa N, Marino FE, Liu FF, Kahn BB *et al*: **A high-fat, ketogenic diet induces a unique metabolic state in mice**. *American journal of physiology Endocrinology and metabolism* 2007, **292**(6):E1724-1739.

113. Baur JA, Pearson KJ, Price NL, Jamieson HA, Lerin C, Kalra A, Prabhu VV, Allard JS, Lopez-Lluch G, Lewis K *et al*: **Resveratrol improves health and survival of mice on a high-calorie diet**. *Nature* 2006, **444**(7117):337-342.
114. Webber BA, Lawson D, Cohen C: **Maspin and Mutant p53 expression in malignant melanoma and carcinoma: use of tissue microarray**. *Applied immunohistochemistry & molecular morphology : AIMM / official publication of the Society for Applied Immunohistochemistry* 2008, **16**(1):19-23.
115. Horoszewicz JS, Leong SS, Kawinski E, Karr JP, Rosenthal H, Chu TM, Mirand EA, Murphy GP: **LNCaP model of human prostatic carcinoma**. *Cancer research* 1983, **43**(4):1809-1818.
116. Hayward SW, Dahiya R, Cunha GR, Bartek J, Deshpande N, Narayan P: **Establishment and characterization of an immortalized but non-transformed human prostate epithelial cell line: BPH-1**. *In vitro cellular & developmental biology Animal* 1995, **31**(1):14-24.
117. Sobel RE, Sadar MD: **Cell lines used in prostate cancer research: a compendium of old and new lines--part 1**. *The Journal of urology* 2005, **173**(2):342-359.
118. Janssen T, Raviv G, Camby I, Petein M, Darro F, Pasteels J, Schulman C, Kiss R: **In-vitro characterization of dihydrotestosterone-induced, epidermal growth factor-induced and basic fibroblastic growth factor-induced modifications in the growth dynamics of the human prostate-cancer cell-line lncap, du145 and pc3**. *International journal of oncology* 1995, **7**(5):1219-1225.
119. Pickard RD, Spencer BH, McFarland AJ, Bernaitis N, Davey AK, Perkins AV, Chess-Williams R, McDermott CM, Forbes A, Christie D *et al*: **Paradoxical effects of the autophagy inhibitor 3-methyladenine on docetaxel-induced toxicity in PC-3 and LNCaP prostate cancer cells**. *Naunyn-Schmiedeberg's archives of pharmacology* 2015.
120. Schmitt J, Noble A, Otsuka M, Berry P, Maitland NJ, Rumsby MG: **Phorbol ester stimulates ethanolamine release from the metastatic basal prostate cancer cell line PC3 but not from prostate epithelial cell lines LNCaP and P4E6**. *British journal of cancer* 2014, **111**(8):1646-1656.
121. Semb H, Christofori G: **The tumor-suppressor function of E-cadherin**. *Am J Hum Genet* 1998, **63**(6):1588-1593.
122. Mao Q, Zheng X, Yang K, Qin J, Bai Y, Jia X, Li Y, Xie L: **Suppression of migration and invasion of PC3 prostate cancer cell line via activating E-cadherin expression by small activating RNA**. *Cancer investigation* 2010, **28**(10):1013-1018.
123. Giroldi LA, Schalken JA: **Decreased expression of the intercellular adhesion molecule E-cadherin in prostate cancer: biological significance and clinical implications**. *Cancer metastasis reviews* 1993, **12**(1):29-37.
124. Fan SJ, Wang JA, Yuan RQ, Ma YX, Meng QH, Erdos MR, Brody LC, Goldberg ID, Rosen EM: **BRCA1 as a potential human prostate tumor suppressor: modulation of proliferation, damage responses and expression of cell regulatory proteins**. *Oncogene* 1998, **16**(23):3069-3082.
125. Moro L, Arbini AA, Yao JL, di Sant'Agnese PA, Marra E, Greco M: **Loss of BRCA2 promotes prostate cancer cell invasion through up-regulation of matrix metalloproteinase-9 (vol 99, pg 553, 2008)**. *Cancer Sci* 2014, **105**(7):932-932.
126. Roy R, Chun J, Powell SN: **BRCA1 and BRCA2: different roles in a common pathway of genome protection**. *Nature reviews Cancer* 2012, **12**(1):68-78.
127. Liu Y, West SC: **Distinct functions of BRCA1 and BRCA2 in double-strand break repair**. *Breast cancer research : BCR* 2002, **4**(1):9-13.
128. Vogel C, Marcotte EM: **Insights into the regulation of protein abundance from proteomic and transcriptomic analyses**. *Nature reviews Genetics* 2012, **13**(4):227-232.
129. Neve RM, Chin K, Fridlyand J, Yeh J, Baehner FL, Fevr T, Clark L, Bayani N, Coppe JP, Tong F *et al*: **A collection of breast cancer cell lines for the study of functionally distinct cancer subtypes**. *Cancer cell* 2006, **10**(6):515-527.

130. Wistuba, II, Behrens C, Milchgrub S, Syed S, Ahmadian M, Virmani AK, Kurvari V, Cunningham TH, Ashfaq R, Minna JD *et al*: **Comparison of features of human breast cancer cell lines and their corresponding tumors**. *Clinical cancer research : an official journal of the American Association for Cancer Research* 1998, **4**(12):2931-2938.
131. Engel LW, Young NA, Tralka TS, Lippman ME, O'Brien SJ, Joyce MJ: **Establishment and characterization of three new continuous cell lines derived from human breast carcinomas**. *Cancer research* 1978, **38**(10):3352-3364.
132. Soule HD, Vazguez J, Long A, Albert S, Brennan M: **A human cell line from a pleural effusion derived from a breast carcinoma**. *Journal of the National Cancer Institute* 1973, **51**(5):1409-1416.
133. Horwitz KB, Mockus MB, Lessey BA: **Variant T47D human breast cancer cells with high progesterone-receptor levels despite estrogen and antiestrogen resistance**. *Cell* 1982, **28**(3):633-642.
134. Vranic S, Gatalica Z, Wang ZY: **Update on the molecular profile of the MDA-MB-453 cell line as a model for apocrine breast carcinoma studies**. *Oncology letters* 2011, **2**(6):1131-1137.
135. Jelnes P, Santoni-Rugiu E, Rasmussen M, Friis SL, Nielsen JH, Tygstrup N, Bisgaard HC: **Remarkable heterogeneity displayed by oval cells in rat and mouse models of stem cell-mediated liver regeneration**. *Hepatology* 2007, **45**(6):1462-1470.
136. Hora C, Romanque P, Dufour JF: **Effect of sorafenib on murine liver regeneration**. *Hepatology* 2011, **53**(2):577-586.
137. Affo S, Dominguez M, Lozano JJ, Sancho-Bru P, Rodrigo-Torres D, Morales-Ibanez O, Moreno M, Millan C, Loaeza-del-Castillo A, Altamirano J *et al*: **Transcriptome analysis identifies TNF superfamily receptors as potential therapeutic targets in alcoholic hepatitis**. *Gut* 2013, **62**(3):452-460.
138. Hietaniemi M, Jokela M, Rantala M, Ukkola O, Vuoristo JT, Ilves M, Rysa J, Kesaniemi Y: **The effect of a short-term hypocaloric diet on liver gene expression and metabolic risk factors in obese women**. *Nutrition, metabolism, and cardiovascular diseases : NMCD* 2009, **19**(3):177-183.
139. Langsch A, Giri S, Acikgoz A, Jasmund I, Frericks B, Bader A: **Interspecies difference in liver-specific functions and biotransformation of testosterone of primary rat, porcine and human hepatocyte in an organotypical sandwich culture**. *Toxicology letters* 2009, **188**(3):173-179.
140. Zakhari S: **Bermuda Triangle for the liver: alcohol, obesity, and viral hepatitis**. *Journal of gastroenterology and hepatology* 2013, **28 Suppl 1**:18-25.